## COSMOLOGY, COSMOMICROPHYSICS AND GRAVITATION

# ASPECTS OF STRING PHENOMENOLOGY IN PARTICLE PHYSICS AND COSMOLOGY

I. Antoniadis[1,2]

[1] LPTHE, UMR CNRS 7589 Sorbonne Universités, UPMC Paris 6, F-75005 Paris

[2] A.Einstein Center, Institute for Theoretical Physics, Bern U, Sidlerstrasse 5, CH-3012 Bern

ABSTRACT. We discuss possible connections between several scales in particle physics and cosmology, such the the electroweak, inflation, dark energy and Planck scales. We then describe the phenomenology of a model of supersymmetry breaking in the presence of a tiny (tunable) positive cosmological constant. The model is coupled to the MSSM, leading to calculable soft supersymmetry breaking masses and a distinct low energy phenomenology that allows to differentiate it from other models of supersymmetry breaking and mediation mechanisms.

**Keywords**: String theory, extra dimensions, supersymmetry, scale hierarchies, inflation, de Sitter space

### 1. Introduction

If String Theory is a fundamental theory of Nature and not just a tool for studying systems with strongly coupled dynamics, it should be able to describe at the same time particle physics and cosmology, which are phenomena that involve very different scales from the microscopic four-dimensional (4d) quantum gravity length of $10^{-33}$ cm to large macroscopic distances of the size of the observable Universe $\sim 10^{28}$ cm spanned a region of about 60 orders of magnitude. In particular, besides the 4d Planck mass, there are three very different scales with very different physics corresponding to the electroweak, dark energy and inflation. These scales might be related via the scale of the underlying fundamental theory, such as string theory, or they might be independent in the sense that their origin could be based on different and independent dynamics. An example of the former constrained and more predictive possibility is provided by TeV strings with a fundamental scale at low energies due for instance to large extra dimensions transverse to a four-dimensional braneworld forming our Universe [1]. In this case, the 4d Planck mass is emergent from the fundamental string scale and inflation should also happen around the same scale [2]. We will first review this possibility, focussing on its compatibility with cosmological observations.

We will then adopt a second more conservative approach, assuming that all three scales have an independent dynamical origin. Moreover, we will assume the presence of low energy supersymmetry that allows for an elegant solution of the mass hierarchy problem, a unification of fundamental forces as indicated by low energy data and a natural dark matter candidate due to an unbroken R-parity. The assumption of independent scales implies that supersymmetry breaking should be realized in a metastable de Sitter vacuum with an infinitesimally small (tunable) cosmological constant independent of the supersymmetry breaking scale that should be in the TeV region. In a recent work [3], we studied a simple $N = 1$ supergravity model having this property and motivated by string theory. Besides the gravity multiplet, the minimal field content consists of a chiral multiplet with a shift symmetry promoted to a gauged R-symmetry using a vector multiplet. In the string theory context, the chiral multiplet can be identified with the string dilaton (or an appropriate compactification modulus) and the shift symmetry associated to the gauge invariance of a two-index antisymmetric tensor that can be dualized to a (pseudo)scalar. The shift symmetry fixes the form of the superpotential and the gauging allows for the presence of a Fayet-Iliopoulos (FI) term, leading to a supergravity action with two independent parameters that can be tuned so that the scalar potential possesses a metastable de Sitter minimum with a tiny vacuum energy (essentially the relative strength between the F- and D-term contributions). A third parameter fixes the Vacuum Expectation Value (VEV) of the string dilaton at the desired (phenomenologically) weak coupling regime. An important consistency constraint of our model is anomaly cancellation which has been studied in [5] and implies the existence of additional charged fields under the gauged R-symmetry.

In a more recent work [6], we analyzed a small variation of this model which is manifestly anomaly free without additional charged fields and allows to couple in a straight forward way a visible sector containing the minimal supersymmetric extension of the Standard Model (MSSM) and studied the mediation of super-

symmetry breaking and its phenomenological consequences. It turns out that an additional 'hidden sector' field $z$ is needed to be added for the matter soft scalar masses to be non-tachyonic; although this field participates in the supersymmetry breaking and is similar to the so-called Polonyi field, it does not modify the main properties of the metastable de Sitter (dS) vacuum. All soft scalar masses, as well as trilinear A-terms, are generated at the tree level and are universal under the assumption that matter kinetic terms are independent of the 'Polonyi' field, since matter fields are neutral under the shift symmetry and supersymmetry breaking is driven by a combination of the $U(1)$ D-term and the dilaton and $z$-field F-term. Alternatively, a way to avoid the tachyonic scalar masses without adding the extra field $z$ is to modify the matter kinetic terms by a dilaton dependent factor.

A main difference of the second analysis from the first work is that we use a field representation in which the gauged shift symmetry corresponds to an ordinary $U(1)$ and not an R-symmetry. The two representations differ by a Kähler transformation that leaves the classical supergravity action invariant. However, at the quantum level, there is a Green-Schwarz term generated that amounts an extra dilaton dependent contribution to the gauge kinetic terms needed to cancel the anomalies of the R-symmetry. This creates an apparent puzzle with the gaugino masses that vanish in the first representation but not in the latter. The resolution to the puzzle is based to the so called anomaly mediation contributions [7, 8] that explain precisely the above apparent discrepancy. It turns out that gaugino masses are generated at the quantum level and are thus suppressed compared to the scalar masses (and A-terms).

## 2. Effective Planck mass and the inflation scale

Low scale gravity with large extra dimensions is actually a particular case of a more general framework, where the UV cutoff is lower than the Planck scale due to the existence of a large number of particle species coupled to gravity [9]. Indeed, it was shown that the effective UV cutoff $M_{UV}$ is given by

$$M_{UV}^2 = M_P^2/N\,, \tag{1}$$

where the counting of independent species $N$ takes into account all particles which are not broad resonances, having a width less than their mass. For instance, in braneworld gravity with $n$ large extra dimensions of average size $R$, the particle species are the Kaluza-Klein (KK) excitations of the graviton (and other possible bulk modes), whose number at a given energy scale $E_*$ is given by

$$N \simeq R^n E_*^n\,. \tag{2}$$

Here, we work out the consequences of this scale dependence of the strength of gravity for inferring various quantities during inflation [2], which we take to be driven by a single field for economy of discussion and because the data doesn't compel us to consider otherwise [10]. As is to be expected, all dimensionless observables such as the amplitude and spectral properties of the perturbations are unaffected by the changing strength of gravity at inflationary energies. However, when one tries to *infer* an absolute energy scale for inflation, one finds that it is undetermined commensurate with (1) up to the unknown spectrum of universally coupled species between laboratory scales and the inflationary scale, the details of which we elaborate upon in the following.

According to the inflationary paradigm, the primordial perturbations observed in the CMB were created at horizon crossing during the quasi de Sitter (dS) phase of early accelerated expansion sourced by the inflaton field. Therefore all quantities that enter calculations of primordial correlation functions (which we subsequently relate to observables in the CMB) refer to quantities at the scale at which inflation occurred. We denote all quantities measured at the scale of inflation with a starred subscript. The dominant contribution to the temperature anisotropies comes from adiabatic perturbations [1] sourced by the comoving curvature perturbation $\mathcal{R}$, defined as the conformal factor of the 3-metric $h_{ij}$ in comoving gauge:

$$h_{ij}(t,x) = a^2(t) e^{2\mathcal{R}(t,x)} \hat{h}_{ij}; \quad \hat{h}_{ij} := \exp[\gamma_{ij}] \tag{3}$$

with $\partial_i \gamma_{ij} = \gamma_{ii} = 0$ defining transverse traceless graviton perturbations. The temperature anisotropies are characterized by the dimensionless power spectrum for $\mathcal{R}$, whose amplitude is given by

$$\mathcal{P}_\mathcal{R} := \frac{H_*^2}{8\pi^2 M_*^2 \epsilon_*} = \mathcal{A} \times 10^{-10}, \tag{4}$$

where $\epsilon_* := -\dot{H}_*/H_*^2$, $H_*$ being the Hubble factor during inflation. Given that $\mathcal{R}$ is conserved on superhorizon scales (in the absence of entropy perturbations), this immediately relates to the amplitude of the late time CMB anisotropies, which fixes $\mathcal{A} \sim 22.15$ [10]. The tensor anisotropies are characterized by the tensor power spectrum

$$\mathcal{P}_\gamma := 2\frac{H_*^2}{\pi^2 M_*^2}, \tag{5}$$

Taking the ratio of the above with (4), we find the tensor to scalar ratio

$$r_* := \frac{\mathcal{P}_\gamma}{\mathcal{P}_\mathcal{R}} = 16\epsilon_*. \tag{6}$$

[1] In what follows, we assume that all of the extra species have sufficiently suppressed couplings to the inflaton during inflation (e.g. either through derivative couplings or as Planck suppressed interactions) so that isocurvature perturbations are not significantly generated. This is trivially true for hidden sector fields.

Therefore any determination of $r_*$, either through direct measurements of the stochastic background of primordial gravitational waves or through their secondary effects on the polarization of the CMB [11, 12, 13] allows us in principle to fix the scale of inflation:

$$H_* = M_* \left(\frac{\pi^2 \mathcal{A} r_*}{2 \cdot 10^{10}}\right)^{1/2} := \Upsilon = 1.05 \sqrt{r}_* \times 10^{-4}. \quad (7)$$

We see that any measurements of $r_*$ determines the scale of inflation *up to our ignorance of the effective strength of gravity at the scale* $H_*$, given by $M_* \sim \frac{M_P}{\sqrt{N}}$, where $N$ is the effective number of all universally coupled species up to the scale $H_*$– whether they exist in the visible sector or in any hidden sector. Note that as one lowers the scale of strong gravity, the maximum reheating temperature $T_i$ is necessarily lowered as well, since it cannot be higher than the inflation scale. Conservatively, $T_i$ cannot be too far below the TeV scale without spoiling the standard scenarios of big bang cosmology– in particular, mechanisms for Leptogenesis and Baryogenesis which can occur no lower than the electroweak scale [14]. We note as a consistency check on the above considerations, that although additional species increase the strength of gravity, the ratio $H_*^2/M_*^2$ is independent of $N$ and is fixed by observable quantities. Therefore the effects of strong gravity are evidently negligible during inflation even if $M_*$ is much smaller than the macroscopic strength of gravity $M_{\rm pl}$. Hence inflationary dynamics, in particular the dynamics of adiabatic fluctuations remain weakly coupled independent of $N$ and the usual computation of adiabatic correlators can be implemented [15].

In the case of extra species as KK graviton modes, the fundamental higher-dimensional gravity scale (1) with $N$ given in (2) for $E_* = M_{UV}$ leads to the usual relation between the 4d and $(4+n)$ d Planck scales

$$M_P^2 = M_{UV}^{2+n} R^n \,. \quad (8)$$

On the other hand, during inflation $N$ counts all KK states with mass less than the Hubble scale $H_*$:

$$N = (H_* R)^n \,, \quad (9)$$

and the effective gravity scale becomes

$$M_* = M_P/\sqrt{N} = M_{UV}(M_{UV}/H)^{n/2} \,, \quad (10)$$

where we used the relations (8) and (10). Equation (7) then yields:

$$H_* = M_* \Upsilon = M_{UV}(M_{UV}/H)^{n/2}\Upsilon \;\Rightarrow\; M_{UV}\Upsilon^{2/(n+2)} \,, \quad (11)$$

where we used eq. (10). It follows that $H_*$ is one to three orders of magnitude below the fundamental gravity scale $M_{UV}$ for the range $0.001 \lesssim r_* \lesssim 0.1$. The ratio $H_*/M_*$ is of course fixed by (7). The inflation scale $H_*$ can then be as low as the weak scale in low scale gravity models with large extra dimensions, consistently with observations.

In the following, we assume that the electroweak, inflation, gravity and dark energy scales have an independent dynamical origin and examine the corresponding conditions to the microscopic theories. More precisely, we address the question of supersymmetry breaking in dS space with an infinitesimal (tunable) cosmological constant.

## 3. Conventions

Throughout this paper we use the conventions of [16]. A supergravity theory is specified (up to Chern-Simons terms) by a Kähler potential $\mathcal{K}$, a superpotential $W$, and the gauge kinetic functions $f_{AB}(z)$. The chiral multiplets $z^\alpha, \chi^\alpha$ are enumerated by the index $\alpha$ and the indices $A, B$ indicate the different gauge groups. Classically, a supergravity theory is invariant under Kähler tranformations, viz.

$$\begin{aligned} \mathcal{K}(z,\bar{z}) &\longrightarrow \mathcal{K}(z,\bar{z}) + J(z) + \bar{J}(\bar{z}), \\ W(z) &\longrightarrow e^{-\kappa^2 J(z)} W(z), \end{aligned} \quad (12)$$

where $\kappa$ is the inverse of the reduced Planck mass, $m_p = \kappa^{-1} = 2.4 \times 10^{15}$ TeV. The gauge transformations of chiral multiplet scalars are given by holomorphic Killing vectors, i.e. $\delta z^\alpha = \theta^A k_A^\alpha(z)$, where $\theta^A$ is the gauge parameter of the gauge group $A$. The Kähler potential and superpotential need not be invariant under this gauge transformation, but can change by a Kähler transformation

$$\delta\mathcal{K} = \theta^A \left[r_A(z) + \bar{r}_A(\bar{z})\right], \quad (13)$$

provided that the gauge transformation of the superpotential satisfies $\delta W = -\theta^A \kappa^2 r_A(z) W$. One then has from $\delta W = W_\alpha \delta z^\alpha$

$$W_\alpha k_A^\alpha = -\kappa^2 r_A W, \quad (14)$$

where $W_\alpha = \partial_\alpha W$ and $\alpha$ labels the chiral multiplets. The supergravity theory can then be described by a gauge invariant function

$$\mathcal{G} = \kappa^2 \mathcal{K} + \log(\kappa^6 W \bar{W}). \quad (15)$$

The scalar potential is given by

$$\begin{aligned} V &= V_F + V_D \\ V_F &= e^{\kappa^2 \mathcal{K}} \left(-3\kappa^2 W\bar{W} + \nabla_\alpha W g^{\alpha\bar{\beta}} \bar{\nabla}_{\bar{\beta}} \bar{W}\right) \\ V_D &= \frac{1}{2} \left(\mathrm{Re} f\right)^{-1\ AB} \mathcal{P}_A \mathcal{P}_B, \end{aligned} \quad (16)$$

where W appears with its Kähler covariant derivative

$$\nabla_\alpha W = \partial_\alpha W(z) + \kappa^2 (\partial_\alpha \mathcal{K}) W(z). \quad (17)$$

The moment maps $\mathcal{P}_A$ are given by

$$\mathcal{P}_A = i(k_A^\alpha \partial_\alpha \mathcal{K} - r_A). \tag{18}$$

In this paper we will be concerned with theories having a gauged R-symmetry, for which $r_A(z)$ is given by an imaginary constant $r_A(z) = i\kappa^{-2}\xi$. In this case, $\kappa^{-2}\xi$ is a Fayet-Iliopoulos [17] constant parameter.

## 4. The model

The starting point is a chiral multiplet $S$ and a vector multiplet associated with a shift symmetry of the scalar component $s$ of the chiral multiplet $S$

$$\delta s = -ic\theta\,, \tag{19}$$

and a string-inspired Kähler potential of the form $-p\log(s+\bar{s})$. The most general superpotential is either a constant $W = \kappa^{-3}a$ or an exponential superpotential $W = \kappa^{-3}ae^{bs}$ (where $a$ and $b$ are constants). A constant superpotential is (obviously) invariant under the shift symmetry, while an exponential superpotential transforms as $W \to We^{-ibc\theta}$, as in eq. (14). In this case the shift symmetry becomes a gauged R-symmetry and the scalar potential contains a Fayet-Iliopoulos term. Note however that by performing a Kähler transformation (12) with $J = \kappa^{-2}bs$, the model can be recast into a constant superpotential at the cost of introducing a linear term in the Kähler potential $\delta K = b(s+\bar{s})$. Even though in this representation, the shift symmetry is not an R-symmetry, we will still refer to it as $U(1)_R$. The most general gauge kinetic function has a constant term and a term linear in $s$, $f(s) = \delta + \beta s$.

To summarise,[2]

$$\begin{aligned} \mathcal{K}(s,\bar{s}) &= -p\log(s+\bar{s}) + b(s+\bar{s}), \\ W(s) &= a, \\ f(s) &= \delta + \beta s\,, \end{aligned} \tag{20}$$

where we have set the mass units $\kappa = 1$. The constants $a$ and $b$ together with the constant $c$ in eq. (19) can be tuned to allow for an infinitesimally small cosmological constant and a TeV gravitino mass. For $b > 0$, there always exists a supersymmetric AdS (anti-de Sitter) vacuum at $\langle s+\bar{s}\rangle = b/p$, while for $b = 0$ (and $p < 3$) there is an AdS vacuum with broken supersymmetry. We therefore focus on $b < 0$. In the context of string theory, $S$ can be identified with a compactification modulus or the universal dilaton and (for negative $b$) the exponential superpotential may be generated by non-perturbative effects.

[2] In superfields the shift symmetry (19) is given by $\delta S = -ic\Lambda$, where $\Lambda$ is the superfield generalization of the gauge parameter. The gauge invariant Kähler potential is then given by $\mathcal{K}(S,\bar{S}) = -p\kappa^{-2}\log(S+\bar{S}+cV_R) + \kappa^{-2}b(S+\bar{S}+cV_R)$, where $V_R$ is the gauge superfield of the shift symmetry.

The scalar potential is given by:

$$\begin{aligned} V &= V_F + V_D \\ V_F &= a^2 e^{\frac{b}{l}} l^{p-2}\left\{\frac{1}{p}(pl-b)^2 - 3l^2\right\} \quad l = 1/(s+\bar{s}) \\ V_D &= c^2\frac{l}{\beta+2\delta l}(pl-b)^2 \end{aligned} \tag{21}$$

In the case where $S$ is the string dilaton, $V_D$ can be identified as the contribution of a magnetized D-brane, while $V_F$ for $b = 0$ and $p = 2$ coincides with the tree-level dilaton potential obtained by considering string theory away its critical dimension [18]. For $p \geq 3$ the scalar potential $V$ is positive and monotonically decreasing, while for $p < 3$, its F-term part $V_F$ is unbounded from below when $s+\bar{s} \to 0$. On the other hand, the D-term part of the scalar potential $V_D$ is positive and diverges when $s+\bar{s} \to 0$ and for various values for the parameters an (infinitesimally small) positive (local) minimum of the potential can be found.

If we restrict ourselves to integer $p$, tunability of the vacuum energy restricts $p = 2$ or $p = 1$ when $f(s) = s$, or $p = 1$ when the gauge kinetic function is constant. For $p = 2$ and $f(s) = s$, the minimization of $V$ yields:

$$b/l = \alpha \approx -0.183268 \quad , \quad p = 2 \tag{22}$$

$$\frac{a^2}{bc^2} = A_2(\alpha) + B_2(\alpha)\frac{\Lambda}{b^3c^2} \approx -50.6602 + \mathcal{O}(\Lambda) \tag{23}$$

where $\Lambda$ is the value of $V$ at the minimum (i.e. the cosmological constant), $\alpha$ is the negative root of the polynomial $-x^5+7x^4-10x^3-22x^2+40x+8$ compatible with (23) for $\Lambda = 0$ and $A_2(\alpha)$, $B_2(\alpha)$ are given by

$$A_2(\alpha) = 2e^{-\alpha}\frac{-4+4\alpha-\alpha^2}{\alpha^3-4\alpha^2-2\alpha} \;;\; B_2(\alpha) = 2\frac{\alpha^2 e^{-\alpha}}{\alpha^2-4\alpha-2} \tag{24}$$

It follows that by carefully tuning $a$ and $c$, $\Lambda$ can be made positive and arbitrarily small independently of the supersymmetry breaking scale. A plot of the scalar potential for certain values of the parameters is shown in figure 1.

At the minimum of the scalar potential, for nonzero $a$ and $b < 0$, supersymmetry is broken by expectation values of both an F and D-term. Indeed the F-term and D-term contributions to the scalar potential are

$$\begin{aligned} V_F|_{s+\bar{s}=\frac{\alpha}{b}} &= \frac{1}{2}a^2b^2e^\alpha\left(1-\frac{2}{\alpha}\right)^2 > 0, \\ V_D|_{s+\bar{s}=\frac{\alpha}{b}} &= \frac{b^3c^2}{\alpha}\left(1-\frac{2}{\alpha}\right)^2 > 0\,. \end{aligned} \tag{25}$$

The gravitino mass term is given by

$$(m_{3/2})^2 = e^{\mathcal{G}} = \frac{a^2b^2}{\alpha^2}e^\alpha\,. \tag{26}$$

Due to the Stueckelberg coupling, the imaginary part of $s$ (the axion) gets eaten by the gauge field, which acquires a mass. On the other hand, the Goldstino, which

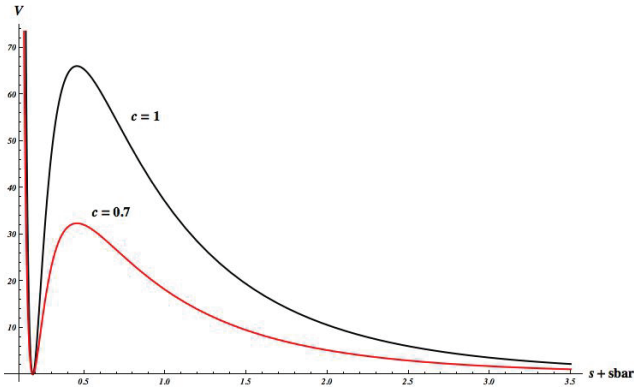


Figure 1: A plot of the scalar potential for $p = 2$, $b = -1$, $\delta = 0$, $\beta = 1$ and $a$ given by equation (23) for $c = 1$ (black curve) and $c = 0.7$ (red curve).

is a linear combination of the fermion of the chiral multiplet $\chi$ and the gaugino $\lambda$ gets eaten by the gravitino. As a result, the physical spectrum of the theory consists (besides the graviton) of a massive scalar, namely the dilaton, a Majorana fermion, a massive gauge field and a massive gravitino. All the masses are of the same order of magnitude as the gravitino mass, proportional to the same constant $a$ (or $c$ related by eq. (23) where $b$ is fixed by eq. (22)), which is a free parameter of the model. Thus, they vanish in the same way in the supersymmetric limit $a \to 0$.

The local dS minimum is metastable since it can tunnel to the supersymmetric ground state at infinity in the $s$-field space (zero coupling). It turns out however that it is extremely long lived for realistic perturbative values of the gauge coupling $l \simeq 0.02$ and TeV gravitino mass and, thus, practically stable; its decay rate is [5]:

$$\Gamma \sim e^{-B} \quad \text{with} \quad B \approx 10^{300}\,. \tag{27}$$

## 5. Coupling a visible sector

The guideline to construct a realistic model keeping the properties of the toy model described above is to assume that matter fields are invariant under the shift symmetry (19) and do not participate in the supersymmetry breaking. In the simplest case of a canonical Kähler potential, MSSM-like fields $\phi$ can then be added as:

$$\begin{aligned} \mathcal{K} &= -\kappa^{-2}\log(s+\bar{s}) + \kappa^{-2} b(s+\bar{s}) + \sum \varphi\bar{\varphi}, \\ W &= \kappa^{-3} a + W_{MSSM}, \end{aligned} \tag{28}$$

where $W_{MSSM}(\phi)$ is the usual MSSM superpotential. The squared soft scalar masses of such a model can be shown to be positive and close to the square of the gravitino mass ($\text{TeV}^2$). On the other hand, for a gauge kinetic function with a linear term in $s$, $\beta \neq 0$ in eq. (20), the Lagrangian is not invariant under the shift symmetry

$$\delta\mathcal{L} = -\theta\frac{\beta c}{8}\,\epsilon^{\mu\nu\rho\sigma} F_{\mu\nu} F_{\rho\sigma}. \tag{29}$$

and its variation should be canceled. As explained in Ref. [5], in the 'frame' with an exponential superpotential the R-charges of the fermions in the model can give an anomalous contribution to the Lagrangian. In this case the 'Green-Schwarz' term $\text{Im} s F\tilde{F}$ can cancel quantum anomalies. However as shown in [5], with the minimal MSSM spectrum, the presence of this term requires the existence of additional fields in the theory charged under the shift symmetry.

Instead, to avoid the discussion of anomalies, we focus on models with a constant gauge kinetic function. In this case the only (integer) possibility[3] is $p = 1$. The scalar potential is given by (21) with $\beta = 0$, $\delta = p = 1$. The minimization yields to equations similar to (22), (23) and (24) with a different value of $\alpha$ and functions $A_1$ and $B_1$ given by:

$$\begin{aligned} b\langle s+\bar{s}\rangle &= \alpha \approx -0.233153 \\ \frac{bc^2}{a^2} &= A_1(\alpha) + B_1(\alpha)\frac{\Lambda}{a^2 b} \approx -0.359291 + \mathcal{O}(\Lambda) \\ A_1(\alpha) &= 2e^{\alpha}\alpha\frac{3-(\alpha-1)^2}{(\alpha-1)^2}\ ,\ B_1(\alpha) = \frac{2\alpha^2}{(\alpha-1)^2}\,, \end{aligned} \tag{30}$$

where $\alpha$ is the negative root of $-3+(\alpha-1)^2(2-\alpha^2/2) = 0$ close to $-0.23$, compatible with the second constraint for $\Lambda = 0$. However, this model suffers from tachyonic soft masses when it is coupled to the MSSM, as in (28). To circumvent this problem, one can add an extra hidden sector field which contributes to (F-term) supersymmetry breaking. Alternatively, the problem of tachyonic soft masses can also be solved if one allows for a non-canonical Kähler potential in the visible sector, which gives an additional contribution to the masses through the D-term.

Let us discuss first the addition of an extra hidden sector field $z$ (similar to the so-called Polonyi field [19]). The Kähler potential, superpotential and gauge kinetic function are given by

$$\begin{aligned} \mathcal{K} &= -\kappa^{-2}\log(s+\bar{s}) + \kappa^{-2} b(s+\bar{s}) + z\bar{z} + \sum \varphi\bar{\varphi}\,, \\ W &= \kappa^{-3} a(1+\gamma\kappa z) + W_{\text{MSSM}}(\varphi)\,, \\ f(s) &= 1 \quad , \quad f_A = 1/g_A^2\,, \end{aligned} \tag{31}$$

where $A$ labels the Standard Model gauge group factors and $\gamma$ is an additional constant parameter. The existence of a tunable dS vacuum with supersymmetry

[3] If $f(s)$ is constant, the leading contribution to $V_D$ when $s+\bar{s} \to 0$ is proportional to $1/(s+\bar{s})^2$, while the leading contribution to $V_F$ is proportional to $1/(s+\bar{s})^p$. It follows that $p < 2$; if $p > 2$, the potential is unbounded from below, while if $p = 2$, the potential is either positive and monotonically decreasing or unbounded from below when $s+\bar{s} \to 0$ depending on the values of the parameters.

breaking and non-tachyonic scalar masses implies that $\gamma$ must be in a narrow region:

$$0.5 \lesssim \gamma \lesssim 1.7\,. \tag{32}$$

In the above range of $\gamma$ the main properties of the toy model described in the previous section remain, while Re$z$ and its F-auxiliary component acquire non vanishing VEVs. All MSSM soft scalar masses are then equal to a universal value $m_0$ of the order of the gravitino mass, while the $B_0$ Higgs mixing parameter is also of the same order:

$$\begin{aligned} m_0^2 &= m_{3/2}^2\left[(\sigma_s+1)+\frac{(\gamma+t+\gamma t)^2}{(1+\gamma t)^2}\right], \\ A_0 &= m_{3/2}\left[(\sigma_s+3)+t\frac{(\gamma+t+\gamma t^2)}{1+\gamma t}\right], \\ B_0 &= m_{3/2}\left[(\sigma_s+2)+t\frac{(\gamma+t+\gamma t^2)}{(1+\gamma t)}\right], \end{aligned} \tag{33}$$

where $\sigma_s = -3+(\alpha-1)^2$ with $\alpha$ and $t \equiv \langle \mathrm{Re}\, z\rangle$ determined by the minimization conditions as functions of $\gamma$. Also, $A_0$ is the soft trilinear scalar coupling in the standard notation, satisfying the relation [20]

$$A_0 = B_0 + m_{3/2}\,. \tag{34}$$

On the other hand, the gaugino masses appear to vanish at tree-level since the gauge kinetic functions are constants (see (31)). However, as mentioned in Section , this model is classically equivalent to the theory[4]

$$\begin{aligned} \mathcal{K} &= -\kappa^{-2}\log(s+\bar{s}) + z\bar{z} + \sum_\alpha \varphi\bar{\varphi}, \\ W &= \left(\kappa^{-3}a(1+z) + W_{\rm MSSM}(\varphi)\right)e^{bs}\,, \end{aligned} \tag{35}$$

obtained by applying a Kähler transformation (12) with $J = -\kappa^{-2}bs$. All classical results remain the same, such as the expressions for the scalar potential and the soft scalar masses (33), but now the shift symmetry (19) of $s$ became a gauged R-symmetry since the superpotential transforms as $W \longrightarrow We^{-ibc\theta}$. Therefore, all fermions (including the gauginos and the gravitino) transform[5] as well under this $U(1)_R$, leading to cubic $U(1)_R^3$ and mixed $U(1)\times G_{\rm MSSM}$ anomalies. These anomalies are cancelled by a Green-Schwarz (GS) counter term that arises from a quantum correction to the gauge kinetic functions:

$$f_A(s) = 1/g_A^2 + \beta_A s \quad \text{with} \quad \beta_A = \frac{b}{8\pi^2}\left(T_{R_A} - T_{G_A}\right), \tag{36}$$

where $T_G$ is the Dynkin index of the adjoint representation, normalized to $N$ for $SU(N)$, and $T_R$ is the Dynkin index associated with the representation $R$ of dimension $d_R$, equal to 1/2 for the $SU(N)$ fundamental. An implicit sum over all matter representations is understood. It follows that gaugino masses are non-vanishing in this representation, creating a puzzle on the quantum equivalence of the two classically equivalent representations. The answer to this puzzle is based on the fact that gaugino masses are present in both representations and are generated at one-loop level by an effect called Anomaly Mediation [7, 8]. Indeed, it has been argued that gaugino masses receive a one-loop contribution due to the super-Weyl-Kähler and sigma-model anomalies, given by [8]:

$$\begin{aligned} M_{1/2} = -\frac{g^2}{16\pi^2}\times\big[&(3T_G - T_R)m_{3/2} + (T_G - T_R)\mathcal{K}_\alpha F^\alpha \\ &+2\frac{T_R}{d_R}(\log\det\mathcal{K}|_R\,'')_{,\alpha}F^\alpha\Big]. \end{aligned} \tag{37}$$

The expectation value of the auxiliary field $F^\alpha$, evaluated in the Einstein frame is given by

$$F^\alpha = -e^{\kappa^2\mathcal{K}/2}g^{\alpha\bar{\beta}}\bar{\nabla}_{\bar{\beta}}\bar{W}. \tag{38}$$

Clearly, for the Kähler potential (31) or (35) the last term in eq. (37) vanishes. However, the second term survives due to the presence of Planck scale VEVs for the hidden sector fields $s$ and $z$. Since the Kähler potential between the two representations differs by a linear term $b(s+\bar{s})$, the contribution of the second term in eq. (37) differs by a factor

$$\delta m_A = \frac{g_A^2}{16\pi^2}(T_G - T_R)be^{\kappa^2\mathcal{K}/2}g^{\alpha\bar{\beta}}\bar{\nabla}_{\bar{\beta}}\bar{W}, \tag{39}$$

which exactly coincides with the 'direct' contribution to the gaugino masses due to the field dependent gauge kinetic function (36) (taking into account a rescaling proportional to $g_A^2$ due to the non-canonical kinetic terms).

We conclude that even though the models (31) and (35) differ by a (classical) Kähler transformation, they generate the same gaugino masses at one-loop. While the one-loop gaugino masses for the model (31) are generated entirely by eq. (37), the gaugino masses for the model (35) after a Kähler transformation have a contribution from eq. (37) as well as from a field dependent gauge kinetic term whose presence is necessary to cancel the mixed $U(1)_R\times G$ anomalies due to the fact that the extra $U(1)$ has become an R-symmetry giving an R-charge to all fermions in the theory. Using (37), one finds:

$$\begin{aligned} M_{1/2} = -\frac{g^2}{16\pi^2}m_{3/2}[&(3T_G - T_R) - \\ &(T_G - T_R)\left((\alpha-1)^2 + t\frac{\gamma+t+\gamma t^2}{1+\gamma t}\right)\Big] \end{aligned} \tag{40}$$

[4] This statement is only true for supergravity theories with a non-vanishing superpotential where everything can be defined in terms of a gauge invariant function $G = \kappa^2\mathcal{K} + \log(\kappa^6 W\bar{W})$ [21].

[5] The chiral fermions, the gauginos and the gravitino carry a charge $bc/2$, $-bc/2$ and $-bc/2$ respectively.

For $U(1)_Y$ we have $T_G = 0$ and $T_R = 11$, for $SU(2)$ we have $T_G = 2$ and $T_R = 7$, and for $SU(3)$ we have $T_G = 3$ and $T_R = 6$, such that for the different gaugino masses this gives (in a self-explanatory notation):

$$M_1 = 11\frac{g_Y^2}{16\pi^2}m_{3/2}\left[1-(\alpha-1)^2-\frac{t(\gamma+t+\gamma t)}{1+\gamma t}\right],$$
$$M_2 = \frac{g_2^2}{16\pi^2}m_{3/2}\left[1-5(\alpha-1)^2-5\frac{t(\gamma+t+\gamma t^2)}{1+\gamma t}\right],$$
$$M_3 = -3\frac{g_3^2}{16\pi^2}m_{3/2}\left[1+(\alpha-1)^2+\frac{t(\gamma+t+\gamma t^2)}{1+\gamma t}\right] \quad (41)$$

## 6. Phenomenology

The results for the soft terms calculated in the previous section, evaluated for different values of the parameter $\gamma$ are summarised in Table 1. For every $\gamma$, the corresponding $t$ and $\alpha$ are calculated by imposing a vanishing cosmological constant at the minimum of the potential. The scalar soft masses and trilinear terms are then evaluated by eqs. (33) and the gaugino masses by eqs. (41). Note that the relation (34) is valid for all $\gamma$. We therefore do not list the parameter $B_0$.

In most phenomenological studies, $B_0$ is substituted for $\tan\beta$, the ratio between the two Higgs VEVs, as an input parameter for the renormalization group equations (RGE) that determine the low energy spectrum of the theory. Since $B_0$ is not a free parameter in our theory, but is fixed by eq. (34), this corresponds to a definite value of $\tan\beta$. For more details see [22] (and references therein). The corresponding $\tan\beta$ for a few particular choices for $\gamma$ are listed in the last two columns of table 1 for $\mu > 0$ and $\mu < 0$ respectively. No solutions were found for $\gamma \lesssim 1.1$, for both signs of $\mu$. The lighest supersymmetric particle (LSP) is given by the lightest neutralino and since $M_1 < M_2$ (see table 1) the lightest neutralino is mostly Bino-like, in contrast with a typical mAMSB (minimal anomaly mediation supersymmetry breaking) scenario, where the lightest neutralino is mostly Wino-like [23].

To get a lower bound on the stop mass, the sparticle spectrum is plotted in Figure 2 as a function of the gravitino mass for $\gamma = 1.1$ and $\mu > 0$ (for $\mu < 0$ the bound is higher). The experimental limit on the gluino mass forces $m_{3/2} \gtrsim 15$ TeV. In this limit the stop mass can be as low as 2 TeV. To conclude, the lower end mass spectrum consists of (very) light charginos (with a lightest chargino between 250 and 800 GeV) and neutralinos, with a mostly Bino-like neutralino as LSP ($80 - 230$ GeV), which would distinguish this model from the mAMSB where the LSP is mostly Wino-like. These upper limits on the LSP and the lightest chargino imply that this model could in principle be excluded in the next LHC run.

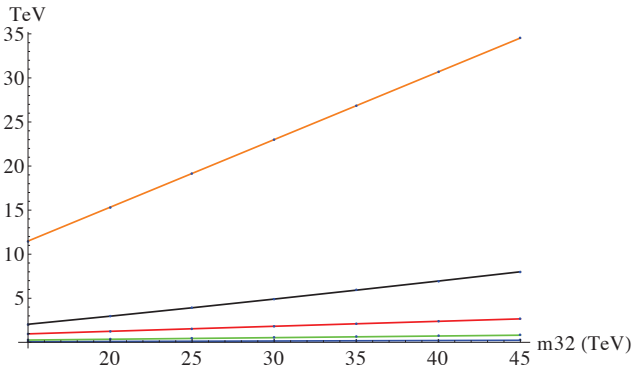


Figure 2: The masses (in TeV) of the sbottom (yellow), stop (black), gluino (red), lightest chargino (green) and lightest neutralino (blue) as a function of $m_{3/2}$ for $\gamma = 1.1$ and for $\mu > 0$. No solutions to the RGE were found when $m_{3/2} \gtrsim 45$ TeV. The lower bound corresponds to a gluino mass of 1 TeV.

In order for the gluino to escape experimental bounds, the lower limit on the gravitino mass is about 15 TeV. The gluino mass is then between 1-3 TeV. This however forces the squark masses to be very high ($10 - 35$ TeV), with the exception of the stop mass which can be relatively light ($2 - 15$ TeV).

## 7. Non-canonical Kähler potential for the visible sector

As mentioned already in Section 4, an alternative way to avoid tachyonic soft scalar masses for the MSSM fields in the model (28), instead of adding the extra Palonyi-type field $z$ in the hidden sector, is by introducing non-canonical kinetic terms for the MSSM fields, such as:

$$\mathcal{K} = -\kappa^{-2}\log(s+\bar{s}) + \kappa^{-2}b(s+\bar{s}) + (s+\bar{s})^{-\nu}\sum\varphi\bar{\varphi}$$
$$W = \kappa^{-3}a + W_{MSSM},$$
$$f(s) = 1, \qquad f_A(s) = 1/g_A^2, \quad (42)$$

where $\nu$ is an additional parameter of the theory, with $\nu = 1$ corresponding to the leading term in the Taylor expansion of $-\log(s+\bar{s}-\varphi\bar{\varphi})$. Since the visible sector fields appear only in the combination $\varphi\bar{\varphi}$, their VEVs vanish provided that the scalar soft masses squared are positive. Moreover, for vanishing visible sector VEVs, the scalar potential and is minimization remains the same as in eqs. (refbsalpha). Therefore, the non-canonical Kähler potential does not change the fact that the F-term contribution to the soft scalar masses squared is negative. On the other hand, the visible fields enter in the D-term scalar potential through the derivative of the Kähler potential with respect to $s$. Even though this has no effect on the ground state of the potential, the $\varphi$-dependence of the D-term scalar potential does result in an extra contribution to the

| $\gamma$ | t | $\alpha$ | $m_0$ | $A_0$ | $M_1$ | $M_2$ | $M_3$ | $\tan\beta(\mu>0)$ | $\tan\beta(\mu<0)$ |
|---|---|---|---|---|---|---|---|---|---|
| 0.6 | 0.446 | -0.175 | 0.475 | 1.791 | 0.017 | 0.026 | 0.027 | | |
| 1 | 0.409 | -0.134 | 0.719 | 1.719 | 0.015 | 0.025 | 0.026 | | |
| 1.1 | 0.386 | -0.120 | 0.772 | 1.701 | 0.015 | 0.024 | 0.026 | 46 | 29 |
| 1.4 | 0.390 | -0.068 | 0.905 | 1.646 | 0.014 | 0.023 | 0.026 | 40 | 23 |
| 1.7 | 0.414 | -0.002 | 0.998 | 1.588 | 0.013 | 0.022 | 0.025 | 36 | 19 |

Table 1: The soft terms (in terms of $m_{3/2}$) for various values of $\gamma$. If a solution to the RGE exists, the value of $\tan\beta$ is shown in the last columns for $\mu>0$ and $\mu<0$ respectively.

scalar masses squared which become positive

$$\nu > -\frac{e^{\alpha}(\sigma_s+1)\alpha}{A(\alpha)(1-\alpha)} \approx 2.6\,. \qquad (43)$$

The soft MSSM scalar masses and trilinear couplings in this model are:

$$\begin{aligned} m_0^2 &= \kappa^2 a^2 \left(\frac{b}{\alpha}\right)\left(e^{\alpha}(\sigma_s+1)+\nu\frac{A(\alpha)}{\alpha}(1-\alpha)\right) \\ A_0 &= m_{3/2}(s+\bar{s})^{\nu/2}\,(\sigma_s+3) \qquad (44) \\ B_0 &= m_{3/2}(s+\bar{s})^{\nu/2}\,(\sigma_s+2) \end{aligned}$$

where $\sigma_s$ is defined as in (33), eq. (31) has been used to relate the constants $a$ and $c$, and corrections due to a small cosmological constant have been neglected. A field redefinition due to a non-canonical kinetic term $g_{\varphi\bar{\varphi}} = (s+\bar{s})^{-\nu}$ is also taken into account. The main phenomenological properties of this model are not expected to be different from the one we analyzed in section with the parameter $\nu$ replacing $\gamma$. Gaugino masses are still generated at one-loop level while mSUGRA applies to the soft scalar sector. We therefore do not repeat the phenomenological analysis for this model.

**References**


[1] I. Antoniadis, N. Arkani-Hamed, S. Dimopoulos and G. R. Dvali, Phys. Lett. B **436** (1998) 257 [arXiv:hep-ph/9804398]

[2] I. Antoniadis and S. P. Patil, Eur. Phys. J. **C75** (2015) 182 [arXiv:1410.8845 [hep-th]].

[3] I. Antoniadis and R. Knoops, Nucl. Phys. B **886** (2014) 43 [arXiv:1403.1534 [hep-th]].

[4] F. Catino, G. Villadoro and F. Zwirner, JHEP **1201** (2012) 002 [arXiv:1110.2174 [hep-th]]; G. Villadoro and F. Zwirner, Phys. Rev. Lett. **95** (2005) 231602 [hep-th/0508167].

[5] I. Antoniadis, D. M. Ghilencea and R. Knoops, JHEP **1502** (2015) 166 [arXiv:1412.4807 [hep-th]].

[6] I. Antoniadis and R. Knoops, [arXiv:1507.06924 [hep-ph]].

[7] L. Randall and R. Sundrum, Nucl. Phys. B **557** (1999) 79 [hep-th/9810155]; G. F. Giudice, M. A. Luty, H. Murayama and R. Rattazzi, JHEP **9812** (1998) 027 [hep-ph/9810442].

[8] J. A. Bagger, T. Moroi and E. Poppitz, JHEP **0004** (2000) 009 [hep-th/9911029].

[9] G. Dvali, arXiv:0706.2050 [hep-th]; Int. J. Mod. Phys. A **25** (2010) 602 [arXiv:0806.3801 [hep-th]]; G. Dvali and M. Redi, Phys. Rev. D **77** (2008) 045027 [arXiv:0710.4344 [hep-th]]; R. Brustein, G. Dvali and G. Veneziano, JHEP **0910** (2009) 085 [arXiv:0907.5516 [hep-th]]; G. Dvali and C. Gomez, Phys. Lett. B **674** (2009) 303.

[10] P. A. R. Ade *et al.* [Planck Collaboration], Astron. Astrophys. (2014) [arXiv:1303.5076 [astro-ph.CO]]; arXiv:1303.5082 [astro-ph.CO].

[11] A. G. Polnarev, Sov. Astron. **29**, 607 (1985).

[12] M. Kamionkowski, A. Kosowsky and A. Stebbins, Phys. Rev. Lett. **78**, 2058 (1997) [astro-ph/9609132].

[13] U. Seljak and M. Zaldarriaga, Phys. Rev. Lett. **78**, 2054 (1997) [astro-ph/9609169].

[14] M. Trodden, Rev. Mod. Phys. **71**, 1463 (1999) [hep-ph/9803479]; S. Davidson, E. Nardi and Y. Nir, Phys. Rept. **466**, 105 (2008) [arXiv:0802.2962 [hep-ph]].

[15] C. Cheung, P. Creminelli, A. L. Fitzpatrick, J. Kaplan and L. Senatore, JHEP **0803**, 014 (2008) [arXiv:0709.0293 [hep-th]].

[16] D. Z. Freedman and A. Van Proeyen, Cambridge, UK: Cambridge Univ. Pr. (2012) 607 p.

[17] P. Fayet and J. Iliopoulos, Phys. Lett. B **51** (1974) 461; Phys. Lett. B **69** (1977) 489.

[18] I. Antoniadis, J. -P. Derendinger and T. Maillard, Nucl. Phys. B **808** (2009) 53 [arXiv:0804.1738 [hep-th]].

[19] J. Polonyi, Hungary Central Inst Res - KFKI-77-93 (77,REC.JUL 78) 5p.

[20] H. P. Nilles, Phys. Rept. **110** (1984) 1

[21] S. Ferrara, L. Girardello, T. Kugo and A. Van Proeyen, Nucl. Phys. B **223** (1983) 191

[22] J. R. Ellis, K. A. Olive, Y. Santoso and V. C. Spanos, Phys. Lett. B **573** (2003) 162 [hep-ph/0305212]

[23] T. Gherghetta, G. F. Giudice and J. D. Wells, Nucl. Phys. B **559** (1999) 27 [hep-ph/9904378].

# DISCRETE COSMOLOGY APPLICATION CONCERNING DARK MATTER HALOS

R.D. Brilenkov

Odessa I.I.Mechnikov National University,
Dvoryanskaya st. 2, Odessa 65082, Ukraine,
*ruslan.brilenkov@gmail.com*

ABSTRACT. We applied discrete cosmology for investigation of the density profiles of dark matter (DM) halos of clusters of galaxies. Comparing the derived velocity dispersion with the experimental data for the Coma cluster, we found the effective radius for the mass distribution inside this galaxy cluster. Our estimates give an opportunity to restrict the parameters of the Navarro-Frenk-White profile for considered cluster.

**Keywords**: dark matter, clusters of galaxies.

It is generally known, our Universe is dark: dark energy and dark matter contribute approximately 69% and 26% into total mass-energy balance in the Universe, respectively.

We found potentials, which satisfy the Poisson equation and give us an opportunity to consider motion of test massive bodies and light taking into account gravitational attraction to inhomogeneities inside the galaxies, groups and clusters of galaxies and cosmological expansion of the Universe:

$$\triangle\Phi = \frac{1}{R}\frac{d^2}{dR^2}(R\Phi) = 4\pi G_N \rho_{\rm ph}\,,$$

where $G_N$ is the Newtonian gravitational constant and $\rho_{\rm ph}$ is the physical rest mass density of the bound system.

After that we introduce the distance radius of zero acceleration surface (at which the gravitational attraction and cosmological expansion compensate each other):

$$R_H = \left[\frac{G_N M}{\ddot{a}/a}\right]^{1/3}$$

Using the NFW density profile of DM halo of clusters of galaxies as the most commonly used profile:

$$\rho_{\rm ph}(R) = \frac{4\rho_s}{\frac{R}{R_s}\left(1+\frac{R}{R_s}\right)^2}\,, \quad R_s = \text{const}\,, \quad \rho_s = \rho(R_s)$$

we obtain, with the help of the observable data, the preferable profile parameters for the Coma cluster: $R_{200} \approx 1.77\,h^{-1}\,\text{Mpc} = 2.61\,\text{Mpc}$ and the concentration parameter $c = 3 \div 4$

The most galaxies are concentrated inside a sphere of effective radius $R_{eff} \sim 3.7\,\text{Mpc}$ for the Coma cluster (Abell 1656).

We also found line-of-sight velocity dispersion $1004\,\text{km}\,\text{s}^{-1}$. The observations give very close value $1008\,\text{km}\,\text{s}^{-1}$ for this cluster.

*Acknowledgements.* I would like to thank my supervisors Alexander Zhuk and Maxim Eingorn who helped me to get these results.

**References**

Eingorn M., Zhuk A.: 2012, Hubble flows and gravitational potentials in observable Universe, *JCAP*, **09**, 026; arXiv:1205.2384.

Eingorn M., Kudinova A., Zhuk A.: 2013, Dynamics of astrophysical objects against the cosmological background, *JCAP*, **04**, 010; arXiv:astro-ph/1211.4045.

Eingorn M., Zhuk A.: 2014, Remarks on mechanical approach to observable Universe, *JCAP*, **05**, 024; arXiv:astro-ph/1309.4924.

# THE DOMINANCE OF DARK ENERGY LEADS TO REDUCTION OF THE ENTROPY OF GALAXIES FLOW AND ENTROPY OF THE UNIVERSE

Aleksandr V. Bukalov

The Centre for Physical and Space Research, International Institute of Socionics, Melnikova str., 12, Kyiv-050, 04050, Ukraine, *bukalov.physics@socionic.info*

ABSTRACT. The existence of the Hubble flow recession of galaxies in terms of dominance of dark energy density, vacuum energy, reduces the gravitational entropy of clusters of galaxies, reducing the gravitational entropy of the Universe as a whole. Global dominance of dark energy leads to a decrease in entropy of the Universe within the cosmic event horizon.

**Keywords:** Hubble flow, movement of galaxies, clusters of galaxies, dark energy, entropy of the Universe

The dominance of dark energy in the modern era leads to the dominance of anti-gravitation of gravity on cosmological scales. I.D.Karachentsev (Karachentsev & Kashlbadze, 2006; Karachentsev, 2005; Karachentsev et al., 2009; Karachentsev, Karachentseva & Huchtmeier, 2007) and A.D.Chernin (Chernin, Teerikorpi, Baryshev, 2003; Chernin et al., 2007; Chernin et al., 2009; Chernin et al., 2012; Chernin et al., 2013; Chernin et al., 2007; Chernin et al., 2012; Chernin, 2013; Teerikorpi & Chernin, 2010), studying the motions of galaxies in clusters, have shown that anti-gravity effects manifest themselves not only on a cosmic scale, but the scale of clusters of galaxies, for example – the Local Group, including our galaxy (the Milky Way) galaxy Andromeda and dozens of other smaller galaxies. M. Eingorn and A. Zhuk also studied in detail these issues (Brilenkov, Eingorn & Zhuk, 2015; Eingorn & Zhuk, 2012). Observations and modeling have shown that at distances of 1–3 Mpc from the center of the gravity bounded Local Group of galaxies it is observed the local flow of divergent dwarf galaxies. The velocities of these galaxies are proportional to the distance from the center. A.D.Chernin et al. (2012) have shown that such flows, which are observed in other clusters at different scales, form under the influence of dark energy. So, for Local Groups zone of zero gravity in which the gravitational force is balanced by the force of attraction and anti-gravitation is the $R_{ZG}\approx 1.3\div 1.4$ Mpc. Therefore, when $R>R_{ZG}$ the flow of recession of galaxies starts. A.D.Chernin and colleagues studied the behavior of galaxies streams, build charts based on experimental data and numerical simulation and showed that the phase trajectories of the local stream tend to phase attractor $V=H_xR$, that corresponds to the Hubble law. In this case $H_x=(8\pi G\rho_x/3)^{1/2}$ is determined by the local density of dark energy (Chernin, 2013). Therefore, when $R>R_{ZG}$ flow of receding galaxies starts. In this case the phase trajectories of the local flow tend to phase attractor $V=H_xR$, that is, obey the Hubble law. From experimental diagram of velocities of galaxies we can estimate that the spread of own velocities of galaxies with $R<R_{ZG}$ reaches $\Delta V_{\max}=\pm 150$ km/s, the average is $\Delta V=\pm 70$ km/s, while when $R > R_{ZG}$ velocity spread to the theoretical velocity of Hubble divergence flow averages about $\Delta V= 12$ km/s (Bukalov, 2014). Antigravity of dark energy, or the energy of the vacuum, reduces the dispersion of velocity galaxies. The difference in entropy in areas with $R < R_{ZG}$ and $R > R_{ZG}$ is negative, so "evaporation" of the galaxies from gravitationally bound clusters reduces its gravitational entropy. Thus the antigravitation area causes a decrease in entropy of "gas of galaxies" at different levels of the hierarchy, in clusters and superclusters. In fact, gravitationally bound system, such as a group or cluster of galaxies, has gravitational entropy more than a galaxy outside the gravitational cluster and moving in an anti-gravitational environment. The "evaporation" of the galaxies gravitationally bound cluster reduces its gravitational entropy. Thus, the area of anti-gravitation causes a decrease in the entropy "gas galaxies" at different levels of the hierarchy – in clusters and superclusters.

Based on the results of numerical modeling of flow of galaxies recession, in which were obtained the minimum and maximum velocity of flow $V_{\min}=H_xR(1+2x^{-3}-3x^{-2})^{1/2}$ and $V_{\max}=H_xR(1+3x^{-1/2})$, where $x=R/R_{ZG}$ (Chernin, 2013), we can write in general form the expression for the entropies difference:

$$\Delta S = \ln \frac{(V_{2_{\max}} - V_{2_{\min}})^2}{(V_{1_{\max}} - V_{1_{\min}})^2} . \quad (1)$$

We have obtained the entropy flow of galaxies similar to the gas. But if we use obtained by Chernin A.D. (2013) vacuum cooling factor as ratio of velocities, the logarithm of the square of this factor also provides an estimate of entropy changes. However, we can consider the more general expression for the evaluation of gravitational entropy of the system. We express the acceleration as equivalent to the Unruh vacuum temperature of accelerated moving body, for example a galaxy:

$$\frac{\hbar\ddot{a}}{2\pi c k_B} = \frac{\hbar g}{2\pi c k_B} + \frac{\hbar a}{2\pi c k_B} = -\frac{\hbar GM}{2\pi c k_B R^2} + \frac{\hbar c^2}{2\pi c k_B \cdot 3}\Lambda R , \quad (2)$$

or taking a positive temperature $T_G$, corresponding to the gravitational acceleration $g$, by analogy with the temperature of the black holes, we obtain a negative temperature value of the vacuum $T_v$, which corresponds to the anti-gravity acceleration: $\Delta k_B T = k_B T_G - k_B T_v$.

Thus, the entropy $S_v$ is negative, which means that the effects of the vacuum can be attributed to the negative entropy, or information, that is the ability to the information arranging ordering. This explains the shift to the orderly movement of galaxies at $R>R_{ZG}$.

However, on the scale of the Universe there is a similar law accelerating recession superclusters of galaxies under the influence of dark energy (Chernin, 2013). This means that in a similar manner gravitational entropy decreases at the level of interaction of superclusters of galaxies also. Hence, the dominance of dark energy, or vacuum energy, on cosmological scales leads to the orderly movement of galaxies at the level of clusters and superclusters, reducing gravitational entropy of the Universe as a whole, as was shown earlier by the author (Bukalov, 2014). Therefore, in the Universe, which is expanding with acceleration under the influence of anti-gravity vacuum, gravitational entropy due to the contribution of gravitating matter should decrease with time. Thus, in the present Universe inside the Hubble radius are about $10^9$ clusters of galaxies, like the Local Group. With continued accelerated expansion of the Universe it will be only a local group. All the other galaxies will be an observer outside the event horizon, which tends to $H^{-1} = r_\Lambda$, the radius of de Sitter space. Thus gravitational entropy associated with the supercluster of galaxies decrease in $10^9$ times.

Turning to the cosmological scale and the Friedmann equation:

$$\ddot{a}_U = -\frac{4\pi}{3} G\,(\rho_M + 3p_M)a + (\rho_V + 3p_V)\,a\,, \qquad (3)$$

where $a$ is the scale factor, from $p_M=0$, $\rho_V=-p_V$ we get (Bukalov, 2014).

$$\ddot{a}_U = -\frac{4\pi G}{3}(\rho_M - 2p_V)a\,. \qquad (4)$$

When $a \approx R_H \approx 1.36\cdot 10^{26}$m, $\Omega_M \approx 0.318$, $\Omega_V = 0.682$, $\Omega_r \approx 5\cdot 10^{-4}$, $z=0$

$$\ddot{a}_U = -\frac{4\pi}{3} G_N \rho_c (0.318(1+z)^3 + \Omega_r (1+z)^4 - 2\cdot 0.682)\cdot R_H = \frac{4\pi}{3} G_N \rho_c \cdot 1.046a = 3.46\cdot 10^{-10}\,\mathrm{m\cdot s^{-2}}. \qquad (5)$$

$$\Delta\ddot{a}_V = g - 2\ddot{a}_V \qquad (6)$$

$$k_B \Delta T = k_B T_g - 2k_B T_V = -1.046 k_B T_H = -k_{B'} T_U \qquad (7)$$

$$T_U = \frac{\hbar \ddot{a}_U}{2\pi c k_B} = 1.4\cdot 10^{-30}\ \mathrm{K}. \qquad (8)$$

This is the temperature of the quantum radiation of accelerated body to the outside distant observer. According to M.B. Mensky (1978) such temperature is negative. Therefore for the Universe the entropy change will be:

$$\frac{\partial S_U}{\partial t} \approx \frac{S_U}{t_U} \approx -2.4\cdot 10^{52}\ \mathrm{J/s}. \qquad (9)$$

Thus, when $z<0.745$, $\partial S_U / \partial t < 0$.

From our results it follows that the vacuum is a reservoir of negative entropy, or ordering, which manifests itself in the period of its domination. Therefore, the vacuum can induce an increase in ordering of the movement patterns the universe. This impact is **the macroscopic quantum cosmological effect**.

The existence of the Hubble flow of receding galaxies under the domination of dark energy density, vacuum energy, leads to a decrease of gravitational entropy of galaxy clusters, reducing gravitational entropy of the universe as a whole.

With the gradual disappearance of black holes with their entropy and radiation, as well as the galaxies themselves over the cosmic event horizon, the entropy of the observable universe will only decrease, and negative entropy, or the degree of ordering of information, will increase asymptotically approaching a constant value.

**References**


Birrell N.D., Davies P.C.W. Quantum fields in curved space. Cambridge University Press, 1982.

Bisnovatyi-Kogan G.S., Chernin A.D.: 2012, *Astrophys. Space Sci*., **338**, 337.

Bukalov A.V.: 2014, in Proc. of 14*th International Gamow Summer School*.

Chernin A., Teerikorpi P., Baryshev Yu.: 2003, *Adv. Space Res*., **31**, 459; astro-ph/0012021.

Chernin A.D. et al.: 2007, *Astron. Astrophys*., **467**, 933.

Chernin A.D. et al.: 2007, *Astron. Astrophys. Trans*., **26,** 275.

Chernin A.D. et al.: 2009, *Astron. Astrophys*., **507**, 1271.

Chernin A.D. et al.: 2012, *Astron. Astrophys*., **539**, 4.

Chernin A.D. et al.: 2012, *Astron. Rep*., **56**, 653.

Chernin A.D. et al.: 2013, *Astron. Astrophys*., **553**, 101.

Chernin A.D.: 2013, *UFN* (*Uspehi fiz. nauk*), **183**, 741.

Egan C.A., Lineweaver C.H.: 2010, *Astrophys. J*., **710**, 1825; arXiv:0909.3983 [astro-ph.CO].

Brilenkov R., Eingorn M., Zhuk A.: 2015, arXiv: 1507.07234.

Eingorn M., Zhuk A.: 2012, arXiv:1205.2384.

Gibbons G.W., Hawking S.W.: 1977, *Phys. Rev*. D, **15**, 2738.

Karachentsev I.D., Kashlbadze O.G.: 2006, *Astrophys.,* **49**, 3.

Karachentsev I.D.: 2005, *Astron. J*., **129**, 178.

Karachentsev I.D. et al.: 2009, *Mon. Not. R. Astron. Soc*., **393**, 1265.

Karachentsev I.D., Karachentseva V.E., Huchtmeier W.K.: 2007, *Astron. Lett*., **33**, 512.

Mensky M.B.: 1978, *TMF*, **115 (2)**, 215.

Perlmutter S. et al.: 1999, *Astrophys. J*., **517**, 565.

Riess A.G. et al.: 1998, *Astron. J*., **116**, 1009.

Teerikorpi P., Chernin A.D.: 2010, *Astron. Astrophys*., **516**, A93.

# THE MODEL FOR FINAL STAGE OF GRAVITATIONAL COLLAPSE MASSLESS SCALAR FIELD

V.D. Gladush[1], D.V. Mironin[2]

Dnipropetrovsk National University, Gagarin Ave, 725014, Ukraine,
[1]*vgladush@gmail.com*, [2]*dmyronin1993@mail.ru*

ABSTRACT. It is known that in General relativity, for some spherically symmetric initial conditions, the massless scalar field (SF) experience the gravitational collapse (Choptuik, 1989), and arise a black hole (BH). According Bekenstein, a BH has no "hair scalar", so the SF is completely under the horizon. Thus, the study of the final stage for the gravitational collapse of a SF is reduced to the construction of a solution of Einstein's equations describing the evolution of a SF inside the BH. In this work, we build the Lagrangian for scalar and gravitational fields in the spherically symmetric case, when the metric coefficients and SF depends only on the time. In this case, it is convenient to use the methods of classical mechanics. Since the metric allows an arbitrary transformation of time, then the corresponding field variable ($g_{00}$) is included in the Lagrangian without time derivative. It is a non-dynamic variable, and is included in the Lagrangian as a Lagrange multiplier. A variation of the action on this variable gives the constraint. It turns out that Hamiltonian is proportional to the constraint, and so it is zero. The corresponding Hamilton-Jacobi equation easily integrated. Hence, we find the relation between the SF and the metric. To restore of time dependence we using an equation $\partial L / \partial \dot{q} = \partial S / \partial q$ After using a gauge condition, it allows us to find solution. Thus, we find the evolution of the SF inside the BH, which describes the final stage of the gravitational collapse of a SF. It turns out that the mass BH associated with a scalar charge $G$ of the corresponding SF inside the BH ratio $M = G/(2\sqrt{\kappa})$.

**Keywords:** scalar field, black hole, Einstein equations.

## 1. Introduction

One of the most interesting objects in astrophysical and cosmological applications of General relativity (GR) is a scalar field. However, the models with scalar field known only for the simplest configurations, due to the difficulties of obtaining analytical solutions. So for a massless scalar field in General relativity is widely known spherically symmetric static solution of Fisher (1948) and its various later modifications (Janis, Newman, Winicour (1968); Wyman (1981); Agnese and La Camera. (1985)). Analytical solutions for the system of static scalar and electromagnetic fields in General relativity for spherical symmetry built Bronnikov (1972), Zaitsev, Kolesnikov and Radynov (1972), and then Korkina (1976) in different coordinate systems. All these solutions are unstable and have naked singularity. It turns out that for systems with a scalar field analogue of Birkhoff theorem on the uniqueness of the solution fails, and in addition, there is no conserved scalar charge. Therefore, a static configuration with a scalar field which satisfies the Einstein equations, due to negligible fluctuations, coming out of this mode and begins to evolve.

For dynamic spherically symmetric problems, due to the obvious difficulties in obtaining solutions of Einstein's equations in closed form, most of the work performed numerically. Roberts (1989) has built one of the few analytical solutions in closed form. Initially, he scheduled to use it as a counter-example to the hypothesis of cosmic censorship. However, later Brady (1994); Oshiro, Nakamura and Tomimatsu (1994) rediscovered this solution in the context of critical gravitational collapse

Spherically symmetric collapse of a scalar field is the perfect model for studying the dynamics of strong field in general relativity. Therefore, in this model used analytical and numerical methods. In particular, Christodoulou (1987) rigorously established global existence and uniqueness of solutions of the Einstein equations for a scalar field. He proved that the space of General relativity together with spherically symmetric scalar field with a sufficiently weak (in some sense) initial data evolves in Minkowski space-time, while the class sufficiently strong data forms a BH.

The behavior of the scalar field near the threshold of BH formation was first investigated Choptuik (1993). He numerically solved the Einstein equations for spherically symmetric systems of the gravitational and massless scalar fields with minimal coupling. He studied the gravitational collapse for different sets of one-parameter families of the initial data. For example, they can be taken as a family of Gaussian pulses

$$\varphi(0,v) = pv^2 \exp(-(v-v_0)^2/\sigma^2).$$

Suppose that for a given family the parameter $p$ is chosen in such a way that for small values of $p$ the gravitational field in during the evolution of is too weak to form a BH (the field is scattered), while for large values of parameter p is formed BH. Then between these two limits, there is a critical value of this parameter $p^*$ in which first formed the BH. Solutions for which $p < p^*$ are called subcritical and solving for $p > p^*$ – supercritical, respectively. Choptuik proved that in the collapse may occur arbitrarily small BH. Moreover, when $p > p^*$ the mass of the BH is given by

$$M_{BH}(p) \propto \left| p - p^* \right|^{\beta},$$

where the exponent β has a universal value $\gamma \simeq 0.374$ for all 1-parameter families of scalar field data. There are still a number of other features critical gravitational collapse of a scalar field, for example, discrete and continuous self-similarity, and others. Work Choptuik is an example of when the discovery of a new phenomenon in General relativity was done numerically. The discovery of universal properties of critical collapse is one of significant achievements the numerical relativity (Novikov & Frolov, 2001).

## 2. The action and its reduction

Consider the evolution of spherically symmetric massless scalar field in the supercritical case, when $p > p^*$. In this case, at the final stage of the gravitational collapse is formed the black hole with a mass $M_{BH}(p)$. The residual relaxation phenomena associated with scattering of the remnants of the scalar field at infinity, do not affect the black hole and can be ignored.

According to the no-hair theorem Chase (1970) and Bekenstein (1972), the BH has no of neutral "scalar hairs" (as, indeed, and charged), therefore on the final stage of the gravitational collapse a scalar field is completely under the horizon, inside a black hole. Beyond the BH, we have the free vacuum gravitational field described by the Schwarzschild solution. Thus, the study of the final stage the gravitational collapse a scalar field, by definition, is to construction of the solution of Einstein equations describing the evolution of scalar field inside the BH and satisfying appropriate boundary conditions.

In view with the above, we assume that the space-time inside a BH is described by the spherically symmetric metric, depending on time

$$ds^2 = e^{\nu(t)} c^2 dt^2 - e^{\lambda(t)} dr^2 - e^{\mu(t)} d\sigma^2,$$
$$d\sigma^2 = d\theta^2 + \sin^2\theta d\alpha^2.$$

For simplicity, consider the evolution of the homogeneous scalar field ψ = ψ(t). Note that the metric admits an arbitrary gauge transformation time $t = t(\tilde{t})$, which induces the transformation of the metric coefficient $e^{\tilde{\nu}} = e^{\nu}\left(dt/d\tilde{t}\right)^2$ .Thus, there is a gauge arbitrariness in the definition of the metric function $e^{\nu} = N^2$.

$$S = \int \Lambda \sqrt{-g}\, d^4 x.$$
$$\Lambda = -\frac{1}{4\pi}\left[\frac{c^4}{4k} R - \frac{1}{2} g^{\mu\nu} \varphi_{,\mu} \varphi_{,\nu}\right].$$

Here scalar curvature R in this case is equal to

$$R = -2e^{-\mu} - \frac{e^{-\nu}}{c^2}(2\ddot{\mu} + \ddot{\lambda} + \frac{3}{2}\dot{\mu}^2 + \dot{\mu}\dot{\lambda} - \dot{\mu}\dot{\nu} + \frac{1}{2}\dot{\lambda}^2 - \frac{1}{2}\dot{\nu}\dot{\lambda}),$$
$$\sqrt{-g} = e^{\mu + (\nu+\lambda)/2} \sin\theta,$$

where the point denotes $d/dx^0$. After the integration over the angles, the action takes the form

$$S = \int L dx^0 dr,$$

$$L = \frac{1}{2c^2}[\frac{c^4}{2k}(2\ddot{\mu} + \ddot{\lambda} + \frac{3}{2}\dot{\mu}^2 + \dot{\mu}\dot{\lambda} - \dot{\mu}\dot{\nu} + \frac{1}{2}\dot{\lambda}^2 - \frac{1}{2}\dot{\nu}\dot{\lambda}) + \dot{\varphi}^2]e^{\frac{\lambda-\nu}{2}+\mu} + \frac{c^4}{2k} e^{\frac{\nu+\lambda}{2}}.$$

Since the Lagrangian and the field variables is independent from the coordinate *r*, it possible to be limited to the one-dimensional system with the action

$$\tilde{S} = \int L dx^0.$$

Extracting total time derivative, we obtain an effective Lagrangian

$$\tilde{L} = -\frac{1}{2c^2}\left[\frac{c^4}{2k}\left(\frac{1}{2}\dot{\mu}^2 + \dot{\mu}\dot{\lambda}\right) - \dot{\varphi}^2\right] e^{\frac{\lambda-\nu}{2}+\mu} + \frac{c^4}{2k} e^{\frac{\nu+\lambda}{2}}.$$

For diagonalization of the Lagrangian, we make a change of field variables

$$\mu = \omega - \lambda, \qquad \nu = \rho - \lambda.$$

Then

$$\tilde{L} = \frac{1}{2}\left[\frac{\dot{\varphi}^2}{c^2} - \frac{c^3}{4k}\left(\dot{\omega}^2 - \dot{\lambda}^2\right)\right] e^{\omega - \rho/2} + \frac{c^4}{2k} e^{\rho/2}.$$

In the new variables, the metric takes the form

$$ds^2 = e^{-\lambda}\left(e^{\rho} c^2 dt^2 - e^{\omega} d\sigma^2\right) - e^{\lambda} dr^2.$$

## 3. The equation of Hamilton-Jacobi in the minisuperspace

To solve the problem under consideration is convenient to use the methods of classical mechanics. From the point of view of the classical mechanics, the metric coefficients and a scalar field in the resulting Lagrangian are the generalized coordinates (coordinates of a minisuperspace Wheeler-DeWitt).

Note that the metric allows arbitrary gauge transformation of time, and the corresponding metric variable $e^{\rho}$ enters the Lagrangian without time derivative. Therefore, it is a non-dynamic variable and is included in the Lagrangian as the Lagrange multiplier. Variation of the Lagrangian on this variable gives us the constraint:

$$\frac{\partial \tilde{L}}{\partial \rho} = -\frac{1}{4}\left[\frac{\dot{\varphi}^2}{c^2} - \frac{c^2}{4k}\left(\dot{\omega}^2 - \dot{\lambda}^2\right)\right] e^{\omega - \rho/2} + \frac{c^4}{4k} e^{\rho/2} = 0.$$

Next, we find momenta, conjugate of the dynamic variables $\{\varphi, \omega, \lambda\}$ :

$$p_{\varphi} = \frac{\partial \tilde{L}}{\partial \dot{\varphi}} = \frac{\dot{\varphi}}{c^2} e^{\omega - \rho/2}, \qquad p_{\omega} = \frac{\partial \tilde{L}}{\partial \dot{\omega}} = -\frac{c^2}{4k}\dot{\omega} e^{\omega - \rho/2},$$
$$p_{\lambda} = \frac{\partial \tilde{L}}{\partial \dot{\lambda}} = \frac{c^2}{4k}\dot{\lambda} e^{\omega - \rho/2},$$

and Hamiltonian

$$H = \frac{1}{2}\left[\left(c^2 p_\varphi{}^2 - \frac{4k}{c^2}\left(p_\omega{}^2 - p_\lambda{}^2\right)\right)e^{\frac{\rho}{2}-\omega}\right] - \frac{c^4}{2k}e^{\frac{\rho}{2}}.$$

Comparing the Hamiltonian with the constraint, it is easy to see that they are proportional

$$H = -2\frac{\partial\widetilde{L}}{\partial\rho}.$$

Hence, by virtue of Lagrangian constraint $\partial L / \partial\rho = 0$ it follow the Hamiltonian constraint

$$\frac{1}{2}c^2 p_\varphi{}^2 - \frac{2k}{c^2}\left(p_\omega{}^2 - p_\lambda{}^2\right)e^{\frac{\rho}{2}-\omega} - \frac{c^4}{2k}e^{\frac{\rho}{2}} = 0.$$

The latter is a consequence of the invariance of the theory with respect to gauge transformations $t = t(\widetilde{t})$ Next, substituting momenta

$$p_\varphi = \frac{\partial S}{\partial\varphi}, \qquad p_\lambda = \frac{\partial S}{\partial\lambda}, \qquad p_\omega = \frac{\partial S}{\partial\omega}$$

in the Hamiltonian constraint, we come to the Hamilton-Jacobi equation (HJE)

$$c^2\left(\frac{\partial S}{\partial\varphi}\right)^2 - \frac{4k}{c^2}\left(\frac{\partial S}{\partial\omega}\right)^2 + \frac{4k}{c^2}\left(\frac{\partial S}{\partial\lambda}\right)^2 = \frac{c^4}{k}e^{\omega}.$$

This equation is one-dimensional minisuperspace analogue of the Peres equation in the functional derivatives in a superspace. The variable $e^{\rho/2}$ is not included in the GJE and is not related with the minisuperspace dynamics. Thus, the 3-geometry minisuperspace with coordinates φ, $e^{\lambda}$, $e^{\omega}$ is defined by diffeomorphic invariant way. It is easy to see that this equation is the GJE for the geodesic in minisuperspace in terms minisupermetric (in a potential space). Indeed, let us rewrite the action for the diagonalized Lagrangian

$$\widetilde{S} = \int\left[\left(\frac{\dot{\varphi}^2}{2c^2} - \frac{c^3}{8k}\left(\dot{\omega}^2 - \dot{\lambda}^2\right)\right)e^{\omega-\rho/2} + \frac{c^4}{2k}e^{\rho/2}\right]dx^0.$$

Nondynamical variable can be eliminated. In order to do this we find the variable $e^{\rho/2}$ from the constraint equation

$$e^{\rho/2} = \frac{\sqrt{k}}{c^2}\sqrt{\frac{\dot{\varphi}^2}{c^2} - \frac{c^2}{4k}\left(\dot{\omega}^2 - \dot{\lambda}^2\right)}e^{\omega/2},$$

and substitute into the action. The result is

$$\widetilde{S} = \int\widetilde{L}dx^0 = \frac{c^2}{\sqrt{k}}\int e^{\omega/2}\sqrt{\frac{\dot{\varphi}^2}{c^2} - \frac{c^2}{4k}\left(\dot{\omega}^2 - \dot{\lambda}^2\right)}dx^0.$$

From here we have

$$\widetilde{S} = \frac{c^2}{\sqrt{k}}\int e^{\omega/2}\sqrt{\frac{d\varphi^2}{c^2} - \frac{c^2}{4k}\left(d\omega^2 - d\lambda^2\right)}.$$

It is easy to show that the equations resulting from the variational principle $\delta S = 0$ together with the constraint are equivalent to the Einstein equations for the original metric. Taking the differential from the action and placed in the square, we obtain the interval in a minisuperspace

$$d\widetilde{S} = \frac{c^2}{\sqrt{k}}e^{\omega/2}\sqrt{\frac{d\varphi^2}{c^2} - \frac{c^2}{4k}\left(d\omega^2 - d\lambda^2\right)},$$

$$d\widetilde{s}^2 = G_{ab}dq^a dq^b = \frac{c^4}{k}e^{\omega}\left[\frac{d\varphi^2}{c^2} - \frac{c^2}{4k}\left(d\omega^2 - d\lambda^2\right)\right].$$

**4. Solutions of the Hamilton-Jacobi equation**

We are searching the solution GJE in the form

$$S = a\lambda + b\varphi + V(\omega).$$

Then the function V(ω) is determined by the integral

$$V(\omega) = \int\sqrt{A^2 - e^{\omega}\varepsilon^2}\,d\omega,$$

where

$$A^2 = a^2 + \frac{c^4}{4k}b^2, \qquad \varepsilon^2 = \frac{c^6}{4k^2}.$$

Thus, we find for the action

$$S = a\lambda + b\varphi + \int\sqrt{A^2 - e^{\omega}\varepsilon^2}\,d\omega.$$

From the relations

$$\frac{\partial S}{\partial a} = \ln N, \qquad \frac{\partial S}{\partial b} = \varphi_0,$$

we find the connection between the scalar field φ and metric functions λ, $e^{\omega}$ In order to restore the time dependence, we use the equation

$$p_\omega = \frac{\partial L}{\partial\dot{\omega}} = \frac{\partial S}{\partial\omega}.$$

As a result, we obtain

$$-\frac{c^2}{4k}e^{\omega-\rho/2}\dot{\omega} = \sqrt{A^2 - e^{\omega}\varepsilon^2}.$$

Choosing the gauge condition

$$e^{\rho/2} = 1,$$

we find

$$\int\frac{e^{\omega}d\omega}{\sqrt{A^2 - e^{\omega}\varepsilon^2}} = -\frac{4k}{c^2}t.$$

Hence we obtain the equation

$$e^{\omega} = B^2 - c^2t^2.$$

Where

$$B^2 = \frac{k}{c^2}\left(\frac{4k}{c^4}a^2 + b^2\right).$$

Thus the metric takes the form

$$ds^2 = e^{-\lambda}\left(e^{\rho}c^2dt^2 - \left(B^2 - c^2t^2\right)d\sigma^2\right) - e^{\lambda}dr^2.$$

Furthermore, we find the remaining variables φ and λ, as function of time t. From the relations

$$\frac{\partial S}{\partial a} = \ln N, \qquad \frac{\partial S}{\partial b} = \varphi_0,$$

it follows that

$$\lambda + a\int \frac{d\omega}{\sqrt{A^2 - e^{\omega}\varepsilon^2}} = \ln N,$$

$$\varphi + \frac{c^4 b}{4k}\int \frac{d\omega}{\sqrt{A^2 - e^{\omega}\varepsilon^2}} = \varphi_0 .$$

Taking into account

$$e^{\omega} = B^2 - c^2 t^2, \qquad B^2 = \frac{k}{c^2}\left(\frac{4k}{c^4}a^2 + b^2\right),$$

$$A^2 = a^2 + \frac{c^4}{4k}b^2, \qquad \varepsilon^2 = \frac{c^6}{4k^2},$$

from here we find

$$e^{\lambda} = N\left|\frac{B+ct}{B-ct}\right|^p, \qquad p = \frac{2ak}{Bc^3},$$

$$\varphi = \varphi_0 + \frac{cb}{2B}\ln\left|\frac{B+ct}{B-ct}\right|,$$

where

$$B^2 = \frac{1}{c^6}\left(4k^2a^2 + kb^2c^4\right), \qquad \text{N=const.}$$

Thus, the metric and the scalar field inside the BH take the form

$$ds^2 = N^{-1}\left(\frac{B+ct}{B-ct}\right)^{-p}\left[c^2dt^2 - \left(B^2 - c^2t^2\right)d\sigma^2\right] -$$

$$- N\left(\frac{B+ct}{B-ct}\right)^{p} dr^2.$$

$$\varphi = \varphi_0 + \frac{cb}{2B}\ln\left|\frac{B+ct}{B-ct}\right|, \qquad -B < ct < B .$$

### 5. Determination constants

To find the constant, we can use the correspondence principle. When the scalar field vanishes, the resulting solution should be the same with the Schwarzschild solution in the T-region. Therefore, we put b= 0, $\varphi_0 = 0$. Then

$$B = \frac{2ka}{c^3}, \qquad \text{p=1.}$$

$$ds^2 = N^{-1}\left[\frac{2ka/c^3 + ct}{2ka/c^3 - ct}c^2dt^2 - \left(\frac{2ka}{c^3} - ct\right)^2 d\sigma^2\right] -$$

$$- N\frac{2ka/c^3 + ct}{2ka/c^3 - ct}dr^2.$$

After replacing

$$T = \frac{2ka}{c^4} - t,$$

we have

$$ds^2 = N^{-1}\left[\left(\frac{4ka}{c^4T} - 1\right)^{-1} c^2dT^2 - c^2T^2d\sigma^2\right] -$$

$$- N\left(\frac{4ka}{c^4T} - 1\right)dr^2.$$

This metric coincides with the Schwarzschild solution

$$ds^2 = \left(1 - \frac{2km}{c^2R}\right)c^2dt^2 - \left(1 - \frac{2km}{c^2R}\right)^{-1} dR^2 - R^2d\sigma^2$$

in the T-region, when we replace cT → R, r → ct and choice the constants N = 1, $a = mc/2$ . Thus, the solution can be written in the form

$$ds^2 = \left(\frac{B+ct}{B-ct}\right)^{-p}\left[c^2dt^2 - \left(B^2 - c^2t^2\right)d\sigma^2\right] -$$

$$- \left(\frac{B+ct}{B-ct}\right)^{p} dr^2,$$

$$\varphi = \varphi_0 + \frac{G}{2B}\ln\left|\frac{B+ct}{B-ct}\right|,$$

$$-B < ct < B, \qquad B = \frac{1}{c^2}\sqrt{k^2m^2 + kG^2},$$

$$p = \frac{km}{\sqrt{k^2m^2 + kG^2}},$$

where we introduced the scalar charge $G = cb$.

### 6. Conclusion

In the obtained solution about free scalar field, except the scalar charge, any other constants should not be. Therefore, we should put m = 0 and p= 0. Then we have

$$B = \frac{\sqrt{k}G}{c^2}.$$

In this case, the metric and scalar field take the form

$$ds^2 = c^2dt^2 - dr^2 - c^2\left(t_G^2 - t^2\right)d\sigma^2,$$

$$\varphi = \frac{c}{2\sqrt{k}}\ln\left|\frac{t_G + t}{t_G - t}\right|, \qquad -t_G < t < t_G .$$

where we have introduced the constant

$$t_G = \frac{B}{c} = \frac{\sqrt{k}G}{c^3}.$$

We take into account that at a maximum expansion (at the boundary of BH), when $t = t_G$, the scalar field vanishes, $\varphi_0 = 0$. This metric correspond the scalar field confinement under the horizon BH by the gravitational interaction.

Note that the spatial part of the metric describes a metric of hypercylinder $R^1 \otimes S^2$.

$$dl^2 = dr^2 + c^2\left(t_G^{\,2} - t^2\right)d\sigma^2 .$$

Here $R = c\sqrt{t_G^{\,2} - t^2}$ is the radius of hypercylinder, which when time changing within $-t_G < t < t_G$ first increases $0 < \mathrm{R} < \mathrm{c}\,t_G$, and then decreases $\mathrm{c}\,t_G > \mathrm{R} > 0$. At t= $t_G$ we have a singularity. The radius R = $t_G$ corresponds to the horizon in the Schwarzschild metric.

Note that this solution has an analogue in the R-region, which are considered by Denisova at al (1999). Their metrics can be rewritten as

$$ds^2 = c^2dt^2 - dR^2 - \left(R^2 - R_0^{\,2}\right)d\sigma^2 .$$

Where $R_0^{\,2} < R^2 < \infty$ .When $R^2 = R_0^{\,2}$ this metric has a naked singularity. This metric corresponds to a scalar field coupled gravitational interaction

$$\psi = \frac{c^2}{2\sqrt{k}}\ln\frac{R - R_0}{R + R_0},$$

and physically is not connected with the interior of a black hole with collapsing scalar field, because it is another solution.

Note that after replacing the time coordinate

$$T = \sqrt{t_G^{\,2} - t^2}\,, \qquad 0 < T < t_G\,,$$

the obtained metric inside a BH with a scalar field takes the form

$$ds^2 = \frac{c^2dT^2}{t_G^{\,2}/T - 1} - dr^2 - c^2T^2d\sigma^2 .$$

It turns out that scalar curvature $R^{\alpha}_{\beta\alpha\gamma}g^{\beta\gamma}$ and Krechman invariant $K = R_{\alpha\beta\alpha\gamma}R^{\alpha\beta\alpha\gamma}$ on the boundary $t = 0$ $(T = t_G)$ are the finite quantities, while in the center, when $t = t_G$ $(T = 0)$ they go to infinity. Since the boundary $t = 0$ $(T = t_G)$ is regular, therefore it can be matched with the external vacuum solution for the BH, i.e. with the Schwarzschild metric. From the matched condition of the angular parts of the metrics, we obtain the relation between the scalar charge *G*, collapsed scalar field, and the BH mass *M*:

$$G = 2M\sqrt{k}\,.$$

Note that the mass function

$$M = \frac{c^2}{2k}R\left(1 + \left(\nabla R\right)^2\right),$$

for the given solution takes the form

$$M = \frac{c^2}{2k}\frac{c^2t_G^{\,2}}{c\sqrt{t_G^{\,2} - t^2}}.$$

Hence, at the boundary value of time $t = 0$, we have

$$M(0) = \frac{c^2}{2k}ct_G = \frac{G}{2\sqrt{k}}.$$

This again confirms the connection the BH mass with the scalar charge into the BH. In the center of $t = t_G$ and mass function diverge.

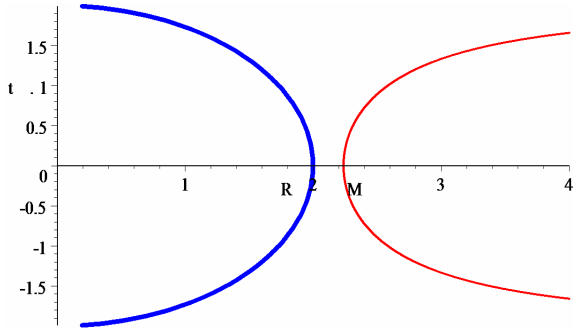


Figure 1: The behavior of the mass function and the hypercylinder radius in universe with homogeneous scalar field.

The behavior of the mass function and the hypercylinder radius represented on the figure 1.

Here, the ordinate represents time t, and abscissa is the radius of hypercylinder R and the mass function M. We see that when the time changes from $-t_G$ to $t_G = \sqrt{k}G/c^3 = 2kM/c^3$ the hypercylinder radius grows from zero, reaches the maximum is equal to $ct_G = \sqrt{k}G/c^2 = 2kM/c^2$ at $t = 0$ and then decreases again to zero. At the same time the mass function simultaneously decreases and reaches a minimum is equal of the mass $M(0) = c^3/2kt_G = G/2\sqrt{k} = M_{BH}$ external BH at $t = 0$ is and rises again to infinity.

Therefore, we obtained formulas describing the evolution of the homogeneous scalar field inside the BH. It corresponds to the final stage of the gravitational collapse some scalar field with such initial conditions that lead to the homogeneous distribution of the scalar field inside the BH.

**References**

Fisher I.Z.: 1948, *JETF*, **18**, 636.
Janis A.I, Newman E.T., Winicour J.: 1968, *Phys. Rev. Lett.* **20**, 878.
Wyman M.: 1981, *Phys. Rev. D*, **24**, 839.
Agnese A.G., La Camera M.: 1985, *Phys. Rev. D*, **31**, 1280.
Bronnikov K.A.: 1972, *Preprint ITF*-72-20P.
Zaitsev N.A., Kolesnikov S.M., Radynov A.G.: 1972, *Preprint ITF*-72-21P.
Korkina M.P.: 1976, *Preprint ITF*-76-93P.
Roberts M.D.: 1989, *GRG*, **21**, 907.
Brady P.R.: 1994, *Class. Quant. Grav.*, **11**, 1255.
Oshiro Y., Nakamura K., Tomimatsu A.: 1994, *Prog. Theor. Phys*. (arXiv: gr-qc/9402017).
Christodoulou D.: 1987, *Commun. Math. Phys*. **109**, 613.
Choptuik M.W.: 1993, *Phys. Rev. Letters* **70**, 9.
Novikov I.D, Frolov V.P.: 2001, *UFN*, **171**, 307.
Chase J.E.: 1970, *Commun. Math. Phys*., **19**, 276.
Bekenstein J.D.: 1972, *Phys. Rev. Letters*, **28**, 452; 1972, *Phys. Rev. D,* **5**, 1239 and 2403.
Denisova I.P., Mehta B.V., Zubrilo A.A.: 1999, *GRG*, **31**, 821.

# FIVE DIMENSIONAL BOOSTS AND ELECTROMAGNETIC FIELD IN KALUZA-KLEIN THEORY

V.D. Gladush[1], Nadim Al-Shawaf[2]

[1] Dnipropetrovsk National University, Gagarin Ave, 725014, Ukraine, *vgladush@gmail.com*
[2] Uppsala University, Sweden, *tms2006@gmail.com*

ABSTRACT. A stationary, spherically symmetric, 5D Kaluza-Klein theory exhibits 5D boosts. After reduction of 5D vacuum Einstein action of a diagonal 5D metric, we obtained Einstein equations with energy-momentum tensor of a massless scalar field. Applying a 5D boost generates a non-diagonal metric with an electric field. This electric field is trivial, since it can be removed by a reverse 5D boost. Existence of such kind of trivial fields is analyzed on the example previously known solutions. Transformation properties of physical fields relative to 5D boosts examined. This symmetry is a subgroup of $SL(3,R)$ symmetries of 5D equations, rewritten in $3+2$-decomposition in stationary, spherically symmetric case. This symmetry also can be used to generate new solutions. The solution with trivial electric field is obtained from diagonal 5D metric by a simple symmetry transformation, which reduces to the coordinate 5D boosts.

**Keywords**: Kaluza-Klein theory, decomposition, electric field, symmetry.

## 1. Introduction

In a framework of the usual 5D Kaluza-Klein theory (KK), we consider $M^5$ space with the following 5D metric:

$$ {}^{(5)}ds^2 = {}^{(5)}g_{AB}dx^A dx^B, \qquad (1) $$

where $\{A, B = 0,1,2,3,4\} = \{\mu,\nu = 0,1,2,3\} \cup \{4\}$, $x^\mu$ –are space-time coordinates, $x^4 = z$ – fifth coordinate.

As it is known, KK theory is based on two postulates:

1. Cylindrical condition, according to which, the space $M^5$ admits a space-like Killing vector $\vec{\xi}$. In the corresponding coordinate system it has the form $\vec{\xi} = \partial/\partial z$, that leads to metric's independence of the fifth coordinate $z$, that is ${}^{(5)}g_{AB} = {}^{(5)}g_{AB}(x^\mu)$.

2. Closure condition, which states that the space $M^5$ is closed relative to coordinate $z$.

Four dimensional physical space can be derived by dimensional reduction of $M^5$ space, and it's corresponding action. This can be accomplished by orthogonal $4+1$ splitting of $M^5$ space, and then projecting all quantities on the physical space-time $M^4$. In result we get the following form of the 5D metric:

$$ \begin{aligned} {}^{(5)}ds^2 &= {}^{(5)}g_{\mu\nu}dx^\mu dx^\nu + 2{}^{(5)}g_{\mu 4}dx^\mu dx^4 + {}^{(5)}g_{44}dz^2 \\ &= V^{-1}h_{\mu\nu}dx^\mu dx^\nu - V^2\left(dz + A_\mu dx^\mu\right)^2, \end{aligned} \qquad (2) $$

where:

$$ {}^{(5)}g_{\mu\nu} = V^{-1}h_{\mu\nu} - V^2 A_\mu A_\nu\,, \qquad (3) $$

$$ {}^{(5)}g_{4\nu} = -V^2 A_\nu, \quad {}^{(5)}g_{44} = -V^2\,. \qquad (4) $$

This splitting leads to the following physical space-time metric:

$$ h_{\mu\nu} = {}^{(5)}g_{\mu\nu} - \frac{{}^{(5)}g_{4\nu}\,{}^{(5)}g_{4\mu}}{{}^{(5)}g_{44}}\,, \qquad (5) $$

and the following electromagnetic field:

$$ A_\nu = \frac{{}^{(5)}g_{4\nu}}{{}^{(5)}g_{44}}\,, \qquad (6) $$

while the scalar field is:

$$ V^2 = -\left(\vec{\xi},\vec{\xi}\right) = -{}^{(5)}g_{44}\,. \qquad (7) $$

After orthogonalization of the 5D action

$$ S = -\frac{1}{4\pi L}\int d^5x\sqrt{{}^{(5)}g}\;\;{}^{(5)}R \qquad (8) $$

we extract a full derivative, and then integrating by the periodic coordinate $z$ we get:

$$ \begin{aligned} S &= -\frac{1}{4\pi L}\int d^4x\sqrt{h}\,\left\{{}^{(4)}R - \frac{1}{2}\frac{(\nabla V)^2}{V^2} + \right. \\ &+ \left. \frac{V^3}{4}F_{\mu\nu}F^{\mu\nu}\right\}. \end{aligned} \qquad (9) $$

Using the following natural variable substitution:

$$ V = e^{\varphi/\sqrt{3}} \qquad (10) $$

we get the following 5D metric:

$$\begin{aligned} {}^{(5)}ds^2 &= e^{-\varphi/\sqrt{3}} h_{\mu\nu} dx^\mu dx^\nu - \\ &- e^{2\varphi/\sqrt{3}} \left(dz + A_\mu dx^\mu\right)^2 \end{aligned} \tag{11}$$

and following 4D action of Einstein's form:

$$\begin{aligned} S &= -\frac{1}{4\pi L} \int d^4x \sqrt{h} \left\{ {}^{(4)}R - \frac{1}{2} \left(\nabla\varphi\right)^2 + \right. \\ &+ \left. \frac{1}{4} e^{\sqrt{3}\varphi} F_{\mu\nu} F^{\mu\nu} \right\} . \end{aligned} \tag{12}$$

where $F_{\mu\nu} = A_{\nu,\mu} - A_{\mu,\nu}$ is an electromagnetic tensor, $\varphi$ is a massless scalar field.

In summary, 5D variational principle for 5D manifold with a metric that subject to cylindrical and closure conditions, is equivalent to a 4D variation principle of a system with an interacting scalar, electromagnetic and gravitational fields, and above mentioned action.

## 2. Stationary space of 5D theory and boosts

Suppose that on $M^5$ space, in addition to the space-like Killing vector $\vec{\xi}_4$, there is also a time-like Killing vector $\vec{\xi}_0 = \partial/\partial x^0$ orthogonal to space directions. Thus we have

$$ortgonal \vec{\xi}_a = \frac{\partial}{\partial x^a} \qquad (a = 0, 4). \tag{13}$$

Those two vectors induce a "2+3 splitting" of $M^5$ space, and the metric becomes:

$$\begin{aligned} {}^{(5)}ds^2 &= {}^{(2)}ds^2 + {}^{(3)}ds^2 \\ &= \gamma_{ab}\left(x^k\right) dx^a dx^b - h_{ij}\left(x^k\right) dx^i dx^j , \end{aligned} \tag{14}$$

where $\{a, b = 0, 4\}$ and $\{i, j, k = 1, 2, 3\}$. The Killing vector $\vec{\xi}_a$ is subject to the transformations:

$$\vec{\eta}_{\tilde{a}} = L^b_{\tilde{a}} \vec{\xi}_b = L^b_{\tilde{a}} \frac{\partial}{\partial x^{\tilde{b}}} = \frac{\partial}{\partial x^{\tilde{a}}} , \tag{15}$$

where $\vec{\eta}_{\tilde{a}}$ – new Killing vectors, $L^b_{\tilde{a}}$ – a constant invertible matrix. Herewith, this "2+3 splitting" of the metric (14) is form invariant. This transformation, can be also induced by the following linear coordinate transformation $\{x^0, x^4\} = \{x^a\}$ :

$$\begin{gathered} \tilde{x}^{\tilde{a}} = L^{\tilde{a}}_b x^b , \quad L^b_{\tilde{a}} L^{\tilde{a}}_c = \delta^b_c , \\ \det \left\| L^b_a \right\| = L^0_0 L^4_4 - L^0_4 L^4_0 = \pm 1 . \end{gathered}$$

In this text we will use only the positive sign. This transformations keeps the interval ${}^{(2)}ds^3$ structure unchanged. While the 2D metric $\gamma_{ab}(x^k)$ transforms according to:

$$\tilde{\gamma}_{\tilde{a}\tilde{b}}\left(\tilde{x}^k\right) = L^b_{\tilde{a}} L^b_{\tilde{b}} \gamma_{ab}\left(x^k\right) .$$

Let the metrics $\tilde{\gamma}_{\tilde{a}\tilde{b}}\left(\tilde{x}^k\right)$ and $\gamma_{ab}\left(x^k\right)$ are asymptotically flat, i.e. in spatial infinity our metric metric is pseudo-euclidean:

$$\lim_{r\to\infty} \gamma_{ab}\left(x^k\right) = \eta_{ab}, \ \lim_{r\to\infty} \tilde{\gamma}_{\tilde{a}\tilde{b}}\left(\tilde{x}^k\right) = \eta_{\tilde{a}\tilde{b}} ,$$

where $\eta_{ab}$ – is 2D Minkowski tensor. Then:

$$\begin{aligned} \eta_{\tilde{a}\tilde{b}} &= \lim_{r\to\infty} \tilde{\gamma}_{\tilde{a}\tilde{b}}\left(\tilde{x}^k\right) = \lim_{r\to\infty} L^a_{\tilde{a}} L^b_{\tilde{b}} \gamma_{ab}\left(x^k\right) \\ &= L^a_{\tilde{a}} L^b_{\tilde{b}} \lim_{r\to\infty} \gamma_{ab}\left(x^k\right) = L^a_{\tilde{a}} L^b_{\tilde{b}} \eta_{ab} . \end{aligned}$$

Thus, those transformations, at infinity approaches 2D Lorentz transformations, or 5D boosts in $\{x^a\} = \left\{x^0 = t,\ x^4 = z\right\}$ coordinates, with a property:

$$L^a_{\tilde{a}} L^b_{\tilde{b}} \eta_{ab} = \eta_{\tilde{a}\tilde{b}} . \tag{16}$$

In consequence, we have 2D Lorentz transformations:

$$\begin{aligned} x^0 &= \frac{\tilde{x}^0 + v\tilde{x}^4/c}{\sqrt{1 - V^2/c^2}} = \tilde{x}^0 \cosh\alpha + \tilde{x}^4 \sinh\alpha , \\ x^4 &= \frac{\tilde{x}^4 + v\tilde{x}^0/c}{\sqrt{1 - V^2/c^2}} = \tilde{x}^0 \sinh\alpha + \tilde{x}^4 \cosh\alpha , \end{aligned}$$

where:

$$\tanh\alpha = \frac{v}{c} ,$$

Herewith, the physical quantities transforms as:

$$\tilde{h}_{\tilde{0}\tilde{0}} = -\frac{\det\gamma_{ab}}{\sqrt{-V^{-1}h_{00}\sinh^2\alpha + V^2\left(A_0\sinh\alpha + \cosh\alpha\right)^2}} ;$$

$$\tilde{A}_{\tilde{0}} = \frac{\left(V^{-3}h_{00} - A_0^2 - 1\right)\tanh\alpha - A_0\left(1 + \tanh^2\alpha\right)}{V^{-3}h_{00}\tanh^2\alpha - \left(A_0\tanh\alpha + 1\right)^2} ;$$

$$\tilde{V}^2 = -V^{-1}h_{00}\sinh^2\alpha + V^2\left(A_0\sinh\alpha + \cosh\alpha\right)^2 .$$

Note that the metric' determinant

$$\det\gamma_{ab} = \gamma_{00}\gamma_{44} - \left(\gamma_{04}\right)^2 = -\frac{h_{00}}{V} = inv \tag{17}$$

actually an invariant.

Those transformations, physically corresponds to using a moving frame of reference of the fifth coordinate $\tilde{x}^4$, which according to the Kaluza-Klein postulates, is closed.

Let our initial metric be diagonal, this will correspond to that there is no electromagnetic field. Owing to 5D boosts, and bearing in mind that $\gamma_{04} = 0$, and $A_0 = \gamma_{04}/\gamma_{44} = 0$ we get:

$$\tilde{h}_{\tilde{0}\tilde{0}} = \frac{-Vh_{00}}{\sqrt{V^2\cosh^2\alpha - V^{-1}h_{00}\sinh^2\alpha}} , \tag{18}$$

$$\tilde{A}_{\tilde{0}} = \frac{\left(V^{-1}h_{00} - V^2\right)\tanh\alpha}{V^{-1}h_{00}\tanh^2\alpha - V^2} , \tag{19}$$

$$\tilde{V}^2 = V^2\cosh^2\alpha - V^{-1}h_{00}\sinh^2\alpha . \tag{20}$$

So we see that after 5D Lorentz transformations, the metric becomes non-diagonal. In 4D physical spacetime it will correspond the appearance of the electromagnetic field. This means that we actually generating electromagnetic field with its corespondent effective electric charge. This electric field corresponds to a global 5D boost, so we call it trivial field, due to the fact that applying backward 5D boost (by coordinate transformation $\tilde{x}^{\tilde{a}} = L^{\tilde{a}}_{b} x^{b}$) this field can be removed (a removable electric charge).

To find the condition under which this electromagnetic field can be removed, we consider the transformation of the metric ${}^{(2)}ds^2$ by the 2D boost $x^b = L^b_{\tilde{a}} \tilde{x}^{\tilde{a}}$ :

$$\tilde{\gamma}_{\tilde{a}\tilde{b}}\left(\tilde{x}^{k}\right) = L^{a}_{\tilde{a}} L^{b}_{\tilde{b}} \gamma_{ab}\left(x^{k}\right), \quad (21)$$

$$\det\left(\tilde{\gamma}_{\tilde{a}\tilde{b}}\right) = \det\gamma_{ab} = inv\,. \quad (22)$$

From this we have:

$$\tilde{\gamma}_{\tilde{0}\tilde{0}} = \gamma_{00}\cosh^2\alpha + \gamma_{04}\sinh 2\alpha + \gamma_{44}\sinh^2\alpha \quad (23)$$

$$\tilde{\gamma}_{\tilde{0}\tilde{4}} = \frac{1}{2}\left(\gamma_{00}+\gamma_{44}\right)\sinh 2\alpha + \gamma_{04}\cosh 2\alpha\,, \quad (24)$$

$$\tilde{\gamma}_{\tilde{4}\tilde{4}} = \gamma_{00}\sinh^2\alpha + \gamma_{04}\sinh 2\alpha + \gamma_{44}\cosh^2\alpha \quad (25)$$

The requirement $\tilde{\gamma}_{\tilde{0}\tilde{4}} = 0$ leads us to the needed condition for 5D metric to be diagonalizable:

$$\frac{\gamma_{04}\left(x^{k}\right)}{\gamma_{00}\left(x^{k}\right)+\gamma_{44}\left(x^{k}\right)} = -\frac{1}{2}\tanh 2\alpha = const\,. \quad (26)$$

In terms of physical quantities, this conditions takes the form:

$$\frac{V^{-3}h_{00} - A_0^2 - 1}{A_0} = \coth\alpha + \tanh\alpha = const\,. \quad (27)$$

While the rest of the metric components will transform as:

$$\tilde{\gamma}_{\tilde{0}\tilde{0}} = \frac{\gamma_{00}\cosh^2\alpha - \gamma_{44}\sinh^2\alpha}{\cosh 2\alpha}\,, \quad (28)$$

$$\tilde{\gamma}_{\tilde{4}\tilde{4}} = \frac{\gamma_{44}\cosh^2\alpha - \gamma_{00}\sinh^2\alpha}{\cosh 2\alpha}\,. \quad (29)$$

Analyzing the conditions that will keep fifth coordinate space-like (i.e. conserve metric signature) when electric field is generated, with a consideration of the initial values $\gamma_{04} = 0$, and $A_0 = \gamma_{04}/\gamma_{44} = 0$, we have:

$$\tilde{V}^2 = V^2\cosh^2\alpha - V^{-1}h_{00}\sinh^2\alpha \geq 0$$

$$\frac{v^2}{c^2} = \tanh^2\alpha \leq \frac{V^3}{h_{00}} = \frac{\left(\gamma_{44}\right)^2}{-\det\gamma_{ab}} = \frac{-\gamma_{44}}{\gamma_{00}}\,.$$

Thus, the allowed global boosts is when the coordinate velocity not larger than:

$$v \leq c\sqrt{-\frac{\gamma_{44}}{\gamma_{00}}}\,. \quad (30)$$

For asymptotically flat space, we conclude the expected result of $v \leq c$. With higher speeds, horizons are formed, and the meaning of fifth coordinate does change.

## 3. Examples of a removable and unremovable electric charge

### *3.1. A removable electric charge*

In Chodos and Detweiler (1982) work, they obtained the following solution:

$${}^{(5)}ds^2 = -e^{\mu}dt^2 + 2\tilde{A}dtdx + \varphi^2 dx^2 + \\ +e^{\beta}\left[dr^2 + r^2 d\sigma^2\right] \quad (31)$$

$$= {}^{(4)}ds^2 + \varphi^2\left(dx + Adt\right)^2\,,$$

$${}^{(4)}ds^2 = -e^{\nu}dt^2 + e^{\beta}\left[dr^2 + r^2 d\sigma^2\right] \quad (32)$$

$$A = \frac{\tilde{A}}{\varphi^2},\ \ e^{\nu} = e^{\mu} + \frac{\tilde{A}^2}{\varphi^2} \quad (33)$$

where

$$\varphi^2 = a_1\psi^{p_1} + a_2\psi^{p_2},\ \ \psi = \left(\frac{r-B}{r+B}\right)^{\lambda/2B}, \quad (34)$$

$$e^{\nu} = e^{\beta}e^{\mu} + \frac{\tilde{A}}{\varphi^2} = \frac{\psi^2}{\varphi^2}\,, \quad (35)$$

$$e^{\beta} = \left(1 - \frac{B^2}{r^2}\right)^2 \frac{1}{\psi^2}\,, \quad (36)$$

$$\tilde{A} = \sqrt{-a_1 a_2}\left(\psi^{p_1} - \psi^{p_2}\right)\,, \quad (37)$$

$$e^{\mu} = a_2\psi^{p_1} + a_1\psi^{p_2}\,, \quad (38)$$

$$A = \frac{\tilde{A}}{\varphi^2} = \frac{\sqrt{-a_1 a_2}\left(\psi^{p_1} - \psi^{p_2}\right)}{a_1\psi^{p_1} + a_2\psi^{p_2}}\,, \quad (39)$$

$$E \equiv F_{rt}e^{-\nu/2} = \frac{Q}{r^2\varphi^3}e^{-\beta/2}\,, \quad (40)$$

$$p_{1,2} = 1 \pm \sqrt{1+\kappa},\ \kappa = 4\left(\frac{4B^2}{\lambda^2} - 1\right), \quad (41)$$

$$Q^2 = -a_1 a_2\left(1+\kappa\right)\frac{\lambda^2}{G}\,, \quad a_1 + a_2 = 1\,, \quad (42)$$

where $a_1$, $a_2$, $p_1$, $p_2$, $\lambda$, and $B$– constants.

We rewrite this metric in the form:

$${}^{(5)}ds^2 = -\left(a_2\psi^{p_1} + a_1\psi^{p_2}\right)dt^2 + \\ +2\left(\sqrt{-a_1 a_2}\left(\psi^{p_1} - \psi^{p_2}\right)\right)dtdx + \\ +\left(a_1\psi^{p_1} + a_2\psi^{p_2}\right)dx^2 + e^{\beta}\left[dr^2 + r^2 d\sigma^2\right]$$

or:

$${}^{(5)}ds^2 = -\psi^{p_2}\left(\sqrt{a_1}dt + \sqrt{-a_2}dx\right)^2 + \\ +\psi^{p_1}\left(\sqrt{-a_2}dt + \sqrt{a_1}dx^2\right)^2 + \\ e^{\beta}\left[dr^2 + r^2 d\sigma^2\right]\,. \quad (43)$$

Now we see that the transformation:

$$T = \sqrt{a_1}t + \sqrt{-a_2}x\,, \quad (44)$$
$$X = \sqrt{-a_2}t + \sqrt{a_1}x \quad (45)$$

will give us the diagonal form of the metric:

$$-{}^{(5)}ds^2 = \psi^{p_2}dT^2 - \psi^{p_1}dX^2 - e^{\beta}\left[dr^2 + r^2 d\sigma^2\right], \quad (46)$$

So we have here an example of the removable electric field (charge).

In their work, authors claims that this is a general spherically symmetric solution of KK theory. However, in a general solution, there should be 4 independent parameters, more precisely: $m$– mass, $q$– electromagnetic charge, $g$– scalar charge, $v$– boost parameter. But here we have actually only three parameter: $m$, $g$, $v$, moreover, electromagnetic charge is actually some function of the rest of parameters, $q = q(v, m, g)$. So for the obtained electric field is an open question about the sense of the thus obtained electric field and charge

Frolov et al. (1987) carried out a formal embedding of the Kerr metric in the flat space $M^5$, and then applied a boost. By this procedure they obtaining electromagnetic field, and even the scalar field. Of course, those are trivial fields, that can be removed by another global boost. Note that those authors reference to works of Gibbons (1982), Gibbons and Wiltshire (1985), where this method been developed.

We note also the work Vladimirov and Popov (1982), which uses a similar method of generating an electric field.

Apart from the question of the interpretation of this removable electric field, there are still problems related to the relationship between the the closure condition space 5D and 5D boost. In addition to that, it is appropriate to ask if there are solutions where electromagnetic field $A_0$ is unremovable by this procedure, and with an independent charge parameter $q$.

### *3.2. Unremovable Electric Charge*

In work Gladush (1980), there is a solution of spherically-symmetric configuration of interacting scalar, electromagnetic and gravitational fields of 5D KK theory, with the following reduced metric and Lagrangian:

$$\Lambda = -\frac{1}{4\pi}\left[\frac{c^4}{4\kappa}{}^{(4)}R - \frac{1}{2}\left(\nabla\psi\right)^2 + \right.$$
$$\left. + \frac{1}{4}F_{\mu\nu}F^{\mu\nu}e^{\psi\sqrt{6}}\right], \quad (47)$$

$${}^{(5)}ds^2 = \frac{1}{2}e^{-\psi\sqrt{2/3}}{}^{(4)}ds^2 - e^{2\psi\sqrt{2/3}}\left(dz + fdt\right)^2\,, \quad (48)$$

where 4D metric is:

$${}^{(4)}ds^2 = e^{\nu}dt^2 - e^{-\nu}\left[dr^2 + \left(r^2 - a^2\right)d\sigma^2\right] \quad (49)$$

while the gravitational potential, scalar field, and electric field are:

$$e^{\nu} = u^{G\sqrt{3\kappa}/2a}\left[\frac{A+1}{2}u^{-p} - \frac{A-1}{2}u^{p}\right]^{-1/2} \quad (50)$$

$$\psi = -\frac{1}{4}\ln\left[u^{\frac{G}{a}}\left(\frac{A+1}{2u^p} - \frac{A-1}{2u^{-p}}\right)^{\sqrt{\frac{3}{\kappa}}}\right] \quad (51)$$

$$f = \frac{q}{2p}\frac{1-u^{2p}}{A+1-(A-1)\,u^{2p}}\,, \quad (52)$$

$$u = \frac{r-a}{r+a}\,, \quad p = \frac{\sqrt{\kappa^2m^2 - \kappa q^2}}{a}\,, \quad (53)$$

$$A = \frac{\pm\kappa m}{\sqrt{\kappa^2m^2 - \kappa q^2}}\,, \quad (54)$$

$$a^2 = \kappa^2m^2 - \kappa q^2 + \kappa G^2\,, \quad \kappa^2m^2 - \kappa q^2 > 0 \quad (55)$$

Here, we have three independent parameters $\{m,\, q,\, G\}$, and the forth parameter $v$ can be included by applying some boost. There is no global transformation with constant coefficients, that can be used to remove the electromagnetic field, thus this field is unremovable.

In the work of Bronikov and Shikin (1977) a similar problem is solved for a system of interacting scalar, electromagnetic and gravitational fields, and with an action similar to above mentioned. But the field was interpreted not in the context of 5D theory. Also they used harmonic time gauge for the metric. However if we analyze it in the context of 5D theory, one finds that the electric field here as well is unremovable.

## 4. A symmetrical approach for constructing new solutions of 5D KK theory

For stationary spaces, in KK theory there is a method of constructing solutions by using internal symmetries of KK equations. This method has been developed in the papers of Maison Kramer and Neugebauer (1969), Maison (1979), Dobiasch and Maison (1982), Clement (1986), Cvetic and Youm (1995) and others.

The stationary metric(14) 5D KK theory in 2+3 splitting: be rewritten as:

$$ds^2 = \gamma_{ab}\left(x^k\right)dx^a dx^b - \frac{\tilde{h}_{ij}}{\tau}\left(x^k\right)dx^i dx^j\,, \quad (56)$$
$$\tau = \left|\det\left\|\gamma_{ab}\right\|\right|\,. \quad (57)$$

Then the 5D lagrangian for vacuum 5D space of KK theory is:

$$L = \sqrt{{}^{(5)}g}{}^{(5)}R\,,$$

by omitting the divergence, it can be rewritten as Lagrangian for the 4D space

$$L = \sqrt{\tilde{h}}\left\{ {}^{(3)}R - \frac{1}{4}\left[\gamma^{ab}\gamma^{cd}\gamma_{ac,k}\gamma^{,k}_{bd,l} + \gamma^2\left(\tau^{-1}\right)_{,k}\left(\tau^{-1}\right)_{,l}\right]\tilde{h}^{kl}\right\} . \quad (58)$$

Furthermore, we introduce a symmetrical unimodular matrix $3 \times 3$:

$$\chi = \begin{pmatrix} \gamma_{ab} & 0 \\ 0 & \tau^{-1} \end{pmatrix} , \quad (59)$$

such that $\det\chi = 1$ . Then the Lagrangian can be rewritten as ($\sigma$-model):

$$L = \sqrt{\tilde{h}}\left\{ {}^{(3)}R - \frac{1}{4}Sp\left(\gamma^{-1}\gamma_{,k}\gamma^{-1}\gamma^{,k}\right)\right\} . \quad (60)$$

From this we get the following equations:

$$\left(\chi^{-1}\chi^{,k}\right)_{;k} = 0 , \quad (61)$$

$${}^{(3)}R_{ij} = \frac{1}{4}Sp\left(\chi^{-1}\chi_{,i}\chi^{-1}\chi_{,j}\right) . \quad (62)$$

This system is invariant under group $SL(3,R)$ transformations of 3D matrices:

$$\chi \longrightarrow N\chi N^T , \quad N \in SL(3,R) . \quad (63)$$

To force this metric $\gamma_{ab}$ be asymptotically flat space, we should have at infinity:

$$\chi = \begin{pmatrix} 1 & & \\ & -1 & \\ & & -1 \end{pmatrix} . \quad (64)$$

Only the subgroup $SO(1,2)$ of the group $SL(3,R)$ can satisfy this property. Now we can generate new solutions by applying some transformation of the group SO(1,2) to a known solution. For the class of metrics under our consideration, we only need the transformations $\widetilde{SO}(1,2) \subset SO(1,2)$, which can conserve the block structure of the matrix $\chi$.

We see that the analyzed Lorentz transformation $L(2) = O(1,1)$ is actually a subgroup of $\widetilde{SO}(1,2)$ $\tilde{x}^{\tilde{a}} = L^{\tilde{a}}_b x^b$. So we have:

$$O(1,1) \subset \widetilde{SO}(1,2) \subset SO(1,2) \subset SL(3,R) .$$

While the transformed matrix $\chi$ has the structure:

$$N = \begin{pmatrix} L^{\tilde{a}}_b & 0 \\ 0 & 1 \end{pmatrix} , \quad (65)$$

where $L^{\tilde{a}}_b$ are the 2D boosts matrix, that reduces to the Lorentz coordinate transformations. The set of solutions that can be obtained by this method is not very big. The group $O(1,1)$ that induced by coordinate transformation can give us solutions only with trivial electric field. Hence we see the place of coordinate transformations that generate the trivial electric fields, among the entire set of transformations SO(1,2), which in the general case generate a nontrivial field.

We also see that the physically significant transformations $\widetilde{SO}(1,2)$ – are a map of one KK space (solution) to another one, that can not be reduced to simple coordinate transformations.

## 5. Conclusion

We observed that a phenomenon of generating an electric field can be interpreted as 5D rotation. In general, electric field is a result of local 5D rotations of 5D manifold (i.e. existence of local inertial 5D reference frames), that defined by additional local dynamical degrees of freedom. The corresponding integral of motion gives the conserved charge, as an independent parameter, This is the case of non trivial unremovable electrical field (charge).

## References


Chodos A., Detweiler S.: 1982, *GRG,* **14**, 879.

Frolov V., Zelnikov I, Bleyer U.: 1987, *Annalen der Physik,* **7**, 371.

Gibbons G.: 1982, *Nucl. Phys.,* **B207**, 337.

Gibbons G., Wiltshire D.: 1985, *University of Cambridge preprint.*

Vladimirov Yu. S., Popov A.D.: 1982, *Problems in Gravitation Theory and Particle Theory.* Atomizdat, Moscow, **13**, 66.

Gladush V.D.: 1980, *Izv. Vuzov, Fiz.,* **3**, 74.

Bronikov K., Shikin G.: 1977, *Izv. Vuzov, Fiz.,* **9**, 25.

Kramer Von D., Neugebauer G.: 1969, *Annalen der Physik,* **1-2**, 479.

Maison D.: 1979, *GRG,* **10**, 717.

Dobiasch P., Maison D.: 1982, *GRG,* **14**, 231.

Clement G.: 1986, *GRG,* **18**, 861.

Cvetic M., Youm D.: 1995, arXiv:hep-th/9503082.

# STABILITY OF STELLAR SYSTEMS ORBITING SGR A*

Magd E. Kahil

October University for Modern Sciences and Arts (MSA),
October City, Giza, Egypt,
Egyptian Relativity Group (ERG)
*mkahil@msa.eun.eg*

ABSTRACT. Path equations of different orbiting objects in the presence of very strong gravitational fields are essential to examine the impact of its gravitational effect on the stability of each system. Implementing an analogous method, used to examine the stability of planetary systems by solving the geodesic deviation equations to obtain a finite value of the magnitude of its corresponding deviation vectors. Thus, in order to know whether a system is stable or not, the solution of corresponding deviation equations may give an indication about the status of the stability for orbiting systems.Accordingly, two questions must be addressed based on the status of stability of stellar objects orbiting super-massive black holes in the galactic center.
1. Would the deviation equations play the same relevant role of orbiting planetary systems for massive spinning objects such as neutron stars or black holes?
2. What type of field theory which describes such a strong gravitational field?

**Keywords**: Stellar systems: Stability – Galaxy: SgrA* – Strong fields: bi-metric theory – Path and Path deviation equations: Orbiting particles.

## 1. Introduction

The problem of stability in our study is centered only on examining the stability of orbits in a very strong gravitational fields. In our Galaxy, S-stars are counted to be good candidates, to explain such a phenomenon. S-Stars are of spectral class B, that have been traced near infrared. The characteristic behavior of these stars as they are very fast orbital motions around the Galactic Center, with orbital periods more than 16 years, high eccentricities $e > 0.2$, and their distances from the Galactic Center is between $10^0 - 10^2 mpc$ (Han, 2014), which is greater than the center's radius $r >> r_g$ where $r_g$ its Schwarzschild radius. Also, a stringent condition is taken based on $\frac{m}{M} < 10^{-5}$, where $m$ and $M$ are masses of stellar object and center of SgrA* respectively (Iorio, 2011). One of most brightest member of this group is S2, which takes about 16 years to revolve about the center of Galaxy with a radial speed $10,000 km/sec$ and its mass is about $15 m_{sun}$ (Meyer et al., 2012). Recently, another type of stars S0-102 with lesser brightness and shorter period about 11.5 years. Unlike, the orbits of satellites, planets or pulsars in the galactic center the orbital periods are much longer leading to the relativistic effects increase more steeply with small radius and very high velocities than classical effects leading to the involvement of relativity is strongly appear around the peri-center passage. Accordingly, S-stars can be counted as clocks in orbit around a black hole moving on geodesics (Angelil et al., 2014). Any slight effective perturbation on these trajectories can be obtained by obtaining its corresponding geodesic deviation equations.

In general the problem of stability is not only related to geodesic deviation equations, but to path deviation equations of spinning object for a point mass particle (Mohseni, 2010), which can also be extended to be charged and spinning charged objects. However, a slight problem can be emerged which is the solution of these deviation equations are completely affected by a coordinate system. Yet, Wanas and Bakry (2008) developed an approach based on determining a scalar value of the geodesic deviation capable for detecting the status of stability of any a certain planetary system in the presence of weak gravitational fields (Wanas & Bakry, 2008).

In the present work, we are going to examine stability conditions in the presence of a strong gravitational field, using Verozub's version of bi-metric theory of gravity, which is one of the most appealing theories (Verozub, 2015).

## 2. Equations of motion for orbiting objects

It is well known that from observational methods, to confirm that both planetary and stellar objects are exhibiting two types of motion revolving and spinning to become stable in their orbits. From this perspective, it is important to study stability of these systems by causing a slight perturbation that affects these com-

bined motion and checks whether the object remains in the orbit or lose it forever. Such a technique is required to solve the path deviation equations of these objects. Accordingly, it is vital to obtain these equations from perturbing the original path equation. In case of planets/stellar objects, several authors have recommended Mathisson-Papapetrou- Dixon equations (MPD) to be most reliable set of equation for describing such a situation (Dixon, 1970).

$$\frac{DP^{\mu}}{DS} = F^{\mu}, \tag{1}$$

$$\frac{DS^{\mu\nu}}{DS} = M^{\mu\nu}, \tag{2}$$

where $P^{\mu}$ is the momentum vector, $F^{\mu} = \frac{1}{2}R^{\mu}_{\nu\rho\delta}S^{\rho\delta}U^{\nu}$, $R^{\alpha}_{\beta\rho\sigma}$ is the Riemann curvature, $\frac{D}{Ds}$ is the covariant derivative with respect to a parameter $S$,$S^{\alpha\beta}$ is the spin tensor, and $M^{\mu\nu} = P^{\mu}U^{\nu} - P^{\nu}U^{\mu}$ such that $U^{\alpha} = \frac{dx^{\alpha}}{ds}$ is the unit tangent vector to the geodesic.
Using the following identity on both equations (1) and (2)

$$A^{\mu}_{;\nu\rho} - A^{\mu}_{;\rho\nu} = R^{\mu}_{\beta\nu\rho}A^{\beta}, \tag{3}$$

such that $A^{\mu}$ is an arbitrary vector. Multiplying both sides with vectors, $U^{\rho}$ and $\Psi^{\nu}$ as well as using the following condition (Heydri-Fard et al., 2005)

$$U^{\alpha}_{;\rho}\Psi^{\rho} = \Psi^{\alpha}_{;\rho}U^{\rho}, \tag{4}$$

and $\Psi^{\alpha}$ is its deviation vector associated to the unit vector tangent $U^{\alpha}$. Also in a similar way:

$$S^{\alpha\beta}_{;\rho}\Psi^{\rho} = \Phi^{\alpha\beta}_{;\rho}U^{\rho},$$

one obtains the corresponding deviation equations (Mohseni, 2010)

$$\frac{D\Phi^{\mu}}{DS} = F^{\mu}_{;\rho}\Psi^{\rho}, \tag{5}$$

$$\frac{D\Phi^{\mu\nu}}{DS} = M^{\mu\nu}_{;\rho}\Phi^{\rho} \tag{6}$$

where $\Phi^{\alpha}$, $\Phi^{\alpha\beta}$ are the spin path deviation and the spin tensor deviation associated to a path characterized by a parameter S and $(;)$ is the covariant derivative in Riemannian spaces.
In our study, it is worth mentioning that in case of S-systems, the orbiting systems are becoming MPD with $S^{\mu\nu}$ is constant.
Thus,

$$\frac{DU^{\mu}}{DS} = \frac{1}{2m}F^{\mu}, \tag{7}$$

$$\frac{DS^{\mu\nu}}{DS} = 0, \tag{8}$$

with taking into consideration that

$$S^{\mu\nu}U_{\mu} = 0.$$

Accordingly, one transform $V^{\alpha}$ to $U^{\alpha}$ in the following way:

$$V^{\alpha} = U^{\alpha} + \sigma\frac{D\Psi^{\alpha}}{Ds}$$

where $V^{\alpha} = \frac{dx}{dS}$ the tangent vector describing the spinning motion, $S$ its associated geodesic parameter and $\sigma$ ia an arbitrary parameter acting as a spin angular momentum ratio (Bini & Gerlalico, 2014).
Thus,

$$\frac{D}{DS}V^{\alpha} = \frac{D}{Ds}(U^{\alpha} + \sigma\frac{D\Psi^{\alpha}}{Ds})\frac{ds}{dS}$$

as well as

$$S^{\mu\nu} = \hat{s}(\Psi^{\mu}U^{\nu} - \Psi^{\nu}U^{\mu}),$$

such that $\sigma = \frac{\hat{s}}{m}$. Thus,

$$\frac{D}{DS}V^{\alpha} = \frac{\hat{s}}{m}R^{\mu}_{\nu\rho\sigma}U^{\rho}\Psi^{\sigma}U^{\beta}\frac{ds}{dS},$$

Let $\frac{ds}{dS} = 1$, we obtain

$$\frac{D}{DS}V^{\alpha} = \frac{\hat{s}}{m}R^{\mu}_{\nu\rho\sigma}U^{\rho}\Psi^{\sigma}U^{\beta}, \tag{9}$$

the above equation gives an indication that the path equation of a spinning particle is expressed in terms of its corresponding geodesic deviation vector.

Such a result can be also extended to study the motion of binary pulsar, PSR-J0737-3039. It is composed of two neutrons stars, located at a distance $10^9 km$ from the Galactic Center, of negligible intrinsic rotations regrading to the orbital period of about 2.4 hours, and their total mass is about $0.7M_{sun}$. This can give that

$$\frac{D}{DS}V_1^{\alpha} - \frac{D}{DS}V_2^{\alpha} = \frac{D}{Ds}(U^{\alpha} + \sigma_1\frac{D\Psi^{\alpha}}{Ds})\frac{ds}{dS} - \frac{D}{Ds}(U^{\alpha} + \sigma_2\frac{D\Psi^{\alpha}}{Ds})\frac{ds}{dS}.$$

where $\sigma_1$ and $\sigma_2$ the angular momentum ratio of each neutron star of this binary pulsar, to obtain the following equation

$$\frac{D}{DS_1}V_1^{\alpha} - \frac{D}{DS_2}V_2^{\alpha} = (\sigma_1 - \sigma_2)R^{\alpha}_{\rho\delta\beta}U^{\delta}U^{\rho}\Psi^{\beta},$$

in which $V_1^{\alpha}$ and $V_2^{\alpha}$ are two tangent vector associated to each spinning object in the binary system.
Consequently, we find out that

$$\frac{D\bar{V}^{\alpha}}{DS} = (\sigma_1 - \sigma_2)R^{\alpha}_{\rho\delta\beta}U^{\delta}U^{\rho}\Psi^{\beta} \tag{10}$$

such that, $\bar{V}^{\alpha} = V_1^{\alpha} - V_2^{\alpha}$.

### 3. The relationship between stability and geodesic deviation

It is well known that stability of planetary / stellar systems can be represented by a path deviation equation for an orbiting object.
Consequently, the stability tensor can be defined as follows:

$$H^{\alpha}_{\gamma}\Psi^{\gamma} = R^{\alpha}_{\beta\omega\gamma}U^{\beta}U^{\omega} \tag{11}$$

where $H^{\alpha}_{\gamma}$ is the stability tensor defined as (Di Bari & Cipriani, 2000).

Thus geodesic deviation equation may be expressed in terms of stability tensor;

$$\frac{D^2\Psi^{\alpha}}{DS^2} = H^{\alpha}_{\beta}\Psi^{\beta} \tag{12}$$

which is reduced to

$$\frac{d^2\Psi^{\mu}}{dS^2} + 2\Gamma^{\mu}_{\nu\rho}\frac{d\Psi^{\nu}}{dS}U^{\rho} + \Gamma^{\mu}_{\nu\rho,\sigma}U^{\nu}U^{\rho}\Psi^{\sigma} = 0, \tag{13}$$

provided that (Di Bari & Cipriani, 2000)

$$g_{\mu\nu}\Psi^{\mu}\Psi^{\nu} = constant.$$

Also, equation (9) and (10) can be written in terms of stability tensor in following way

$$\frac{D}{DS}V^{\alpha} = \sigma R^{\mu}_{\sigma}\Psi^{\sigma}, \tag{14}$$

and

$$\frac{D\bar{V}^{\alpha}}{DS} = (\sigma_1 - \sigma_2)H^{\alpha}_{\beta}\Psi^{\beta}. \tag{15}$$

Such a result for linearized systems gives rise to indicate that geodesic deviation vector can determine the spin path equation for S-stars and binary pulsar that are expressed by MPD equations. In order to obtain the solution, one must solve its corresponding field equation and define a certain coordinate system, to obtain the value of the deviation vector.
However, Wanas and Bakry (1995) introduced an approach, for examining the stability problem for any planetary system, being a covariant coordinate independent which can be explained in the following way (Wanas & Bakry, 1995)).
Let $\Psi^{\alpha}(S)$ is obtained from the solutions of the deviation equation in a given interval [a,b] in which $\Psi^{\alpha}(S)$ behave monotonically. These quantities can become sensors for measuring the stability of the system are

$$q^{\alpha} \overset{def.}{=} \Psi^{\alpha}(S) = C^{\alpha}f(S), \tag{16}$$

where $C^{\alpha}$ are constants and $f(S)$ is a function known from the metric. If $f(S) \to \infty$, the system becomes unstable otherwise it is stable. This approach has been applied previously in examining the stability of some cosmological models (Wanas & Bakry, 1995) using two geometric structures (Wanas, 1986). The above approach has been modified by obtaining the scalar value of the deviation vector which gives rise to become independent of any coordinate system (Wanas & Bakry, 2008)

$$q \overset{def.}{=} \lim_{s\to b}\sqrt{\Psi^{\alpha}\Psi_{\alpha}}. \tag{17}$$

If $q \to \infty$ then the system is unstable, otherwise it is always stable.

Now for spinning objects with precession, we suggest the above condition be extended to include the spin deviation tensor $\Phi^{\mu\nu}$ as

$$\bar{q} \overset{def.}{=} \lim_{s\to b}\sqrt{\Phi^{\alpha\beta}\Phi_{\alpha\beta}}. \tag{18}$$

Thus, for such a member in stellar/planetary system is stable, if and only if the magnitude of the scalar value of both spin deviation vectors $\Phi^{\alpha}$ and spin deviation tensors $\Phi^{\alpha\beta}$ to be real numbers respectively. i.e. either $q \to \infty$ or $\bar{q} \to \infty$ the assigned member is unstable. Accordingly, a strong stability condition must be admitted if both $q$ and $\bar{q}$ are satisfying the following conditions:

$$\lim_{s\to\infty}(\Phi_{\alpha}\Phi^{\alpha}) = 0, \tag{19}$$

and

$$\lim_{s\to\infty}(\Phi_{\alpha\beta}\Phi^{\alpha\beta}) = 0. \tag{20}$$

### 4. Geodesic and geodesic deviation: The Bazanski approach

Geodesic and geodesic deviation equations can be obtained simultaneously by using the Bazanski Lagrangian (Bazanski, 1989):

$$L = g_{\alpha\beta}U^{\alpha}\frac{D\Psi^{\beta}}{DS}, \tag{21}$$

where $L$ is the lagrangian function.
Thus, it can be found clearly, if one takes the variation with respect to the deviation vector $\Psi^{\rho}$ to get geodesic equations:

$$\frac{dU^{\alpha}}{dS} + \Gamma^{\alpha}_{\mu\nu}U^{\mu}U^{\nu} = 0. \tag{22}$$

Also, the same technique can be applied to get the variation with respect to the tangent vector $U^{\rho}$ to get the geodesic deviation equations:

$$\frac{D^2\Psi^{\alpha}}{DS^2} = R^{\alpha}_{.\beta\gamma\delta}\Psi^{\gamma}U^{\beta}U^{\delta}. \tag{23}$$

The above Lagrangian has been modified to describe the path equation of a charged object to take the following form (Kahil, 2006);

$$L = g_{\alpha\beta}U^{\alpha}\frac{D\Psi^{\beta}}{DS} + \frac{e}{m}F_{\alpha\beta}U^{\alpha}\Psi^{\beta}$$

where $\frac{e}{m}$ is the ratio of charge to mass of any charged object, $F_{\mu\nu}$ is an electromagnetic field tensor. Taking the variation with respect to $\Psi^{alpha}$ one obtains

$$\frac{dU^\alpha}{d\bar{S}} + \Gamma^\alpha_{\mu\nu} U^\mu U^\nu = \frac{e}{m} F^\mu_{.\nu} U^\nu. \tag{24}$$

While taking the variation with respect to $U^\alpha$ one obtains its corresponding deviation equations:

$$\frac{D^2\Psi^\alpha}{DS^2} = R^\alpha_{.\mu\nu\rho} U^\mu U^\nu \Psi^\rho + \frac{e}{m}(F^\alpha_{.\nu} \frac{D\Psi^\nu}{Ds} + F^\alpha_{.\nu;\rho} U^\nu \Psi^\rho). \tag{25}$$

Also the corresponding Papapetrou Equation for rotating objects without precession can be obtained from the following Lagrangian:

$$L = g_{\alpha\beta} U^\alpha \frac{D\Psi^\beta}{DS} + \frac{1}{2m} F_\mu \Psi^\mu \tag{26}$$

Taking the variation with respect to $\Psi^\alpha$, we obtain the spin path equation,

$$\frac{dU^\alpha}{dS} + \Gamma^\alpha \mu\nu U^\mu U^\nu = \frac{1}{2} F^\alpha \tag{27}$$

and taking the variation with respect to $U^\alpha$, we obtain the spin deviation equation

$$\frac{D^2\Psi^\alpha}{DS^2} = R^\alpha_{\beta\gamma\delta} U^\beta U^\gamma \Psi^\delta + \frac{1}{2} F^\alpha_{;\rho} \Psi^\rho. \tag{28}$$

In case of the Dixon equation for spinning charged objects can be obtained in a similar way from the following Lagrangian

$$L = g_{\alpha\beta} U^\alpha \frac{D\Psi^\beta}{DS} + \frac{1}{2m}(F_\mu + eF_{\mu\nu} U^\nu)\Psi^\mu. \tag{29}$$

Taking the variation with respect to $\Psi^\mu$ we obtain

$$\frac{dV^\alpha}{dS} + \Gamma^\alpha_{\mu\nu} U^\mu U^\nu = \frac{e}{m} F^\mu_{.\nu} U^\nu + \frac{1}{2m} F^\mu. \tag{30}$$

While its corresponding deviation equation can be obtained by taking the variation with respect to $U^\alpha$

$$\frac{D^2\Psi^\alpha}{DS^2} = R^\alpha_{.\mu\nu\rho} U^\mu U^\nu \Psi^\rho + \frac{e}{m}(F^\alpha_{.\nu} U^\nu)_{;\rho} \Psi^\rho + \frac{1}{2} F^\alpha_{;\rho} \Psi^\rho. \tag{31}$$

Similarly, we can modified the Lagrangian (21) to obtain spin equation and spin deviation equation for rotating objects with precession in the following way:

$$L = g_{\alpha\beta} P^\alpha \frac{D\Psi^\beta}{DS} + F_\alpha \Phi^\alpha \tag{32}$$

where

$$P^\alpha = mU^\alpha + U_\beta \frac{DS^{\alpha\beta}}{DS}.$$

In order to obtain an equation of spinning object with precession, we take the variation with respect to the deviation vector $\Phi^\alpha$

$$\frac{DP^\alpha}{DS} = F^\alpha. \tag{33}$$

And for its spin deviation equation, we take the variation with respect to $U^\alpha$ to become:

$$\frac{D^2\Phi^\alpha}{DS^2} = R^\alpha_{.\mu\nu\rho} P^\mu U^\nu \Phi^\rho + F^\mu_{;\rho} \Phi^\rho. \tag{34}$$

While for its precession part it can be obtained using the following condition:

$$P_\mu S^{\mu\nu} = 0,$$

to give

$$\frac{DS^{\alpha\beta}}{DS} = P^\mu U^\nu - P^\nu U^\mu.$$

## 5. Stability of motion in bimetric theory of gravity: the Verozub approach

In this section, we are showing that the treatment of the stability problem in strong fields may be explained in the presence of bimetric theory of gravity. This type of bimetric theories was proposed by Rosen in 1940, who regarded gravity can be expressed in flat space. Due to considering that, all objects of the Riemannaian space are functions in Minkowski space (Rosen, 1973). But such a type of visualization gives no physical meaning, with inconsistency with observations as well as there is no relation between the two metrics (Verozub, 2015). Recently, Verozub has introduced a new version of bimetric theory of gravity, stemmed from a well known principle of Poincare that properties of space-time are relative to the properties of used measuring instruments,together with the Einstein idea of the relativity of properties of space-time with respect to the distribution of matter (Verozub, 2008).

It is well known that in general relativity that test particles in gravitational field move on geodesics in a Riemanannian space. Accordingly, one may figure out that the differential equations for obtaining the metric tensor $g_{\mu\nu}(x)$ of any distribution of matter must keep the geodesic equations invariant under coordinate transformations. Surprisingly, it can be found that these equations are also invariant under geodesic mapping of space time $V$ into $\bar{V}$ upon replacing $\Gamma^\mu_{\alpha\beta} \to \bar{\Gamma}^\mu_{\alpha\beta}$ of the Christoffel symbols in any fixed coordinate system to become

$$\bar{\Gamma}^\mu_{\alpha\beta} = \Gamma^\mu_{\alpha\beta} + \delta^\mu_\alpha \phi_\beta + \delta^\mu_\beta \phi_\alpha \tag{35}$$

where $\phi_\mu(x)$ is a vector field. Moreover, transformations of the metric tensors are obtained by solving the

partial differential equation

$$\bar{g}_{\mu\nu;\alpha} = 2\phi_\alpha(x)\bar{g}_{\beta\gamma}(x) + \phi_\beta(x)\bar{g}_{\gamma\alpha}(x) + \phi_\gamma(x)\bar{g}_{\alpha\beta}(x), \tag{36}$$

in which the semi-colon is related here to the covariant derivative of $V$.

Thus, this field can be expressed in a Riemannian space in terms of two metrics before and after the geodesic mapping of from one space time into another in the following way:

$$\phi_\alpha = \frac{1}{n+1}(\bar{\Gamma}^\mu_{\alpha\mu} - \Gamma^\mu_{\alpha\mu}) = \frac{1}{2(n+1)}\frac{\partial}{\partial x^\alpha} ln|\frac{\bar{g}}{g}|. \tag{37}$$

Thus, Verozub's version of bimetric theory of gravity has two important results, geodesic transformations are playing the role of gauge transformations while coordinates transformation are acting the same way as in electrodynamics. It also gives a full description of motion of small particles of a perfect isentropic fluid able to describe gravity in strong gradational fields of a super-massive black hole Sgr A* at the Galactic Center. Also, the theory has neither singularities nor event horizon.

From this perspective, we aim to study stability of orbiting objects like S2 and binary pulsar PSR-J0737-3039, by obtaining their geodesic and geodesic deviations vectors.

Implementing Verzob's version one can find that the trajectories of a test particles are geodesics are in the co-moving reference frame, (CRF), described by $g_{\mu\nu}(\psi)$, such that $\psi_{\mu\nu}$ is a tensor field of spin 2 gravity, as found in Riemananain space of non zero curvature. While, the same test particle is observed in an inertial reference frame (IRF) as a point mass moves under the influence of a force field $\psi_{\mu\nu}$, as existed in Minkwoskian space (Verozub 2008).

Accordingly, the line element of the IRF is defined as follows:

$$d\sigma^2 = \eta_{\mu\nu}(x)dx^\mu dx^\nu, \tag{38}$$

where $\eta_{\mu\nu}$ is the Minkowski metric and its corresponding CRF line element is defined as

$$dS^2 = g_{\mu\nu}(\psi)dx^\mu dx^\nu \tag{39}$$

leading to define its corresponding affine connection:

$$\bar{\Gamma}^\alpha_{\beta\rho} = \frac{1}{2}g^{\alpha\delta}(\psi)(g_{\beta\delta,\rho} + g_{\delta\rho,\beta} - g_{\beta\rho,\delta}).$$

Applying the Bazanski approach, we obtain geodesic and geodesic deviation equations of Verozub's version for bimetric theory of gravity:

$$L(\psi) = g_{\alpha\beta}(\psi)U^\alpha\frac{D\Psi^\beta}{DS} \tag{40}$$

This can be seen clearly if one takes the variation with respect to the deviation vector $\Psi^\rho$ to get the geodesic equations:

$$\frac{dU^\alpha}{dS} + \bar{\Gamma}^\alpha_{\mu\nu}(\psi)U^\mu U^\nu = 0 \tag{41}$$

Also, the same technique can be applied to get the variation with respect to the tangent vector $U^\rho$ to get the geodesic deviation equations:

$$\frac{D^2\Psi^\alpha}{DS^2} = \bar{R}^\alpha_{.\beta\gamma\delta}(\Psi)\Psi^\gamma U^\beta U^\delta \tag{42}$$

where $\bar{R}$ is the Riemann Curvature described by the affine connection $\bar{\Gamma}^\alpha_{\beta.\rho\sigma}$ for the (CRF). Thus the stability equation in this case becomes:

$$\frac{D^2\Psi^\alpha}{DS^2} = \hat{H}^\alpha_{.\gamma}(\psi)\Psi^\gamma. \tag{43}$$

as $\hat{H}^\alpha_{.\beta}$ is the stability tensor defined in CRF. Thus, the deviation vector in CRF in Riemannian space can be expressed as a separation vector of these particles under the action of a force field $\psi_{\mu\nu}$ in Minkowkian space, which can be reduced to (Verozub, 2015):

$$\frac{\partial^2\eta^\alpha}{\partial^2\tau} + \frac{\partial^2 U}{\partial x^\alpha \partial x^\beta}\eta^\beta = 0, \tag{44}$$

where $\eta^\alpha = \frac{\partial x^\alpha}{\partial\xi}$, $x^\mu = x^\mu(\tau,\xi)$ such that $\eta^\alpha$ is the separation vector and $U$ is the gravitational potential as measured in the flat space. If we apply the Wanas-Bakry condition on the scalar of the separation vector between two geodesics in a Minkowski space we can easily find

$$\tilde{q} = \lim_{\tau\to\bar{b}}\sqrt{\eta^\alpha\eta_\alpha}$$

, where the solutions of $\eta(\tau)$ in a given interval $[\bar{a},\bar{b}]$ behave monotonically. If $\tilde{q}\to\infty$ then the system is unstable, otherwise it is always stable. Consequently, the strong stability condition becomes

$$\lim_{\tau\to\infty}(\eta_\alpha\eta^\alpha) = 0. \tag{45}$$

Accordingly, we can conclude that in a strong gravitational field, in covariant stability condition is examined by obtaining the scalar value of its associated separation vectors as defined in IRF rather than its equations. Such an approach gives the finiteness of the scalar value for the separation vector an indicator to decide whether the orbiting system is stable or not.

## 6. Discussion and concluding remarks

In this study,we have examined the stability of rotating objects in the presence of very strong gravitational field. One of most promising theories is the bimetric version of Verozub. The objects are considered as test particles due to to the stringent condition $\frac{m}{M} < 10^{-5}$, e.g the S-stars are considered as test particles moving on geodesics and acting as clocks for the SgrA*. It has been assumed that the stability criterion may be estimated its status by extending the covariant stability condition method of Wanas-Bakry to examine S-stars

and PSR J0737-3039. The stability of these systems are mainly dependent on obtaining the corresponding deviation vectors and then finding their scalar value in each case. Yet, an additive step may be obtained due to Verozub's bimetric theory, is the scalar part of the separation vectors obtained in IRF as defined in flat space is becoming a good candidate to examine the stability condition.

Moreover, we have obtained a relationship between the spin tensor of a rotating object with its corresponding deviation vector. This result leads to identify the stability condition without finding out the spin deviation vector as an indicator of stability conditions, and examining only the stability condition on their corresponding deviation vector. Accordingly, we have obtained a quick method to estimate whether the system is stable or not without going to lengthy calculation to determine the scalar value for the spin deviation vector, such an advantage works in favor of testing stability conditions for S-stars or binary pulsars orbiting SgrA*.

*Acknowledgments.* The author would like to thank Professor A.Zhuk and the organizing committee of the Conference of Fifth Gammov for their hospitality and good atmosphere of discussions during the conference period.

**References**

Angelil R., Saha P.: 2014, *MNRS*, **444(2)**, 3780.
Bazanski S.L.: 1989, *J. Math. Phys.*, **30**, 1018.
Bini D., Geralico A.: 2014, *Phys Rev.*, **D84**,104012.
Di Bari M., Cipriani P.: 2000, *Chaotic Universe*, 444.
Dixon W.G.: 1970, *Proc. R. Soc. London, Ser. A*, **314**, 499.
Han Wen-Biao: 2014, *A&A*, **14**, 1415.
Heydrai-Fard, Mohseni, M., Sepanigi, H.R.: 2005, *Phys. Lett. B*, **626**, 230.
Iorio L.: 2011, *Phys. Rev.*, **D84**, 124001.
Kahil M.E.: 2006, *J. Math. Physics*, **47**, 052501.
Meyer et al.: 2012, *Science*, **125506**.
Mohseni M.: 2010, *Gen. Rel. Grav.*, **42**, 2477.
Papapetrou A.: 1951, *Proc. R. Soc. London, Ser. A*, **209**, 248.
Rosen N.: 1973, *Gen. Relativ. and Gravit.*, **4**, 435.
Verozub L.: 2008, *Annalen der Physik*, **27**, 28.
Verozub L.: 2015, *Space-time Relativity and Gravitation*, Lamberg Acadamic Publishing.
Wanas M.I.: 1986, *Astrophys. Space Sci.*, **127**, 21.
Wanas M.I., Bakry M.A.: 1995, *Astrophys. Space Sci.*, **228**, 239.
Wanas M.I., Bakry M.A.: 2008, *Proc. MGXI, part C*, 2131.

# PERTURBATIONS OF FRIEDMAN-LEMAITRE-ROBERTSON-WALKER SPACETIMES IN GEROCH-HELD-PENROSE FORMALISM

J.Novák

Department of theoretical physics, Charles University,
V Holešovičkách 2, Prague-Libeň, 180 00, Czech republic, *jan.janno.novak@gmail.com*

ABSTRACT. We will use Geroch-Held-Penrose formalism for decoupling of quantity $d\Psi_4$, which is responsible for tensorial perturbations, in Bianchi equations. We will concentrate on the case, where we eliminate the source terms.

**Keywords**: Friedman-Lemaitre-Robertson-Walker spacetime, Geroch-Held-Penrose formalism, Newman-Penrose formalism, Weyl scalars

## 1. Introduction

Our goal is to use the Geroch-Held-Penrose formalism (GHP - formalism) in reformulation of perturbations of Friedman-Lemaitre-Robertson-Walker spacetime (FLRW ST). GHP - formalism (a more compact version of NP - formalism) is a convenient formalism, because it allows us to work with partial differential equations of the first order. The scalar and tensor perturbations are for us the most interesting because of the origin of structure. I will show, how to apply the GHP-formalism for decoupling of the quantity $d\psi_4$ in Bianchi equation. These calculations are done for the case of the simplified right-hand side (RHS without sources).

## 2. NP-formalism

NP- and GHP-formalisms are mathematical approaches which help us, for example, in perturbation theory to simplify calculations in standard General Relativity. We decompose the metric with respect to the null tetrad and then we project all quantities on this tetrad (in the NP-formalism). The basic quantities are spin-coefficients - projections of the derivatives of the null tetrad, then projections of the Ricci tensor and already mentioned Weyl scalars. We could then rewrite the Einstein's equations by the 18 Ricci, 8+3 Bianchi and 4 commutation equations, which are only first order PDE's, when we define new derivatives in the direction of the tetrad ($D$,$\Delta$, $\delta$, $\overline{\delta}$). Let us to introduce, for illustration, the basic quantities and equations now:

Table 1: Spin coefficients

| | | |
|---|---|---|
| $\alpha = \frac{1}{2}(S_{214} + S_{344})$ | $\nu = S_{242}$ | $\tau = S_{312}$ |
| $\beta = \frac{1}{2}(S_{213} + S_{343})$ | $\kappa = S_{311}$ | $\sigma = S_{313}$ |
| $\gamma = \frac{1}{2}(S_{212} + S_{342})$ | $\pi = S_{241}$ | $\mu = S_{243}$ |
| $\epsilon = \frac{1}{2}(S_{211} + S_{341})$ | $\rho = S_{314}$ | $\lambda = S_{244}$ |

we will denote the 12 spin coefficients by $S_{ijk}$ (standard notation is with $\gamma$), where the three indices mean, which element of the tetrad we are using (where the null tetrad is defined in standard way), Table 1.

For example:

$$\rho = m^{\mu} l_{\mu;\nu} \overline{m}^{\nu}$$

Projections of the Ricci tensor (we will omit the brackets by tetrad indices in this part of thesis):

$$\Phi_{(i)(j)},\ i,j = 0,1,2,3,$$

$$\Phi_{(0)(0)} = -\frac{1}{2} R_{\mu\nu} l^{\mu} l^{\nu}$$

So, let's define the projections of the Ricci tensor by the following notation, [1]:

$$\begin{aligned}
&\Phi_{00} = -\frac{1}{2}R_{11}, \Phi_{01} = -\frac{1}{2}R_{13}, \Phi_{10} = -\frac{1}{2}R_{14},\\
&\Phi_{12} = -\frac{1}{2}R_{23}, \Phi_{21} = -\frac{1}{2}R_{24}, \Phi_{22} = -\frac{1}{2}R_{22},\\
&\Phi_{11} = -\frac{1}{4}(R_{12} + R_{34}), \Lambda = \frac{1}{12}(R_{12} - R_{34}),\\
&\Phi_{02} = -\frac{1}{2}R_{33}, \Phi_{20} = -\frac{1}{2}R_{44}.
\end{aligned} \tag{1}$$

Weyl scalars (5 in dimension 4):

$$\Psi_i,\ i = 0,1,2,3,4 \tag{2}$$

$$\Psi_0 = l^\mu m^\nu l^\rho m^\sigma C_{\mu\nu\rho\sigma},$$
$$\Psi_1 = l^\mu n^\nu l^\rho m^\sigma C_{\mu\nu\rho\sigma},$$
$$\Psi_2 = l^\mu m^\nu \overline{m}^\rho n^\sigma C_{\mu\nu\rho\sigma},$$
$$\Psi_3 = n^\mu l^\nu n^\rho \overline{m}^\sigma C_{\mu\nu\rho\sigma},$$
$$\Psi_4 = n^\mu \overline{m}^\nu n^\rho \overline{m}^\sigma C_{\mu\nu\rho\sigma}. \quad (3)$$

Now we present one Ricci, one Bianchi and one commutation relation:

Ricci identities (18 equations)

$$D\rho - \delta^*\kappa - \rho^2 - \sigma\overline{\sigma} - \rho\epsilon - \rho\overline{\epsilon} + \overline{\kappa}\tau + (3\alpha + \overline{\beta} - \pi)\kappa = \Phi_{00}, \quad (4)$$

Bianchi identities (11 equations)

$$-\delta^*\Psi_0 + D\Psi_1 + (4\alpha - \pi)\Psi_0 - 2(2\rho + \epsilon)\Psi_1 =$$
$$\delta\Phi_{00} - 3\kappa\Psi_2 - D\Phi_{01} + 2(\epsilon + \overline{\rho})\Phi_{01} - \overline{\kappa}\Phi_{02} +$$
$$+ (\overline{\pi} - 2\overline{\alpha} - 2\beta)\Phi_{00} + 2\sigma\Phi_{10} - 2\kappa\Phi_{11}, \quad (5)$$

Commutation relations (4 equations):

$$\Delta D - D\Delta = (\gamma + \overline{\gamma})D + (\epsilon + \overline{\epsilon})\Delta - (\overline{\tau} + \pi)\delta - (\tau + \overline{\pi})\overline{\delta}. \quad (6)$$

We can rotate the tetrad and we can get a transformation property of these quantities. However, there exists also a more compact version of the NP-formalism, so called GHP-formalism. One makes the following redefinitions of the derivative operators:

$$\text{þ} = D - p\epsilon - q\overline{\epsilon}, \quad (7)$$

$$\text{þ}' = \Delta - p\gamma - q\overline{\gamma}, \quad (8)$$

$$\eth = \delta - p\beta - q\overline{\alpha}, \quad (9)$$

$$\eth' = \overline{\delta} - p\overline{\beta} - q\alpha. \quad (10)$$

We have 4 different operators and two, so called, dualities in dimension 4 (star - duality, $(p, q) \to (p, -q)$, is for exchange of the vector $l$ and $m$, the prime duality, $(p, q) \to (-p, -q)$, for the exchange of the $l$ and $n$; we could not use both dualities in HD, because we have odd dimensions)

Table 2: Relations among projections of Ricci tensor

| | | | |
|---|---|---|---|
| $\Phi'_{00} = \Phi_{22}$ | $\Phi'_{11} = \Phi_{11}$ | $\Phi'_{10} = \Phi_{12}$ | $\Phi'_{02} = \Phi_{20}$ |
| $\Phi'_{00} = \Phi_{02}$ | $\Phi'_{01} = -\Phi_{01}$ | $\Phi^*_{10} = \Phi_{12}$ | $\Phi^*_{11} = -\Phi_{11}$ |
| $\Phi^*_{22} = \Phi_{20}$ | $\Phi^*_{12} = \Phi_{10}$ | $\Phi^*_{02} = \Phi_{00}$ | $\Phi^*_{20} = -\Phi_{22}$ |
| $\Lambda' = \Lambda$ | $\Phi^*_{21} = -\Phi_{21}$ | $\Lambda^* = -\Lambda$ | |

Table 3: GHP-type

| | | |
|---|---|---|
| $\Phi_{00} : (2, 2)$ | $\Phi_{01} : (2, 0)$ | $\Phi_{10} : (0, 2)$ |
| $\Phi_{11} : (0, 0)$ | $\Phi_{22} : (-2, -2)$ | $\Phi_{12} : (0, -2)$ |
| $\Phi_{21} : (-2, 0)$ | $\Phi_{20} : (-2, 2)$ | $\Phi_{02} : (2, -2)$ |
| $\Lambda : (0, 0)$ | | |

$$\Sigma\eta, \ \Sigma = \left\{\text{þ}, \ \text{þ}', \eth, \eth'\right\}, \quad (11)$$

where $\Sigma$ is an operator acting on a quantity $\eta$.

But we need the notion of the GHP scalars when we make the following transformations:

$$l^\nu \to \lambda^{-1} l^\nu, \quad (12)$$

$$n^\mu \to \lambda n^\mu, \quad (13)$$

$$m^\rho \mapsto e^{i\theta} m^\rho. \quad (14)$$

We say that a quantity $\eta$ is a GHP-scalar of type $(p, q)$, if it transforms like (analogical definition for the case of higher dimensions is in [2]):

$$\eta \to \lambda^{(p+q)/2} e^{i(p-q)\theta/2} \eta. \quad (15)$$

We will use the star and prime duality in a standard way, [1]. We see the relations among perturbations of Ricci tensor in Table 2.

And the types for these quantities are in Table 3.

## 3.Computations

Now we will apply the GHP-formalism in perturbation theory of FLRW ST. It will be done, of course, in classical manner. However, we obtain a new result with this formalism.

Reference [3] will be of great importance for us, where the following fact can be found: the only non-vanishing spin coefficients for the case of FLRW are $\alpha$, $\beta$, $\gamma$, $\mu$ and $\rho$. These are the same non-zero spin coefficients as for the case of the Schwarzschild solution. This fact can be employed in the analysis of unperturbed equations. This means that we can get rid of

many terms in the resulting equations. We get rid of $\alpha$, $\beta$, $\gamma$ and $\epsilon$ because they are absorbed into $\text{þ}$ and $\eth$ ($\text{þ}'$ and $\eth'$). Together there are 12 spin coefficients, thus there remain yet 8 more: $\tau$, $\sigma$, $\kappa$, $\mu$, $\rho$, $\lambda$, $\pi$ and $\nu$ ;

The course of action will be now the following. We will write the general Bianchi equations for the case of FLRW ST with sources. We will show our result for the special case of simplified right-hand side.

We have the following 2 equations in GHP formalism for the case of FLRW ST. We have 8 equations in standard NP-formalism, but this formalism is even more efficient. (We stress once again that we have sources on the right hand side of the equations contrary to the Schwarzschild ST.) The equations read

$$\begin{aligned}\text{þ}\Psi_1 - \eth'\Psi_0 + \tau'\Psi_0 - 4\rho\Psi_1 + 3\kappa\Psi_2 = \text{þ}\Phi_{01} - \eth\Phi_{00} - \\ -\overline{\pi}\Phi_{00} - 2\overline{\rho}\Phi_{01} + \overline{\kappa}\Phi_{02} + 2\kappa\Phi_{11} - 2\sigma\Phi_{10},\end{aligned} \tag{16}$$

$$\begin{aligned}\text{þ}\Psi_2 - \eth'\Psi_1 - \sigma'\Psi_0 + 2\tau'\Psi_1 - 3\rho\Psi_2 + 2\kappa\Psi_3 = \\ \text{þ}'\Phi_{00} - \eth'\Phi_{01} - \overline{\rho}'\Phi_{00} + 2\overline{\tau}\Phi_{01} - 2\rho\Phi_{11} - \\ -\overline{\sigma}\Phi^*_{00} + 2\tau\Phi_{10} + 2\text{þ}\Lambda,\end{aligned} \tag{17}$$

where we defined the NP components of the Weyl tensor in the standard way.

The $\Psi_0$ and $\Psi_4$ are connected with the tensor perturbations, $\Psi_1$ and $\Psi_3$ are connected with the vector perturbations and $\Psi_2$ is connected with the scalar perturbations according to the [3] [1]. [2]

Now we will follow the approach presented in [4]. The difference, as we already mentioned, is that we have sources on the RHS. However, we can make the same steps: we will take the first equation and we will apply operator $\eth$, we make the star duality and we add the first and this modified equation. Then we plug from the Ricci identities, we eliminate some of these combinations of spin coefficients (we make also prime and star dualities of these Ricci identities ) and we arrive at the following result (the second equation could be obtained in a similar way).

[1] We can use their boost weights like an argument.

[2] In the case of non-zero sources we have also other two equations:

$$\begin{aligned}-[\text{þ}' - 2\overline{\tau}^* + \pi^*]\Phi_{01} + [-\text{þ} - 2\tau^* + \overline{\pi}^*]\Phi_{12} + \\ [\eth - 2(\rho^* + \overline{\rho}^*]\Phi_{11} - [-\eth' + \mu^* + \overline{\mu}^*]\Phi_{02} + \\ \overline{\sigma}^*\Phi^*_{02} + \sigma^*\Phi^*_{20} - \overline{\kappa}^*\Phi^*_{12} - \kappa^*\Phi^*_{21} + 3\eth\Lambda = 0,\end{aligned} \tag{18}$$

$$\begin{aligned}[\eth - 2\tau + 2\pi^*]\Phi_{11} - 3\eth\Lambda + [-\text{þ} + 2\rho + \overline{\rho}]\Phi_{12} + \\ [-\text{þ}' - 2\overline{\mu} - \mu]\Phi_{01} + [\eth' - \tau^* + \pi]\Phi_{02} \\ -\kappa\Phi_{22} + \overline{\nu}\Phi_{00} + \sigma\Phi_{21} - \overline{\lambda}\Phi_{10} = 0.\end{aligned} \tag{19}$$

$$\begin{aligned}[\text{þ}'\text{þ} - \eth'\eth - (4\rho' + \overline{\rho}')\,\text{þ} - \rho\text{þ}' + (4\tau' + \overline{\tau})\,\eth + \\ \tau\eth' + 4\rho\rho' - 4\tau\tau' - 2\Psi_2 + 2\Lambda]\Psi_4 + \\ [4\text{þ}\kappa' - 4\eth\sigma' - 4\,(\overline{\rho} - 2\rho)\,\kappa' + \\ 4\,(\overline{\tau} - 2\tau)\,\sigma' + 10\Psi_3]\Psi_3 + \\ \left[-4\sigma'\text{þ}' + 4\kappa'\eth' - 12\kappa'\tau' + 12\rho'\sigma' - 3\Psi_0\right]\Psi_2 = \quad 0.\end{aligned} \tag{20}$$

This equation contains information from both (16) and (17). It is interesting that for this case of FLRW spacetimes, we have cancellations of all extra terms in front of $\Psi_2$ and $\Psi_3$. The terms in the brackets in front of $\Psi_2$ and $\Psi_3$ are exactly the same (except of one term $3\Psi_0\Psi_2$) as for the case of the Schwarzschild spacetime. This means that when we will make perturbations of these equations, the second and third term disappear. So, we obtain a decoupling of the quantity $d\Psi_4$.

This is other new information, when we compare it with [3]. Here we were interested in equations without sources, i.e. when we put just delta-function on the RHS. But in later work we could be interested in the same problem but with sources, as was already suggested in this article. It is an advantage to write all sources in one compact form.

## 4. Conclusion

I have been studying perturbation theory of FLRW ST in GHP formalism. We obtained a new interesting observation, which could be used for other research in the realm of Cosmological Perturbation Theory.

## References

Chandrasekhar S.: 1983, Mathematical theory of black holes, *Oxford University Press*, 668.

Durkee M., Pravda V., Pravdová A., Reall H.S.: 2010, Generalization of the Geroch-Held-Penrose formalism to higher dimensions, *Class.Quantum Grav.*, **27**.

Sharma S., Khanal U.: 2014, Perturbations of FRW ST's in NP formlism, *International Journal of Modern Physics D*.

Stewart J.M., Walker M.: 2014, *Proc. R.Soc. Lond. A*, 49-74.

# THE DETERMINATION OF THE MORPHOLOGICAL TYPES OF GALAXY CLUSTERS USING CLUSTER CARTOGRAPHY

E.A. Panko, S.I. Emelyanov

V.O. Suckomlinsky Nikolaev National University, Kalinenkov Astronomical Observatory
Nikolskaya, 24, Nikolaev, 54030, Ukraine
*panko.elena@gmail.com*

ABSTRACT. We discuss the possibility of using the Cluster Cartography set for the determined the morphological types of galaxy clusters. The applied morphological scheme was proposed by Panko (2013). The morphological types are determined using numerical criteria based on three parameters: concentration to the cluster center, the signs of preferential direction or plane in the cluster (filamentary substructure), and the positions of the brightest galaxies. However, structures like galaxy clusters need visual preview for classification. The Cluster Cartography set constructs the individual cluster map in different forms and allows to estimate previously cluster type.

**Keywords**: Galaxies: clusters: morphological types.

## 1. Introduction

The morphology of galaxy clusters reflects the physical conditions in the cluster space. One can note the galaxy clusters have a special place in hierarchy of large-scale structures. They are the part of a continuous range of large-scale construction of Universe: galaxies ⇒ groups ⇒ clusters ⇒ superclusters ⇒ cosmological large scale structure. Galaxy cluster virialization time is about $10^9$ *yr*, and it is less then Hubble time. In contrary, galaxy superclusters virialization time – about $10^{10.5}$ – is bigger then Hubble time. As a result the galaxy clusters are not biggest bound structures in the Universe, they are only biggest virialized ones. The galaxy clusters are small in comparison to Universe. At the same time, on the galaxy clusters scale, their components have not had a chance to separate during collapse and a cluster is probably a representative sample of the Universe. In particulary, the part of dark matter (DM) in galaxy clusters must be the same, as in whole Universe. The determination of morphological types of galaxy clusters will be useful for detailed study of the large scale structures.

Panko (2013) summarized the classical schemes, including both famous Bautz – Morgan (1970), Rood – Sastry (1971) systems and less popular López-Cruz at al. (1997) and López-Cruz & Gaztanaga (2001) ones. Improved and integrated scheme (Panko 2013) allows to assign the morphological types corresponding to cluster "concentration" (from *C* – compact, to *I* – intermediate, and *O* – open), "flatness signs" (*L* – line or *F* – flat, and no symbol if no indication of flatness is present) and the role of bright galaxies (c*D* or *BG*, if the bright cluster members role is significant). Other peculiarities are noted as *P*. "Flatness signs" can correspond to filamentary substructure or preferential plane in cluster. The designations can be combined, for example *CF*c*D* or *ILP*. Unfortunately, like to morphology of galaxies case, programmatic way does not allow to distinguish morphology without visual preview and control.

We create the Cluster Cartography set (hereafter CC) for simplification of the galaxy clusters classification.

## 2. Observational Data

The CC set was create for morphology classification of galaxy clusters of the "A Catalogue of Galaxy Clusters and Groups" (Panko & Flin, 2006, hereafter PF). The PF Catalogue was constructed on Münster Red Sky Survey Galaxy Catalogue (Ungrue et al., 2003, hereafter MRSS) as the observational basis. Each PF galaxy cluster has the list of galaxies in the cluster field inclusive for each galaxy information accordingly to MRSS, specifically $RA_{2000}$ and $Dec_{2000}$, $r_F$ magnitude, major and minor axes and positional angle of major axis of galaxy best-fitted ellipse (Ungrue et al., 2003).

## 2. The Cluster Cartography set

The cluster map is constructed in rectangular coordinates recalculated into arcseconds. The equatorial coordinates were recalculated to rectangular ones centered in the cluster center by usual way. The CC set allows to construct the cluster map in four modes:

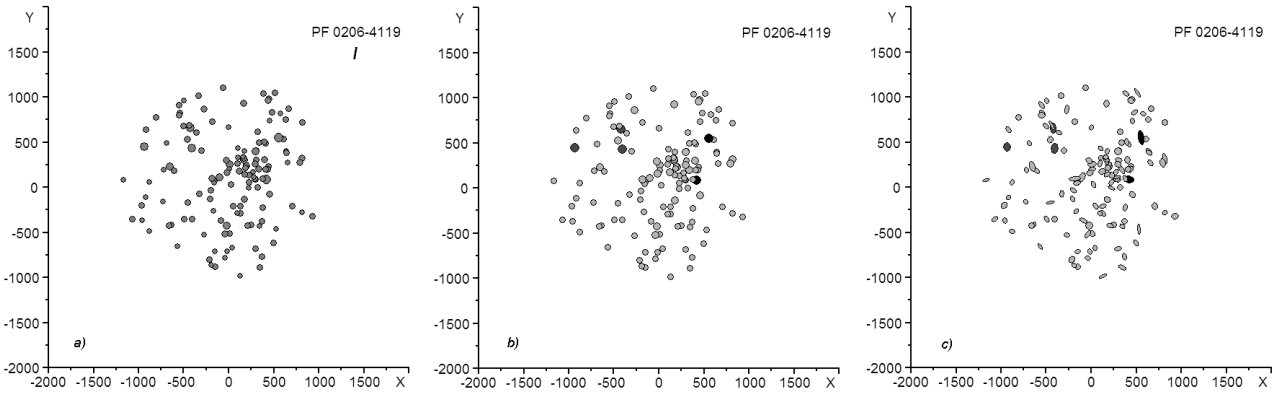


Figure 1: The modes of cluster mapping. All maps constructed for the same $I$-type cluster PF 0206-4119.

– all symbols are circles and have the same size;

– all symbols are circles and the symbol size corresponds to magnitude of galaxy (Fig. 1$a$ and $b$);

– the symbol size corresponds to magnitude of galaxy and each symbol illustrates the galaxy shape and orientation in the projection on the celestial sphere (Fig. 1$c$);

– the symbols illustrates the galaxy shape and orientation in the projection on the celestial sphere, but size of symbol corresponds to galaxy size in arcseconds.

Additionally brightest galaxies can be marked by darker gray shades (Fig. 1$b$ and $c$).

The shown in Fig.1$b$ CC mode allows to estimate the morphological type according to Panko (2013) and the select the clusters for numerical definition. The analyze of distribution of ellipticities of galaxies in the cluster notes to one more parameter in classification – the part of E-type galaxies (Panko & Flin, 2014). E-rich and S-rich galaxy clusters were recognized by Oemler in 1974. The galaxy shape and orientation mode was added for previous estimation of positions of E-type galaxies in the cluster field. In our data set (accordingly to MRSS) we can divide galaxies only to elliptical and non-elliptical. Galaxies with ellipticity $E > 0.5$ can be lenticular or spiral (near edge-on view) or interactive ones. Positions of these galaxies in E-poor clusters is important in connection with Morphology – Density relation (Dressler, 1980).

The diameter of circle symbol $m'$ was calculated using galaxy magnitude $m$ as:

$$m' = 3 \cdot 2^{0.6(18.5-m)} + 6 \qquad (1)$$

The coefficients can be changed in case of need, but for typical map size – $4000 \times 4000$ *arcsec* – the symbol sizes calculated according to (1) are optimal.

The sizes of major and minor axes ($2a$ and $2b$) for shown in Fig. 1$c$ CC mode are calculated from $m'$ and ellipticity $E$ as:

$$2a = \frac{m'}{\sqrt[4]{1-2E+E^2}}; \quad 2b = \frac{(m')^2}{2a} \qquad (2)$$

Note, the ellipticity $E = 1 - \frac{b}{a}$. The equations (2) transform the circle to ellipse with the same area and connect symbol axes with galaxy magnitude. We use MRSS data for maps shown real galaxy size with magnitudes noted as shades of gray in CC mode 4.

## 2. Conclusion

We tested the CC set in different modes on 247 rich PF galaxy clusters. It allows to estimate galaxy cluster morphological type quickly. We will use the CC set in future work for study of 1746 PF galaxy clusters with richness 50 and more. About of 1200 galaxy clusters in this list have no morphological types and using the CC set allows to improve our data set.

*Acknowledgements.* This research has made use of NASA's Astrophysics Data System.

## References

Bautz P. & Morgan W.W.: 1970, *ApJ*, **162**, L149.
Dressler A.: 1980 *ApJ*, **236**, 351.
López-Cruz O., Yee H.K.C., Brown J.P., et al.: 1997, *ApJ*, **475**, L97.
López-Cruz O. & Gaztanaga E.: 2001, *arXiv:astroph/0009028*.
Oemler A.Jr.: 1974, *ApJ*, **194**, 1.
Panko E. & Flin P.: 2006, *J. Astr. Data*, **12**, 1.
Panko E.: 2013, *Odessa Astr. Publ.*, **26**, 90.
Panko E. & Flin P.: 2014, *Odessa Astr. Publ.*, **27**, 32.
Rood H.J. & Sastry G.N.: 1971, *PASP*, **83**, 313.
Ungrue R., Seitter W.C. & Duerbeck, H.W.: 2003, *J. Astr. Data*, **9**,1.

# BIG RIP AND OTHER SINGULARITIES IN ISOTROPIC HOMOGENEOUS COSMOLOGICAL MODELS WITH ARBITRARY EQUATION OF STATE

S.L. Parnovsky

Astronomical Observatory, Taras Shevchenko National University of Kyiv,
3 Observatorna Str., 04053, Kyiv, Ukraine, *par@observ.univ.kiev.ua*

ABSTRACT. We study the possible types of future singularities in the isotropic homogeneous cosmological models for the arbitrary equation of state of the contents of the Universe. We obtain all known types of these singularities as well as two new types using a simple approach. No additional singularity types are possible. We name the new singularities type "Big Squeeze" and "Little Freeze". The "Big Squeeze" is possible only in the flat Universe after a finite time interval. The density of the matter and dark energy tends to zero and its pressure to minus infinity. This requires the dark energy with a specific equation of state that has the same asymptotical behaviour at low densities as the generalised Chaplygin gas. The "Little Freeze" involves an eternal expansion of the Universe. Some solutions can mimic the ΛCDM model.

**Keywords**: Relativistic cosmology

## 1. Introduction

During almost a century, cosmologists considered only two possible scenarios of the future of our Universe – an eternal expansion of open or flat Universe or future recollapse of the closed Universe with the "Big Crunch". Nowadays we know that the Universe contains not only several types of matter, including the dark matter, baryonic matter and massless particles, but also the mysterious dark energy (DE). We know about its existence only for the last few decades. Honestly, we know very little about DE properties, in particular about the DE equation of state.

Even for the simplest type of the DE equation of state

$$p = w\rho \tag{1}$$

with $w = const$, where $p$ is the pressure and $\rho$ is the mass density, the Universe can meet its end in absolutely different way. If $w < -1$ we deal with so-called phantom energy. In this case during the finite time period the matter and energy density, the Hubble parameter $H$ and the scale factor of the Universe $a$ increase to infinity. Such type of possible future singularity was discovered by Caldwell, Kamionkowski and Weinberg (2003) and called "Big Rip".

Note that the latest estimations of the $w$ value do not reject this possibility. The data on the cosmic microwave background spectra from the Planck and WMAP satellites together with ground measurements and data from baryonic acoustic oscillations (BAO) provide the estimation $w = -1.13^{+0.23}_{-0.25}$ at 95% confidence level (CL). The 9-year data from the WMAP satellite plus the determination of the Hubble constant and BAO data provide estimations $w = -1.073^{+0.090}_{-0.089}$ for the flat Universe and $w = -1.19 \pm 0.12$ for the non-flat Universe at 68% CL. Adding 472 type Ia supernovae data improves these estimations to $w = -1.084 \pm 0.063$ and $w = -1.122^{+0.068}_{-0.067}$, respectively.

Thus, the possibility of the "Big Rip" sealing the fate of the Universe is not to be taken lightly. This is not the only theoretically possible type of cosmological singularity except "Big Bang" and "Big Crunch". Their first classification was carried out by Nojiri, Odintsov and Tsujikawa (2005). Four possible types were found for the singularities at $t = t_0$ with finite $t_0$. They include:

- **Type I** $a, \rho, |p| \to \infty$ ("Big Rip")
- **Type II** $a \to a_0; \rho \to \rho_0; |p| \to \infty$ ("sudden")
- **Type III** $a \to a_0; \rho, |p| \to \infty$ (it was named "Big Freeze" lately)
- **Type IV** $a \to a_0; \rho, |p| \to 0$ and higher derivatives of the Hubble parameter $H$ diverge.

There are some singularities with $t_0 = \infty$, too. The "Little Rip" singularity (Frampton, Ludwick and Scherrer, 2012) similar to the "Big Rip", but with eternal expansion is among them.

Some types of singularities were found and demonstrated for some specific equations of state. Cosmologists considered the particular cases of the phantom generalised Chaplygin gas equation of state, tachyon field, scalar fields with specific potentials, etc. Naturally, a question arose, whether all the possible singularity types have been considered.

In this article we try to give an exhaustive answer to this question for the isotropic and homogeneous Universe. To make it worse, in addition to unknown DE equation of state we have three possible signs of space curvature. We are interesting in the complete list of the possible types of future singularities for an arbitrary equation of state for three signs of space curvature. We consider an arbitrary equation of state $p(\rho)$ without any constrains except $\rho \geq 0$. In particular we do not use the strong energy condition $\rho + 3p > 0$.

## 2. The search for future singularities in FLRW Universe

We consider the homogeneous isotropic Universe with the Friedmann-Lemaître-Robertson-Walker (FLRW) metric

$$ds^2 = dt^2 - a(t)^2 \left[d\chi^2 + F^2(\chi) dO^2\right], \qquad (2)$$

where $a(t)$ is the scale factor, $dO^2 = d\Theta^2 + \cos^2(\Theta) d\varphi^2$ is the distance element on a unit sphere, $F(\chi) = \sin(\chi)$ and $k = 1$ for the closed Universe, $F(\chi) = \sinh(\chi)$ and $k = -1$ for the open one, and $F(\chi) = \chi$ and $k = 0$ for the spatially flat models. We use the system of units in which $G = 1$ and $c = 1$. This Universe is filled by all kinds of matter and dark energy with a mass density $\rho$ and an effective pressure $p(\rho)$. In this system of units the energy density $\varepsilon$ coincides with $\rho$. The Einstein equations for the metric (2) reduce to the well-known Friedmann equations. We need the expression for the Hubble parameter $H = a^{-1} da/dt$

$$H^2 = \frac{8\pi}{3}\rho - \frac{k}{a^2} \qquad (3)$$

and the hydrodynamical equation or the energy conservation equation

$$\frac{d\rho}{dt} = -3(\rho + p)H. \qquad (4)$$

The Friedmann equation for the scale factor

$$\frac{d^2 a}{dt^2} = -\frac{4\pi}{3} a(\rho + 3p) \qquad (5)$$

follows from the equations (3) and (4).

### *2.1. Flat model*

We start from the flat model with $k = 0$. The equation (3) provides the expression $H = (8\pi\rho/3)^{1/2}$. After substituting it into (4) we obtain a simple equation with the solution

$$\Delta t = t_0 - t_1 = -\frac{1}{2(6\pi)^{1/2}} \int_{\rho_1}^{\rho_0} \frac{d\rho}{\rho^{1/2}\left(\rho + p(\rho)\right)}. \qquad (6)$$

Here the subscript 1 corresponds to the initial parameters (i.e. $t_1$ is "now") and the subscript 0 corresponds to the parameters of the Universe in the future at time $t_0$ after a time interval $\Delta t$. We will denote the instant of time of any terminal cosmological singularity as $t_0$, and use (6) to analyse their properties. After finding the dependence $\Delta t(\rho)$ we find the inverse function $\rho(\Delta t)$ and $H(\Delta t)$, the integration of the last one gives $\ln(a)$.

The first thing to check is the finiteness of $\Delta t$. If the integral in (6) diverges we obtain $t_0 = \infty$ and this case deals with the asymptotic evolution in the future. An example of such solution is the "Little Rip".

We are going to go over all possible types of singularity. We consider three possible cases for $\rho_0$. It can be infinite, finite and nonzero, or equal to zero. Let us consider it one by one.

#### *2.1.1 Infinite terminal density*

Let us start with a well-known "Big Rip" singularity to illustrate our approach. We consider the equation of state (1). If $w = -1$ we deal with the effective cosmological constant. According to (4) in this case the density and the pressure are constant. If $w > -1$ the values of $\rho$ and $H$ decrease in time because of (4). If $w < -1$ the values of $\rho$ and $H$ increase due to (4) and become infinite at time $t_0$. Equation (6) gives us in this case the relations

$$\rho_1 = \frac{1}{6\pi(1+w)^2 \Delta t^2},\ H = \frac{2}{3|1+w|\Delta t}. \qquad (7)$$

This is the so-called "Big Rip" case. The scale factor of the Universe diverges $a \propto \Delta t^{-\frac{2}{3|1+w|}}$.

A somewhat similar case is when $w$ is not constant, but asymptotically tends to $-1$: $\rho/p \xrightarrow[\rho\to\infty]{} -1$. Let us assume that it follows the power law

$$\rho + p \xrightarrow[\rho\to\infty]{} -A\rho^{\alpha} \qquad (8)$$

with $\alpha < 1$, $A = const$. The integral in (6) is finite at $1/2 < \alpha < 1$. In this case we have the "Big Rip" with $H \propto \Delta t^{1/(1-2\alpha)}$, $\ln a \propto \Delta t^{2(1-\alpha)/(1-2\alpha)}$. It occurs later and has a sharper shape for the same initial value $\rho_1$ in comparison with the equation of state (1).

If $\alpha < 1/2$ the integral in (6) becomes divergent and we have to put $t_0 = \infty$. This is the so-called "Little Rip" introduced in (Frampton, Ludwick and Scherrer, 2012). In this case we rewrite (6) in the form

$$\Delta t = t - t_1 = -\frac{1}{2(6\pi)^{1/2}} \int_{\rho_1}^{\rho(t)} \frac{d\rho}{\rho^{1/2}\left(\rho + p(\rho)\right)}. \qquad (9)$$

This case corresponds to an eternally accelerating expansion of the Universe: $H \propto t^{1/(1-2\alpha)}$, $\ln a \propto t^{2(1-\alpha)/(1-2\alpha)}$.

In the intermediate case $\alpha = 1/2$ we must take into account a possible logarithmic divergence and consider

the equation of state with the asymptote $\rho + p \xrightarrow[\rho\to\infty]{} -A\rho^{1/2}(\ln\rho)^{\beta}$. At $\beta > 1$ we deal with the unconventional "Big Rip" with $\ln\rho \propto \Delta t^{1/(1-\beta)}$, at $\beta < 1$ we deal with the "Little Rip" with $\ln\rho \propto t^{1/(1-\beta)}$. At $\beta = 1$ we consider the equation of state with the asymptotic $\rho + p \xrightarrow[\rho\to\infty]{} -A\rho^{1/2}(\ln\rho)(\ln\ln\rho)^{\gamma}$. There is the "Big Rip" with $\ln\ln\rho \propto \Delta t^{1/(1-\gamma)}$ at $\gamma < 1$ and the "Little Rip" with $\ln\ln\rho \propto t^{1/(1-\gamma)}$ at $\gamma > 1$.

So far we considered cases with $a \xrightarrow[\rho\to\infty]{} \infty$, but this is not required. For example, a type III singularity has finite $t_0$ and $a_0$ values, but $\rho, H, |p| \xrightarrow[t\to t_0]{} \infty$. Let us consider this type of singularity. From $H = a^{-1}da/dt \xrightarrow[t\to t_0]{} \infty$ and $a(t) \xrightarrow[t\to t_0]{} a_0$ we see that $a(t)$ is regular, but $da/dt$ diverges at $t = t_0$. This is possible if the scale factor has a power-law asymptote

$$a(t) \xrightarrow[t\to t_0]{} a_0 - B(t_0 - t)^{\lambda} \tag{10}$$

with $0 < \lambda < 1$. This yilds $H \xrightarrow[t\to t_0]{} \lambda B(t_0 - t)^{\lambda-1}/a_0$. From (3) we obtain for this case $\rho(t) \propto (t_0 - t)^{2(\lambda-1)}$. After substituting these expressions in (4) we get $\rho(t) + p(t) \propto (t_0 - t)^{\lambda-2}$. This corresponds to the equation of state (8) with $\alpha = \frac{2-\lambda}{2-2\lambda}$, $\lambda = \frac{2\alpha-2}{2\alpha-1}$. In this case $\alpha > 1$ and $|p| \propto \rho^{\alpha} \gg \rho$ in the vicinity of the singularity.

Let us consider this type of singularity directly from (6). If $\rho \xrightarrow[t\to t_0]{} \infty$ but $\rho/p \xrightarrow[\rho\to\infty]{} 0$, e.g. $p(\rho) \xrightarrow[\rho\to\infty]{} -A\rho^{\alpha}$ with $\alpha > 1$, $A = const$ we also have a singularity with $H \propto \Delta t^{1/(1-2\alpha)}$, $\ln a \propto \Delta t^{2(1-\alpha)/(1-2\alpha)} = \Delta t^{\lambda}$. Note that at $\alpha < 1$ we get the "Big Rip" case considered above. But in the case of the "Big Freeze" singularity the scale factor tends to some constant value.

If we deal with the power law (10) for the scale factor with some noninteger $\lambda > 1$ we have no "Big Freeze" singularity, but some higher derivatives of $H$ diverge. If $1 < \lambda < 2$ both parts of the Friedmann equation (5) diverge, if $\lambda > 2$ both of them tend to zero. This case corresponds to $\rho \xrightarrow[t\to t_0]{} 0$, $|p| \xrightarrow[t\to t_0]{} \infty$ and we will consider it later.

Is a version of the "Big Freeze" with $t_0 = \infty$ possible? It could be named the "Little Freeze" similarly to the situation with the "Big Rip" and the "Little Rip". In this case instead of (10) we consider an asymptotic behaviour of the scale factor in the form $a(t) \xrightarrow[t\to\infty]{} a_0 - Bt^{\lambda}$ with $\lambda < 0$. According to (3) and (4) we have in this case $\rho(t) \propto t^{2\lambda-2} \xrightarrow[t\to\infty]{} 0$ and $p(t) \propto t^{\lambda-2} \xrightarrow[t\to\infty]{} 0$. This possibility will be considered later, too.

*2.1.2 Finite terminal density*

Let us consider singularities with a nonsingular $\rho \xrightarrow[t\to t_0]{} \rho_0 \neq 0$. In this case all nontrivial solutions require $p + \rho$ factor to diverge or vanish according to (6). In the first case $|p| \to \infty$, the second one corresponds to the crossing the line $\rho + p = 0$. It corresponds to the equation of state of the cosmological constant, separating the phantom energy domain with an effective $w < -1$ from the domain of not so exotic matter $w > -1$. We will see that the possibility of such crossing depends on the parameters of the equation of state.

We start with considering solutions with finite $t_0$. Both cases could be described by a single power-law asymptote of the equation of state

$$\rho + p(\rho) \xrightarrow[\rho\to\rho_0]{} C(\rho - \rho_0)^{\mu} \tag{11}$$

with $C = const$.

At $\mu < 0$ the modulus of the pressure tends to infinity, at $\mu > 0$ the $\rho + p$ reaches zero. The finiteness of $t_0$ is possible only at $\mu < 1$. In this case we have $\rho(t) - \rho_0 \propto \Delta t^{1/(1-\mu)}, \rho(t) + p(t) \propto \Delta t^{\mu/(1-\mu)}$. The singularity with $\mu < 0$ and $|p| \xrightarrow[\rho\to\rho_0]{} \infty$ is referred to as the type II or sudden singularity. The value of $H$ tends to finite $H_0$, so the scale factor linearly increases.

The achievement of $\rho + p = 0$ condition in finite time is possible if $0 < \mu < 1$. Thus, the Universe can change the type of its equation of state from phantom energy to a more ordinary one, but only for such kind of the asymptote of the equation of state.

At $\mu > 1$ we obtain $t_0 = \infty$, i.e. the asymptotic approximation of $\rho + p = 0$ condition. The evolution of such a Universe at the terminal stage practically coincides with the evolution of the flat Universe with a cosmological constant and without any other types of matter. There is no spacetime singularity in this case. Using the approximation (11) we obtain the asymptotes $\rho(t) - \rho_0 \propto t^{1/(1-\mu)}, \rho(t) + p(t) \propto t^{\mu/(1-\mu)} \to 0$ at $t \to \infty$. This solution can mimic the $\Lambda$CDM model.

*2.1.3 Zero terminal density*

This last possibility assumes $\rho_0 = H_0 = 0$, which means that a scale factor tends to some extremum. But this does not means an asymptotic expansion or contraction of the Universe is impossible. One simple example is the case $a \propto t^{\eta}$, $0 < \eta < 1$ when the Universe keeps expanding, but $H$ decreases and tends to zero.

Let us consider the power-law asymptote of the equation of state

$$\rho + p \xrightarrow[\rho\to 0]{} -D\rho^{\nu} \tag{12}$$

and substitute it into (6). The integral in (6) is finite at $\nu < 1/2$, which yilds finite $t_0$. In this case $\rho \propto \Delta t^{2/(1-2\nu)} \xrightarrow[t\to t_0]{} 0$, $H \propto \Delta t^{1/(1-2\nu)} \xrightarrow[t\to t_0]{} 0$, $\rho + p \propto \Delta t^{2\nu/(1-2\nu)}$. If $0 < \mu < 1/2$, pressure tends to zero. This is a type IV singularity. If $\lambda = 1 + 1/(1 - 2\nu)$ is a noninteger number, the higher derivatives of $H \propto \Delta t^{\lambda-1}$ diverge. The condition $0 < \mu < 1/2$ means $\lambda > 2$, so the first derivative of $H$ is finite, as well as both sides of the Friedmann equation (5). The value of

Table 1: Possible cosmological singularities except "Big Bang" and "Big Crunch"

| T | Nickname | EoS | $\rho_0$ | $\lvert p_0\rvert$ | $p_0+\rho_0$ | $a_0$ | $\rho$ | $p+\rho$ | $a$ |
|---|---|---|---|---|---|---|---|---|---|
| | | | | $t\to t_0$, $\Delta t=t_0-t\to 0$ | | | | | |
| I | "Big Rip" | (1), $w<-1$ | $\infty$ | $\infty$ | $-\infty$ | $\infty$ | $\propto\Delta t^{-2}$ | $\propto\Delta t^{-2}$ | $a\propto\Delta t^{-2/(3\lvert 1+w\rvert)}$ |
| I | "Big Rip" | (8), $1/2<\alpha<1$ | $\infty$ | $\infty$ | $-\infty$ | $\infty$ | $\propto\Delta t^{2/(1-2\alpha)}$ | $\propto\Delta t^{2\alpha/(1-2\alpha)}$ | $\ln a\propto\Delta t^{2(1-\alpha)/(1-2\alpha)}$ |
| III | "Big Freeze" | (8), $\alpha>1$ | $\infty$ | $\infty$ | $-\infty$ | $a_0$ | $\propto\Delta t^{2/(1-2\alpha)}$ | $\propto\Delta t^{2\alpha/(1-2\alpha)}$ | $\lambda=(2\alpha-2)/(2\alpha-1)$ |
| II | "sudden" | (11), $\mu<0$ | $\rho_0$ | $\infty$ | $-\infty$ | $a_0$ | $\rho-\rho_0\propto\Delta t^A$ | $\propto\Delta t^{\mu A}$ | $a\to a_0-H_0\Delta t$ |
| IV | | (12), $0<\nu<1/2$ | 0 | 0 | 0 | $a_0$ | $\propto\Delta t^{2/(1-2\nu)}$ | $\propto\Delta t^{2\nu/(1-2\nu)}$ | $\lambda=(2-2\nu)/(1-2\nu)$ |
| New | "Big Squeeze" | (12), $\nu<0$ | 0 | $\infty$ | $-\infty$ | $a_0$ | $\propto\Delta t^{2/(1-2\nu)}$ | $\propto\Delta t^{2\nu/(1-2\nu)}$ | $\lambda=(2-2\nu)/(1-2\nu)$ |
| | | | | $t\to\infty$ | | | | | |
| | "Little Rip" | (8), $0<\alpha<1/2$ | $\infty$ | $\infty$ | $-\infty$ | $\infty$ | $\propto t^{2/(1-2\alpha)}$ | $\propto t^{2\alpha/(1-2\alpha)}$ | $\ln a\propto t^{2(1-\alpha)/(1-2\alpha)}$ |
| | "Little Rip" | (8), $\alpha<0$ | $\infty$ | $\infty$ | 0 | $\infty$ | $\propto t^{2/(1-2\alpha)}$ | $\propto t^{2\alpha/(1-2\alpha)}$ | $\ln a\propto t^{2(1-\alpha)/(1-2\alpha)}$ |
| | "Little Freeze" | (12), $1/2<\nu<1$ | 0 | 0 | 0 | $a_0$ | $\propto t^{2/(1-2\nu)}$ | $\propto t^{2\nu/(1-2\nu)}$ | $a\to a_0-Bt^B$ |
| | "Little Freeze" | (12), $\nu>1$ | 0 | 0 | 0 | $\infty$ | $\propto t^{2/(1-2\nu)}$ | $\propto t^{2\nu/(1-2\nu)}$ | $\ln a\propto t^{2(\nu-1)/(2\nu-1)}$ |

$\lambda$ is the same as in (10). We can introduce the effective barotropic index $w=p/\rho\propto\Delta t^{(2\nu-2)/(1-2\nu)}\to\infty$.

If $\mu<0$ we have $|p|\xrightarrow[t\to t_0]{}\infty$. This is a new type of the future singularity, which we name "Big Squeeze". It combines certain properties of the sudden singularity and the type IV singularity. It corresponds to $1<\lambda<2$ in (10). The first derivative of $H$ and both sides of the Friedmann equation (5) diverge. The asymptotics near this singularity type are $\rho\propto\Delta t^{2/(1-2\nu)}\xrightarrow[t\to t_0]{}0$, $H\propto\Delta t^{1/(1-2\nu)}\xrightarrow[t\to t_0]{}0$, $|p|\propto\Delta t^{2\nu/(1-2\nu)}\xrightarrow[t\to t_0]{}\infty$, $a\xrightarrow[t\to t_0]{}a_0+const\Delta t^{(2-2\nu)/(1-2\nu)}\to a_0$. It requires the equation of state (12) with negative $\nu$. The example is the generalized Chaplygin gas which occurs in some cosmological theories.

At $1/2<\nu<1$ the integral in (6) diverges and $t_0=\infty$. In this case $\rho\propto t^{2/(1-2\nu)}\xrightarrow[t\to\infty]{}0$, $H\propto t^{1/(1-2\nu)}\xrightarrow[t\to\infty]{}0$, $\rho+p\propto t^{2\nu/(1-2\nu)}\xrightarrow[t\to\infty]{}0$, $a\xrightarrow[t\to\infty]{}a_0-Bt^{(2\nu-2)/(2\nu-1)}$. This is the mentioned above solution which could be named the "Little Freeze". In this case the effective barotropic index $w=p/\rho\propto t^{(2\nu-2)/(1-2\nu)}\to\infty$.

At $\nu=1/2$ we can take into account the possible logarithmic factor and consider the asymptotic equation of state $\rho+p\xrightarrow[\rho\to 0]{}-D\rho^{1/2}(\ln\rho)^\beta$. At $\beta>1$ we deal with the unconventional type IV singularity with $\ln\rho\propto\Delta t^{1/(1-\beta)}$, at $\beta<1$ we deal with the "Little Freeze" with $\ln\rho\propto t^{1/(1-\beta)}$. At $\beta=1$ we consider the equation of state with the asymptotic $\rho+p\xrightarrow[\rho\to 0]{}-A\rho^{1/2}(\ln\rho)(\ln\ln\rho)^\gamma$, etc.

At $\nu>1$ we deal with the expanding Universe and $\ln a\propto t^{(2\nu-2)/(2\nu-1)}\xrightarrow[t\to\infty]{}\infty$ at $D>0$ in spite of $H\propto t^{1/(1-2\nu)}\xrightarrow[t\to\infty]{}0$. This is the new "Little Freeze" case. The higher derivatives of $H$ diverge. At $\nu=1$ the Universe expands according to power law $a\propto t^{2/3D}$. The effective barotropic index $w=p/\rho\to-1$.

*2.2. Open and closed models*

The second term in the right-hand side of (3) does not affects the properties of the singularities with $\rho,H\to\infty$ and $\rho\to\rho_0\neq 0, H\to H_0\neq 0$. The only exception is the "Big Crunch" singularity with $a\to 0$ which we do not study in this paper.

But we must revise a possibility of the existence and the properties of singularities with $H\to 0$ or $\rho\to 0$. A simple analysis shows that in all cases we have no new type of singularity. The equation of state (12) with $\nu<1$ could provide the type IV or the "Big Squeeze" singularities only for the flat model.

## 3. Conclusion

We tabulate all main cases of the cosmological singularities in Table 1. T and EoS mean type and equation of state, $\lambda$ corresponds to (10), $A=1/(1-\mu)$, $B=2(1-\nu)/(1-2\nu)$. The terminal values denoted $\rho_0$ and $a_0$ are finite and nonzero. Note that the "Big Squeeze" and the type IV cases are possible only for the flat Universe. The asymptote (11) of the equation of state at $0<\mu<1$ corresponds to changing the type of energy from phantom one to ordinary one or vice versa. At $\mu>1$ it provides an eternal near-ΛCDM expansion of the Universe.

*Acknowledgements.* Publications are based on the research provided by the grant support of the State Fund For Fundamental Research (project F64/42-2015).

## References

Caldwell R.R., Kamionkowski M., Weinberg N.N.: 2003, *Phys. Rev. Lett.*, **91**, 071301.

Nojiri S., Odintsov S.D., Tsujikawa S.: 2005, *Phys. Rev. D*, **71**, 063004.

Frampton P.H., Ludwick K.J., Scherrer R.J.: 2011, *Phys. Rev. D*, **84**, 083001.

# ON THE MECHANISM OF THE FORMATION OF MAGNETO-HYDRODYNAMIC VORTICES IN THE SOLAR PLASMA

E. A. Pashitskii

Institute of Physics, National Academy of Sciences of Ukraine,
pr. Nauki 46, Kyiv, 03680 Ukraine, *pashitsk@iop.kiev.ua*

ABSTRACT. Based on the magnetohydrodynamic (MHD) equations for an incompressible conductive viscous fluid, the possible mechanism of the formation of giant MHD vortices recently discovered in the solar atmosphere (chromosphere) is analyzed. It is assumed that these vortices arise in the regions of the solar surface (photosphere) with ascending flows of hot plasma that arrives from the inner regions of the Sun as a result of thermal convection and is accelerated upward under the action of the chromospheric plasma pressure gradient. It is shown that, under the assumption of plasma incompressibility and flow continuity, the ascending plasma flows induce converging radial plasma flows, which create the convective and Coriolis nonlinear hydrodynamic forces due to the nonzero initial vorticity of the chromospheric plasma caused by Sun's rotation. The combined action of these two forces leads to the exponential acceleration of the solid-body rotation of plasma inside the ascending flow, thereby creating a vortex that generates an axial magnetic field, in agreement with astrophysical observations.

**Keywords:** solar plasma, MHD vortex

## 1. Introduction

Recent publication [1] reported observation of cylindrically symmetric vortex structures with characteristic radii of $R \approx 500$ km in the solar atmosphere in the UV spectral region. There may be more than $10^4$ such structures simultaneously on the Sun's surface. These vortices penetrate through the entire chromosphere reaching the lower layers of the solar corona at an altitude of 2500 km. The existence of such magnetohydrodynamic (MHD) vortices, which were earlier predicted in [2–4], is now confirmed by means of precision optical measurements of the Doppler shifts of the absorption lines of iron, calcium, and helium ions [5] corresponding to the vortex motion of the chromospheric plasma with velocities on the order of 4 km/s. It was suggested in [1] that such MHD vortices could be responsible for the heating of the corona plasma up to temperatures of several million degrees due to dissipation of the energy of Alfvén [6–10] and magnetosonic [11] waves excited by the vortex plasma motion. In [1], vortex structures were simulated numerically by using the MHD equations for a perfectly conducting ideal incompressible fluid with allowance for the processes of radiative energy transfer. It was assumed in [1] that an MHD vortex is accelerated due to its radial compression by converging plasma flows, provided that the initial angular momentum of the vortex is conserved.

However, as will be shown below, an MHD vortex in plasma cannot be regarded as a conservative system in which the angular momentum is constant, because there is a permanent influx of matter with a nonzero vorticity into the vortex core from the surrounding chromospheric plasma, i.e., such a vortex is an open nonequilibrium system. As a result, the mechanism of the formation and evolution of an MHD vortex in the solar chromosphere cannot be considered completely established. In the present work, we analyze a possible mechanism of the formation of an MHD vortex in the solar chromosphere and the accompanying generation of magnetic fields and ohmic heating of the chromospheric plasma in the framework of an approximate description based on the MHD equations for an incompressible viscous fluid with a finite conductivity [12]. It is assumed that such vortices are initiated by the ascending flows of hot plasma that arise in some "hot spots" on the Sun's surface, i.e., in the regions of the photosphere where hot plasma rises from the inner regions of the Sun as a result of convection. This hot plasma expands and rapidly flows upwards in the gravitational field through the surrounding colder chromospheric plasma, whose pressure rapidly drops with altitude. Under the conditions of the flow continuity and plasma incompressibility, the ascending vertical flow creates converging radial flows. At a nonzero initial vorticity of the chromospheric plasma caused by the Sun's rotation, such converging flows give rise to convective and Coriolis nonlinear hydrodynamic forces. The combined action of these two forces leads to the acceleration of the solid–body rotation of plasma in the core of the MHD vortex, similar to the mechanism of the formation of air vortices in the Earth's atmosphere (such as whirlwinds, tornadoes, and typhoons) earlier analyzed in [13]. Here, we analyze axisymmetric vortex solutions to the nonlinear MHD equations with separable variables that satisfy the continuity equation and cause the kinematic and magnetic viscosities of an incompressible conductive fluid to vanish. Such solutions satisfy the principle of the minimum entropy generation in an open nonequilibrium system [13], i.e., correspond to the minimum dissipation rate of the kinetic and magnetic energies of the MHD vortex. It is shown that the vortex state is characterized by the exponential growth of both the azimuthal rotation velocity of the MHD vortex and the axial magnetic field, which qualitatively agrees with the observations [14,15] of the local concentration of the magnetic field under vortex motion of the solar plasma.

Such a growing magnetic field generates an azimuthal electric current in the external shell of the MHD vortex, which should lead to the ohmic heating of plasma in the chromosphere and lower layers of the solar corona. It is shown that, due to the instability of the growing tangential discontinuity of the azimuthal velocity at the boundary of the vortex core, strong local turbulence with an anomalously high viscosity develops in the surface layer, which leads to the dissipation of MHD vortices.

## 2. Basic equations for the description of MHD vortices in the solar chromosphere

To describe MHD vortices in the solar chromosphere, we will use the well-known set of MHD equations for an incompressible viscous conductive fluid [14].

We note that the MHD approximation can be used to describe electron--ion plasma only if the cyclotron radii of ions and electrons, as well as their Debye screening lengths and their free path lengths along the magnetic field, are smaller than the characteristic spatial scales of the problem (in particular, the MHD vortex dimensions). Such an approximation can also be used to describe a weakly ionized plasma with a high particle collision frequency and low electric conductivity. At the same time, plasma in a magnetic field can be assumed to be incompressible if the velocity of its macroscopic motion is lower than both the adiabatic sound speed $c_s = \sqrt{\Gamma P/\rho}$ (where $\Gamma$ is the adiabatic index) and the Alfvén velocity $c_A = H/\sqrt{4\pi\rho}$.

Let us analyze cylindrical axisymmetric (i.e., independent of the azimuthal angle $\varphi$) vortex flows of a conductive fluid (plasma) in which the self-consistent magnetic field has only the azimuthal and axial components, $\mathbf{H}(0, H_\varphi, H_z)$. In this case, the set of MHD equations in cylindrical coordinates with allowance for the gravity acceleration $g$ (which is directed vertically downward, i.e., in negative $z$ direction) takes the form

$$\frac{\partial \upsilon_r}{\partial t} + \upsilon_r \frac{\partial \upsilon_r}{\partial r} + \upsilon_z \frac{\partial \upsilon_r}{\partial z} - \frac{\upsilon_\varphi^2}{r} = -\frac{1}{\rho}\frac{\partial}{\partial r}\left(P + \frac{H_\varphi^2 + H_z^2}{8\pi}\right) + \frac{H_\varphi^2}{4\pi\rho r} + \nu \cdot \Delta \upsilon_r, \quad (1)$$

$$\frac{\partial \upsilon_\varphi}{\partial t} + \upsilon_r \frac{\partial \upsilon_\varphi}{\partial r} + \upsilon_z \frac{\partial \upsilon_\varphi}{\partial z} + \frac{\upsilon_r \upsilon_\varphi}{r} = \frac{1}{4\pi\rho} H_z \frac{\partial H_\varphi}{\partial z} + \nu \cdot \Delta \upsilon_\varphi, \quad (2)$$

$$\frac{\partial \upsilon_z}{\partial t} + \upsilon_r \frac{\partial \upsilon_z}{\partial r} + \upsilon_z \frac{\partial \upsilon_z}{\partial z} = -\frac{1}{\rho}\frac{\partial}{\partial z}\left(P + \frac{H^2}{8\pi}\right) - g + \frac{1}{4\pi\rho} H_z \frac{\partial H_z}{\partial z} + \nu \cdot \Delta \upsilon_z, \quad (3)$$

$$\frac{\partial H_\varphi}{\partial t} + \upsilon_r \frac{\partial H_\varphi}{\partial r} + \upsilon_z \frac{\partial H_\varphi}{\partial z} = H_z \frac{\partial \upsilon_\varphi}{\partial z} + \frac{\upsilon_r H_\varphi}{r} + \nu_m \cdot \Delta H_\varphi, \quad (4)$$

$$\frac{\partial H_z}{\partial t} + \upsilon_r \frac{\partial H_z}{\partial r} + \upsilon_z \frac{\partial H_z}{\partial z} = H_z \frac{\partial \upsilon_z}{\partial z} + \nu_m \cdot \Delta H_z, \quad (5)$$

where $\upsilon_r$, $\upsilon_\varphi$, and $\upsilon_z$ are the radial, azimuthal, and axial components of the hydrodynamic velocity of the fluid, respectively, $\nu$ and $\nu_m$ are the kinematic and magnetic viscosities, and the Laplace operator is

$$\Delta = \frac{\partial^2}{\partial r^2} + \frac{1}{r}\frac{\partial}{\partial r} + \frac{\partial^2}{\partial z^2}. \quad (6)$$

We note that terms $\upsilon_\varphi^2 / r$ and $\upsilon_r \upsilon_\varphi / r$ on the left-hand side of equations (1) and (2) describe the centrifugal force and the local Coriolis nonlinear hydrodynamic force, respectively.

In this case, the continuity equation for an incompressible fluid, $\mathrm{div}\,\boldsymbol{\upsilon} = 0$, and Maxwell's equation for the solenoidal magnetic field, $\mathrm{div}\,\mathbf{H} = 0$, take the form

$$\frac{\partial \upsilon_r}{\partial r} + \frac{\upsilon_r}{r} + \frac{\partial \upsilon_z}{\partial z} = 0; \quad \frac{\partial H_z}{\partial z} = 0. \quad (7)$$

The simplest formal solutions to Eqs. (7) with the separable variables $r$ and $z$ in the region $r \le R_0$ have the form

$$\upsilon_r(r) = -\beta \cdot r; \quad \upsilon_z(z) = \upsilon_{z0} + \alpha \cdot z; \quad H_z = h = const. \quad (8)$$

where the parameters $\alpha$ and $\beta$ are related by the formula

$$(\alpha - 2\beta) = 0. \quad (9)$$

## 3. Ascending flows of plasma in solar chromosphere

The expression for the radial velocity $\upsilon_r(r)$ in Eq. (8) describes an incompressible radial plasma flow converging toward the axis that is induced by the ascending plasma flow the axial velocity of which increases linearly along $z$ axis, $\upsilon_z(z) = \upsilon_{z0} + \alpha z$. According to time-independent equation (3),

$$\upsilon_z \frac{\partial \upsilon_z}{\partial z} = -\frac{1}{\rho}\frac{\partial P}{\partial z} - g + \nu \frac{\partial^2 \upsilon_z}{\partial z^2}, \quad (10)$$

such a velocity can appear under the action of the pressure $P$, which decreases with altitude according to the square law

$$P(z) = P_0 - \rho(az + bz^2), \quad (11)$$

where $a = (\alpha \upsilon_{z0} + g)$ and $b = \alpha^2 / 2$. As will be shown below, such a dependence of the pressure on $z$ can occur in the gravitational field at relatively low altitudes, provided that the plasma temperature sufficiently fast drops with altitude.

Let us suppose that hot plasma in a certain region of radius $R_0$ in the solar photosphere flows up due to thermal convection in the gravitational field. This plasma expands and flows upward under the action of the buoyancy force in the colder denser chromospheric plasma. As the plasma flows up and expands, it plasma cools down, so that its temperature in the initial stage decreases almost linearly with altitude,

$$T(z) \approx T_0 \cdot (1 - \chi z); \qquad \chi = -\left(\frac{\partial \ln T}{\partial z}\right)_{z=0} > 0. \quad (12)$$

In this case, to within second-order terms in $z$, the barometric formula for the pressure of the chromospheric plasma in the Sun's gravitational field takes the form

$$P(z) = P_0 \cdot \exp\left\{-\frac{mgz}{k_B T(z)}\right\} \approx P_0 \cdot \left[1 - \frac{mgz}{k_B T_0} - \frac{mg}{k_B T_0}\left(\chi - \frac{mg}{2k_B T_0}\right)z^2\right]. \quad (13)$$

For $\chi > mg/2k_B T_0$, this formula coincides with the adopted dependence (11) of the pressure on the $z$ coordinate if we set $a = P_0 \cdot mg/k_B T_0$ and $b = (\chi - mg/2k_B T_0)\cdot a$ (where $m$ is the mass of a hydrogen atom). As a result, we obtain two equations for determining two parameters, $\upsilon_{z0}$ and $\alpha$, entering into the expression for the increasing velocity of the ascending flow,

$$\alpha\upsilon_{z0} = g\cdot\left(\frac{c_s^2}{\Gamma}\frac{m}{k_B T_0} - 1\right) > 0, \qquad \alpha^2 = \frac{mg}{k_B T_0}\cdot\left(2\chi - \frac{mg}{k_B T_0}\right) > 0. \quad (14)$$

Taking into account the parameters of plasma in the lower layers of the solar chromosphere ($c_s \approx 10$ km/s and $T_0 \approx 6000$ K) and the value of the gravity acceleration on the Sun's surface ($g \approx 274$ m/s$^2$), we obtain $\alpha\upsilon_{z0} \approx 57.5$ m/s$^2$ and $mg/k_B T_0 \approx 5.5\cdot 10^{-6}$ m$^{-1}$. However, in this case, the parameter $\chi$, which has the dimension of the reciprocal length and characterizes the cooling rate of hot plasma with altitude, remains undefined, due to which the values of $\alpha$ and $\upsilon_{z0}$ cannot be estimated independently (see below).

Note that the radius $R_0$ of the ascending flow should increase with altitude, which prevents separation of the variables $r$ and $z$ in the MHD equations. However, if the longitudinal inhomogeneity scale $L$ of the plasma flow radius is much larger than $R_0$, then, with a high degree of precision, we can set $R_0 = const$, which substantially simplifies the problem and allows us to investigate the main physical processes affecting the dynamics and evolution of MHD vortices in the solar atmosphere by means of an approximate procedure of separation of variables without recourse to complicated computer simulations.

## 4. Solid-body vortex rotation of plasma

Let's assume that at $r \le R_0$ the azimuthal components of the velocity and magnetic field are independent of $z$ and have the form

$$\upsilon_\varphi(r) = \omega\cdot r; \quad H_\varphi(r) = \gamma\cdot r. \quad (15)$$

After the substitution of expressions (8) and (15) into Eqs. (1)–(5), a large number of terms on the right-hand sides (including those containing Laplace operator (6)) vanish. This corresponds to the zero kinematic and magnetic viscosities of the incompressible conductive fluid (plasma), i.e., in fact to the nondissipative solid-body rotation of the MHD vortex core at $r < R_0$.

Substituting Eqs. (8) and (15) into Eqs. (1), (2), (4), and (5) and assuming that the parameters $\gamma, \omega$ and $h$ are functions of $t$, we obtain the following set of first-order equations that describe the dynamics of the MHD vortex core:

$$\omega^2(t) - \beta^2 = \frac{1}{r\rho}\cdot\frac{\partial P}{\partial r} + \frac{\gamma^2(t)}{2\pi\rho}, \quad (16)$$

$$\frac{d\omega}{dt} - 2\beta\cdot\omega(t) = 0, \quad (17)$$

$$\frac{dh}{dt} - \alpha\cdot h(t) = 0. \quad (18)$$

In this case, Eq. (4) is reduced to the condition $d\gamma/dt = 0$, which is a consequence of the mutual compensation of the nonlinear terms $\upsilon_r \partial H_\varphi/\partial r$ and $\upsilon_r H_\varphi/r$ on the right- and left-hand sides of Eq. (4). This allows us to neglect the azimuthal component of the self-consistent magnetic field $H_\varphi$ in the MHD vortex.

Since, according to Eq. (9), we have $\alpha = 2\beta$, solutions to Eqs. (17) and (18) have the form

$$\omega(t) = \omega(0)\cdot e^{\alpha t}, \quad h(t) = h(0)\cdot e^{\alpha t}, \quad (19)$$

where $\omega(0)$ and $h(0)$ are the initial values of the angular plasma rotation velocity and axial magnetic field, respectively.

Equation (16) governs spatial distribution and temporal behavior of plasma pressure in the core of the MHD vortex, which has the following form in the cyclostrophic regime of rotation of an incompressible fluid:

$$P(r,z,t) = \tilde{P}_0 + \frac{\rho r^2}{2}\left[\omega^2(t) + \omega^2(0) - \beta^2\right] - \frac{\rho z^2}{2}\alpha^2(t) - \rho z\tilde{g}, \quad (20)$$

where $\tilde{P}_0$ is the pressure at the vortex axis (see below), and $\tilde{g} = g + \upsilon_{z0}\alpha$.

## 5. Exponential regime of MHD vortex evolution

It follows from Eq. (19) that the angular velocity of the solid-body rotation of the MHD vortex core and the axial component of the self-consistent magnetic field increase exponentially with a characteristic time of $t_{exp} = 1/\alpha$.

We see that the source of the exponential acceleration of the vortex core rotation is the linear increase in the axial velocity of the ascending flow of incompressible plasma, $\upsilon_z(z) = (\upsilon_{z0} + \alpha z)$, as it propagates upward in the gravitational field of the Sun through the solar chromosphere, in which the temperature and pressure decrease with increasing altitude.

The value of $\alpha$ can be estimated by equating the velocity of the ascending flow $\upsilon_z(z) = \upsilon_{z0} + \alpha z$ to the speed of sound at the upper boundary of the solar chromosphere,

$L \approx 2500$ km. In the rarefied upper layers of the chromospheric plasma, the speed of sound is $\tilde{c}_s = \sqrt{2k_B\tilde{T}/m}$, where $\tilde{T} \approx 3\cdot10^4$ K, so that $\tilde{c}_s \approx 20$ km/s. Assuming that $\upsilon_{z0} \le \tilde{c}_s$, we find that $\alpha \le \tilde{c}_s / L \approx 8\cdot10^{-3}$ s$^{-1}$ and the characteristic time of the exponential evolution of the MHD vortex is $t_{\exp} \ge L/\tilde{c}_s \approx 2$ min.

It should be noted that the exponential growth of the axial magnetic field $H_z(t) = h(t)$ qualitatively agrees with the local concentration of the magnetic field during the vortex motion of the chromospheric plasma observed in [14, 15]. In this case, the local Alfvén velocity $c_A(t) = H_z(t)/\sqrt{4\pi\rho}$ inside the vortex core grows exponentially in time (see (19)).

According to expression (20), the plasma pressure on the vortex axis at $z = 0$ in the cyclostrophic regime of vortex rotation is

$$\tilde{P}_0(0,t) \approx P_0 - \frac{\rho R_0^2}{2}\cdot\omega^2(t)\,. \qquad (21)$$

According to Eqs. (19) and (21), this pressure decreases exponentially in time and vanishes at the time

$$t_0 = \frac{1}{2\alpha}\cdot\ln\left[\frac{2P_0}{\rho R_0^2\cdot\omega^2(0)}\right] \approx \frac{1}{\alpha}\cdot\ln\left(c_s/V_0\right), \qquad (22)$$

where $V_0 = R_0\cdot\omega(0)$ is the initial azimuthal velocity of the vortex motion of plasma ($V_0 \ll c_s$). Since the negative pressure in the system leads to instability (collapse), an MHD vortex cannot exist at $t > t_0$. The time $t_0$ can be approximately estimated if we assume that, in the order of magnitude, the initial value of the angular velocity $\omega(0)$ coincides with the average solar atmosphere vorticity caused by the nonuniform (liquid-like) rotation of the Sun's surface with the angular velocity varying with latitude from $\Omega \approx 1/28$ day on the equator to $\Omega \approx 1/33$ day at a latitude of $75°$. Estimates show that the initial vorticity is $\omega(0) \approx 2\cdot10^{-6}$ s$^{-1}$, which is one order of magnitude higher than the vorticity caused by the global Coriolis force on the solar surface.

As a result, the initial azimuthal velocity of plasma at the boundary of a vortex of radius $R_0 \approx 500$ km is $V_0 \approx 1$ m/s. Taking into account that the density of the chromospheric plasma on the Sun's surface is on the order of $\rho \approx 5\cdot10^{-9}$ g/cm$^3$ and the temperature is $T \approx 6000$ K and assuming that the density of hydrogen atoms is $n \approx 3\cdot10^{15}$ cm$^{-3}$, we find using the approximation of an ideal gas that the speed of sound is $c_s \approx 10$ km/s. Hence, with allowance for the above estimate of $\alpha$ and disregarding dissipation of the vortex kinetic energy (see below), we find that the maximum time of the exponential evolution of an MHD vortex is $t_0 \approx 15/\alpha \approx 30$ min.

On the other hand, it should be taken into account that the solid-body rotation of the vortex core begins to decelerate when the azimuthal velocity at $r = R_0$ becomes comparable with the speed of sound, because, at such velocities, the compressibility effects come into play and the fluid (plasma) acquires a nonzero bulk viscosity. Therefore, taking into account the exponential growth of the rotation velocity of the vortex core, the maximum azimuthal velocity $\upsilon_\varphi^{\max}(R_0,t_s) = V_0\cdot exp(\alpha\cdot t_s) \approx c_s$ is reached over a time $t_s = 1/\alpha\cdot\ln(c_s/V_0)$, which coincides with $t_0$. We note that the velocity of the vortex motion of the chromospheric plasma determined from the Doppler shift of the spectral lines is 4 km/s, which is half as large as the speed of sound, whereas according to computer simulations, the vortex velocity at altitudes of 2500 km, where the speed of sound is $c_s \approx 20$ km/s, can reach 15 km/s.

The time $t_0 \approx t_s$ also determines the maximum values of the axial component of the magnetic field inside the vortex core, $H_z = h(0)\cdot\exp(\alpha t_0)$, and the corresponding local Alfvén velocity $c_A^{\max} = \sqrt{h^2(0)/4\pi\rho}\cdot\exp(\alpha t_0)$. Assuming that the factor in front of the exponential in the last expression is on the order of the initial vortex velocity $V_0 \approx 1$ m/s, we find that $c_A^{\max} \approx 10$ km/s. In this case, the magnetic field reaches its maximum value of $H_z^{\max} \approx 250$ G, which agrees with observational data [14, 15].

Note that the excitation of Alfvén and magnetosonic waves in the MHD vortex core cannot lead to vortex deceleration and plasma heating, because the Alfvén velocity grows according to the same exponential law as the azimuthal velocity of plasma rotation, whereas the speed of sound decreases due to a decrease in the pressure in the vortex core.

### 6. Instability of the tangential discontinuity of the azimuthal velocity and local turbulence on the surface of the MHD vortex core

The exponential growth of the angular velocity of the solid-body plasma rotation in the MHD vortex core, where the radial and axial velocities are directly proportional to the radius $r$, is caused, as was mentioned above, by the combined action of the convective and Coriolis nonlinear hydrodynamic forces, which are equal in magnitude. However, in the external region $r \ge R_0$, where the radial and azimuthal velocities are proportional to $r^{-1}$, these forces, as can be easily verified, have opposite signs and exactly balance one other. As a result, there is no acceleration of the initial vorticity $\omega(0)$. Therefore, the azimuthal velocity experiences an exponentially growing jump (tangential discontinuity) at the vortex core boundary.

As was shown for the first time in [13], the exponential growth of the velocity jump leads to the absolute instability of surface perturbations accompanied by the growth of their amplitude according to the double exponential law of the form

$$\left|\xi_k(t)\right| = \left|\xi_k(0)\right|\cdot\exp\left\{\frac{kV_0}{2\alpha}\cdot(e^{\alpha t} - \alpha t)\right\}, \qquad (23)$$

where $\xi_k(0)$ is the initial perturbation with the wavenumber $k$ at $t = 0$.

Such instability develops much faster than the exponential acceleration of the solid-body rotation of the MHD vortex core. As a result, a strongly turbulent state is rapidly established near the vortex surface. Turbulence is localized in a layer of thickness $\delta$, which is comparable with the maximum amplitude of turbulent pulsations $l^* = |\xi_k|_{\max}$. The amplitude reaches its maximum value $|\xi_\kappa|_{\max} \equiv |\xi_k(t_{\max})|$ at the time $t_{\max}$ at which the velocity of turbulent pulsations

$$\tilde{\upsilon}_k(t) \equiv \frac{d\xi_k}{dt} = |\xi_k(t)| \cdot \frac{kV_0}{2} \cdot (\exp\{\alpha t\} - 1) \qquad (24)$$

becomes equal to the speed of sound $c_s$ and the effects of compressibility and finite viscosity come into play. It is well known that the wavenumber $k$ of the most unstable surface perturbations has the same order of magnitude as the reciprocal thickness of the transition layer $1/\delta$. Hence, we have

$$l^* \approx \delta \approx |\xi_k|_{\max} \approx \pi / k_{\max} . \qquad (25)$$

At $\alpha t_{\max} \gg 1$, expression (24) yields

$$t_{\max} \approx \frac{1}{\alpha} \cdot \ln\left(\frac{c_s}{\pi V_0}\right) \le t_0 . \qquad (26)$$

Thus, the peak amplitude of turbulent pulsations cannot exceed

$$|\xi_k|_{\max} = \xi_0 \cdot \exp\left\{\frac{kV_0}{2\alpha} \cdot \exp(\alpha t_0)\right\}. \qquad (27)$$

Taking the logarithm of expression (27) with allowance for relationships (23) and (25), we obtain to within logarithmic accuracy the following transcendental equation for the characteristic scale length of turbulent pulsations $l^*$ and, accordingly, the effective width $\delta$ of the turbulent transition layer on the vortex core boundary:

$$\delta \approx \frac{c_s}{2\alpha \cdot \ln(\delta / \xi_0)} \approx \frac{600}{\ln(\delta / \xi_0)} \text{ km.} \qquad (28)$$

Assuming that the amplitude $\xi_0$ of the initial fluctuations of quasineutral plasma is on the order of the Debye screening length $D = \sqrt{k_B T / 8\pi e^2 n_e}$, which, at a chromospheric plasma temperature of $T \approx 6000$ K and an electron density of $n_e \approx 3 \cdot 10^{15}$ cm$^{-3}$, is $D \approx 10^{-5}$ cm, we find that the thickness of the turbulent region surrounding an MHD vortex is $\delta \approx 25$ km, which corresponds to $\ln(\delta / D) \approx 25$. If the amplitude of turbulent pulsations is known, then, applying the dimensionality analysis, we find that the turbulent viscosity of plasma inside the turbulent layer is $\nu^* \approx c_s \cdot l^* / 3 \approx 8 \cdot 10^7$ m$^2$/s.

The anomalously large effective viscosity of the turbulent layer improves the stability of the MHD vortex core during its evolution. In this regard, it may be supposed that the observed filamentary structure of strong solar flares is caused by the simultaneous formation of a large number of MHD vortices in the photospheric hot spots.

## 7. Deceleration of MHD vortices due to viscous energy dissipation and ohmic losses in the turbulent layer

As we mentioned above, solutions with separable variables correspond to zero kinematic and magnetic viscosities of the incompressible conductive fluid (plasma) both inside the MHD vortex core at $r \le R_0$ and in the external region $r \ge (R_0 + \delta)$. However, the kinetic energy of the vortex should dissipate inside the turbulent surface layer of thickness $\delta \ll R_0$ with an anomalously large turbulent viscosity $\nu^*$. The energy dissipation rate per unit vortex length is determined by the relationship

$$\frac{dE^*_{kin}}{dt} = -\frac{\rho\nu^*}{2} \int dV \left(\frac{\partial \upsilon_\varphi}{\partial r}\right)^2 \approx -\pi R_0 \delta \rho \nu^* \frac{R_0^2 \omega^2(t)}{\delta^2} . \qquad (29)$$

On the other hand, the kinetic energy (per unit length) of the accelerated solid-body rotation of the vortex core is determined by the expression

$$E_{kin}(t) = \pi\rho \int_0^{R_0} r dr \cdot \upsilon_\varphi^2(r,t) = \frac{\pi}{4} \rho R_0^4 \cdot \omega^2(t) . \qquad (30)$$

In this case, the growth rate of the kinetic energy of vortex rotation accelerated under the action of the convective and Coriolis hydrodynamic forces is

$$\frac{dE_{kin}}{dt} = \frac{\pi}{2} \alpha\rho R_0^4 \cdot \omega(t) \frac{d\omega}{dt} \approx \frac{\pi}{2} \alpha\rho R_0^4 \cdot \omega^2(t) . \qquad (31)$$

Comparing expressions (29) and (31), we obtain the following condition for the weak dissipation of the vortex energy: $\nu^* < \alpha \cdot R_0 \cdot \delta / 2$. For the above parameter values, $\nu^* \approx 8 \cdot 10^7$ m$^2$/s, $\alpha \approx 8 \cdot 10^{-3}$ s$^{-1}$, $R_0 \approx 500$ km, and $\delta \approx 25$ km, the left- and the right-hand sides of this inequality are nearly equal to one another, i.e., the rate of kinetic energy dissipation is nearly equal to the energy gain caused by the convective and Coriolis forces. As a result, in the final stage of evolution under the condition of strong turbulence in the surface layer, the MHD vortex reaches a regime of steady-state rotation and gradually dissipates.

There is another energy dissipation mechanism in an MHD vortex that is related to ohmic losses leading to Joule heating. The heat is generated by the electric currents induced by the growing magnetic fields that flow in plasma with a finite conductivity. According to Maxwell's equations

$$\mathrm{rot}\,\mathbf{H} = \frac{4\pi}{c} \cdot \mathbf{j}, \quad \mathrm{rot}\,\mathbf{E} = -\frac{1}{c} \frac{\partial \mathbf{H}}{\partial t} \qquad (32)$$

the generation of magnetic fields during the exponential evolution of MHD vortices should be accompanied by the generation of electric currents $\mathbf{j}$ and electric fields $\mathbf{E}$, which are related to one another via Ohm's law $\mathbf{j} = \sigma\mathbf{E}$. However, taking into account that the vortex evolution is a relatively slow process, we can consider only the first of Maxwell's equations. In particular, the axial magnetic field, which is uniform inside the vortex core and vanishes

in the transition layer of thickness $\delta$, induces the azimuthal current

$$j_\varphi(t) = -\frac{c}{4\pi}\cdot\frac{\partial H_z(t)}{\partial r} \approx -\frac{c\cdot h(t)}{4\pi\delta}. \qquad (33)$$

in this layer.

The azimuthal current of density (33) that flows inside the turbulent surface layer should lead to heat release in this layer, the power of which per unit vortex length is

$$Q \approx 2\pi R_0\delta\cdot j_\varphi^2/\sigma = c^2 R_0\cdot h^2(t)/8\pi\delta\sigma. \qquad (34)$$

Here $\sigma = e^2 n_e\cdot\tau_e/m_e$ is the electron conductivity of the chromospheric plasma with the electron density $n_e \approx 3\cdot10^{15}$ cm$^{-3}$, $m_e$ is the mass of an electron, and $\tau_e \approx 10^{-13}$ s is the average time of electron–electron and electron–ion Coulomb collisions at an electron temperature of $T_e \approx 10^4$ K. Hence, in the order of magnitude, we have $\sigma \approx 10^9$ s$^{-1}$.

As a result, setting $h(t) \approx h(0)\cdot\exp(\alpha t_0)$, we find that the Joule heating power in the final stage of MHD vortex evolution is $Q \approx 1$ MJ/km.

Joule losses must slow down the MHD vortex rotation, determined by relationships (38). The slowing down will be weak if

$$\frac{dE_{kin}(t)}{dt} = \frac{\pi}{2}\alpha\rho R_0^4\cdot\omega^2(t) \gg Q(t). \qquad (35)$$

Taking into account that the angular velocity $\omega(t)$ and the longitudinal magnetic field $h(t)$ grow according to the same exponential law, we can rewrite inequality (43) in the form

$$\frac{c^2\cdot c_A^2(0)}{\pi\alpha\cdot\delta\cdot\sigma\cdot R_0\cdot V_0^2} \ll 1, \qquad (36)$$

which shows that, for the above parameter values, $\alpha \approx 8\cdot10^{-3}$ s$^{-1}$, $\sigma \approx 10^9$ s$^{-1}$, $\delta \approx 25$ km, and $R_0 \approx 500$ km, the Joule losses weakly affect MHD vortex dynamics if $V_0 > c_{A0}$.

Due to ohmic heat release in the MHD vortex shell, additional heating and ionization of the chromospheric plasma, followed by its recombination upon cooling, take place. This should lead to the glow of MHD vortices in the visible and UV spectral regions. Since MHD vortices can reach the lower layers of the solar corona, heat released due to the ohmic heating of plasma, along with that released due to the dissipation of the magnetic and kinetic energies of vortices during their decay, can play a significant role in the heating of the solar corona to temperatures as high as $10^6$ K. However, this issue requires additional study, which goes beyond the scope of the present work.

To conclude, it should be emphasized that the initial local vorticity of the solar plasma in the regions where MHD vortices begin to form can have opposite signs, so that the vortices in different solar hemispheres can rotate in different directions. Accordingly, the self-consistent axial magnetic fields generated by such vortices should have opposite directions. Thus it can be energetically advantageous for the magnetic field lines of the adjacent pairs of such vortices and anti-vortices to be closed into loops, which are indeed often observed in solar atmosphere.

*Acknowledgements.* The author is grateful to A.B. Mikhailovskii, N.S. Erokhin, D.D. Sokolov, and A.V. Stepanov for useful discussions of the problems touched upon in this work, as well as V.I. Pentegov for his help in preparing this manuscript for publication.

**References**

1. Wedermeyer-Böhm S., Scullion E., Steiner O. et al.: 2012, Nature, **486**, 505.
2. Wedermeyer-Böhm S., van der Voort L. R.: 2009, Astron. Astrophys., **507**.
3. De Pontieu B., McIntosh S. W., Carlsson M., et al.: 2007, Science, **318**, 1574.
4. Cirtain J. W., Golub L., Lundquist L., et al.: 2007, Science, **318**, 1580.
5. Lemen J. R., Title A. M., Akin D. J., et al.: 2012, Sol. Phys., **275**, 17.
6. McIntosh S. W., De Pontieu B., Carlsson M., et al.: 2011, Nature, **475**, 477.
7. Fedun V., Shelyag S., Verth G., et al.: 2011, Ann. Geophys., **29**, 1029.
8. Van Ballegooijen A., Asgari-Targhi M., Cranmer S., DeLuca E.: 2011, Astrophys. J., **736**, 3.
9. Kitiashvili I., Kosovichev A., Mansour N., Wray A.: 2011, Astrophys. J., **727**, L50.
10. Attie R., Innes D., Potts H.: 2009, Astron. Astrophys., **493**, L13.
11. Shelyag S., Keys P., Mathioudakis M., Keenan F. P.: 2011, Astron. Astrophys., **526**, A5.
12. Landau L. D., Lifshitz E. M.: *Electrodynamics of Continuous Media* (Fizmatgiz, Moscow, 1959; Pergamon, Oxford, 1960).
13. Pashitskii E. A.: 2010, JETP, **110**, 1026.
14. Balmaceda L., Domingues S. V., Palacios J., et al.: 2010, Astron. Astrophys., **513**.
15. Zhang J., Liu Y.: 2011, Astrophys. J., **741**, L7.

# THE PROPERTIS OF TIDAL FORCES IN THE KERR METRIC

A.M.Rasulova[1,2]

[1]Theoretical Physics and Astronomy Department, The Herzen University, Moika 48 St. Petersburg, 191186, Russia,

[2]Institute of Limnology, RAS, Sevastyanov st. 9. St. Petersburg, 196105, Russia, *ARasulova@gmail.com*

ABSTRACT. The expression for the tidal forces of the two relativistic protons at a distance of the order of the Compton wavelength near a rotating black hole is found. The analysis shows that the tidal forces are dependent on the plane of incidence and sharply increase with increasing Lorentz factor.

**Keywords**: General relativity - geodesic deviation: Black hole - Kerr metric: Tidal forces.

## 1. Introduction

The problem of deviation of geodesic is important in the study of motion of n-interacting particles in strong gravitational fields and in particular, the study of the deformation of the gas and dust clouds in the vicinity of black holes.

When driving two or more closely spaced particles in curved space-time their is a deviation of geodesic lines. General view of the geodesic deviation equation of the n-dimensional Riemannian manifold was obtained by T. Levi-Civita in 1925 Ref. 1. For the 4-dimensional space deviation equation for structureless massless particles was investigated in Refs. 2–3 by J.L. Sing.

The system of units G = c = 1 is used in the paper.

## 2. The Kerr Metric

The Kerr's metric in Boyer-Lindquist coordinates has the form [4]:

$$ds^2 = \rho^2\frac{\Delta}{\Sigma^2}dt^2 - \frac{\Sigma^2}{\rho^2}\left[d\varphi - \frac{2aMr}{\Sigma^2}dt\right]^2 sin^2\theta - \frac{\rho^2}{\Delta}dr^2 - \rho^2 d\theta^2\,, \quad (1)$$

where

$$\Delta = r^2 - 2Mr + a^2\,, \quad (2)$$

$$\rho^2 = r^2 + a^2 cos^2\theta\,, \quad (3)$$

$$\Sigma^2 = (r^2+a^2)^2 - a^2\Delta sin^2\theta\,, \quad (4)$$

and M is the black hole mass, aM its angular momentum $0 \le a \le 1$. The event horizon of the Kerr's black hole corresponds to the coordinate:

$$r_h = M + \sqrt{M^2 - a^2}. \quad (5)$$

The static limit surface is defined by the value:

$$r_{st} = M + \sqrt{M^2 - a^2 cos^2\theta}\,. \quad (6)$$

The region of space-time between the static limit and the event horizon is called ergosphere.

In view of the equation (1) metric tensors are Ref.5:

$$g^{ij} = \begin{pmatrix} \Sigma^2/\rho^2\Delta & 0 & 0 & 2aMr/\rho^2\Delta \\ 0 & -\Delta/\rho^2 & 0 & 0 \\ 0 & 0 & -\frac{1}{\rho^2} & 0 \\ 2aMr/\rho^2\Delta & 0 & 0 & -(\Delta - a^2 sin^2\theta)/\rho^2\Delta sin^2\theta \end{pmatrix}. \quad (7)$$

The nonzero components of the curvature tensor in the Kerr metric have the form [5]:

$$R_{1023} = -aMcos\theta(3r^2 - a^2cos^2\theta)\frac{1}{\rho^6}\,, \quad (8)$$

$$R_{1230} = -\frac{aMcos\theta}{\rho^6}(3r^2 - a^2cos^2\theta)\Sigma^{-2} \times[(r^2+a^2)^2 + 2a^2\Delta sin^2\theta]\,, \quad (9)$$

$$R_{1302} = \frac{aMcos\theta}{\rho^6}(3r^2 - a^2cos^2\theta)\Sigma^{-2} \times[2(r^2+a^2)^2 + a^2\Delta sin^2\theta]\,, \quad (10)$$

$$-R_{3002} = R_{1213} = -\frac{aMcos\theta}{\rho^6}(3r^2 - a^2cos^2\theta) \times\frac{3a\Delta^{1/2}}{\Sigma^2}(r^2+a^2)sin\theta\,, \quad (11)$$

$$-R_{1220} = R_{1330} = -\frac{Mr}{\rho^6}(r^2 - 3a^2cos^2\theta) \times\frac{3a\Delta^{1/2}}{\Sigma^2}(r^2+a^2)sin\theta\,, \quad (12)$$

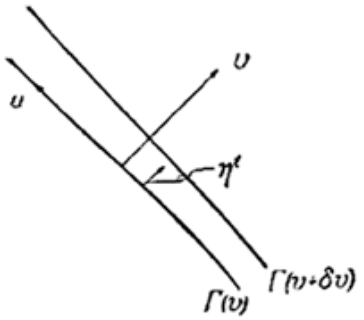


Figure 1: The deviation of curve $\Gamma(v)$ from curve $\Gamma(v+\delta v)$.

$$-R_{1010} = R_{2323} = \frac{Mr}{\rho^6}(r^2 - 3a^2 cos^2\theta) = R_{0202} + R_{0303}\,, \quad (13)$$

$$-R_{1313} = R_{0202} = \frac{Mr}{\rho^6}(r^2 - 3a^2 cos^2\theta)\Sigma^{-2} \times[2(r^2+a^2)^2 + a^2\Delta sin^2\theta]\,, \quad (14)$$

$$-R_{1212} = R_{0303} = -\frac{Mr}{\rho^6}(r^2 - 3a^2 cos^2\theta)\Sigma^{-2} \times[(r^2+a^2)^2 + 2a^2\Delta sin^2\theta]\,. \quad (15)$$

### 3. The equations of geodesic deviation

If there is a pair of adjacent curves $\Gamma(v)$ and $\Gamma(v+\delta v)$ (Fig.1 ), then the equation of geodesic deviation for structureless infinitely close particles has the form:

$$\frac{d^2\eta^i}{ds^2} + R^i_{jkm}U^j\eta^k U^m = 0\,, \quad (16)$$

where $\eta^i$ — infinitesimal vector deviation, $R^i_{jkm} = g^{il}R_{ljkm}$ — Riemann tensor, $U^m$— 4-speed.

A solution of equation (16) is a vector of deviation of world lines that covariantly describes the relative acceleration between geodesic lines.

Let us consider the equations of geodesic deviation in the Kerr metric. We find the equation of geodesic deviation for relativistic structureless particles that have only radial velocity component, hence:

$$U^i = \Gamma(1, V, 0, 0) \quad (17)$$

where $\Gamma = \frac{1}{\sqrt{1-V^2}}$ is Lorentz factor.

From the equations (16) and curvature tensor in the Kerr metric (8)—(15) in this case, the equation of the deviation will have the form:

$$\frac{D^2\eta^0}{ds^2} = \Gamma^2\left[g^{03}(R_{3002} - R_{0303}) + g^{03}V(R_{1230} + R_{1330} - R_{1302}) + V^2(g^{00}R_{1010} - g^{03}R_{1313})\right], \quad (18)$$

$$\frac{D^2\eta^1}{ds^2} = -g^{11}\Gamma^2 R_{1010}(1+V), \quad (19)$$

$$\frac{D^2\eta^2}{ds^2} = g^{22}\Gamma^2\left[R_{0202} + V(R_{1220} + R_{1302}) - R_{1212}V^2\right], \quad (20)$$

$$\frac{D^2\eta^3}{ds^2} = \Gamma^2\left[-g^{33}R_{0303} + g^{33}V(R_{1230} + R_{1330} - R_{1302}) + V^2(g^{03}R_{1010} - g^{33}R_{1313})\right]. \quad (21)$$

From these equations it is seen that the relative acceleration between the infinitely close to the world lines will be directly proportional to the square of the Lorentz factor.

To evaluate the tidal forces of the proton in the Kerr metric we use the following restrictions:

- let proton with mass $m_p = 1.67 \cdot 10^{-27}$kg is in motion along a geodesic so that the deviation is proportional to the Compton wavelength $\lambda^p_C = 1.32 \cdot 10^{-15}$m,
- let movement only occurs in the equatorial plane $\theta = \frac{\pi}{2}$,
- the black hole has the following parameters: $M = 10^6$, $a = 0.98$,
- motion occurs at a coordinate of distance of $r$ from horizon of black hole $r = 10^{-5}r_h$,
- the proton velocity is $V = (1 - 10^{-15})c$.

If we consider the assumptions given above, then calculations made by us lead to the work of the tidal forces $F = 4.156 \cdot 10^9$ Newton's. For example, the same force on the surface of the Sun is about $4.5 \cdot 10^{-26}$ Newtons.

For different values of velocities of particles obtain the tidal forces by numerical calculations for protons are given in the Fig. 2. The graph shows that the tidal forces increase with the speed of the proton in the center of mass of the order of $10^{-19}$ Newtons with $V = 0.9c$ up to $10^{19}$Newtons with $V = (1 - 10^{20})c$.

Dependence of tidal forces on the mass and the specific angular momentum of the black hole is shown in Fig. 3 and Fig. 4 respectively. It is important to note that tidal forces are maximal for black holes of stellar mass and are minimal for a supermassive black holes. For example, if the black hole mass is of about mass of Sun then it creates tidal forces near horizon order $10^{15}$ Newtons and supermassive black holes with mass $10^9 M_\odot$ creates tidal forces order $10^6$ Newtons. A similar effect was observed in Ref. 6 for a Schwarzschild

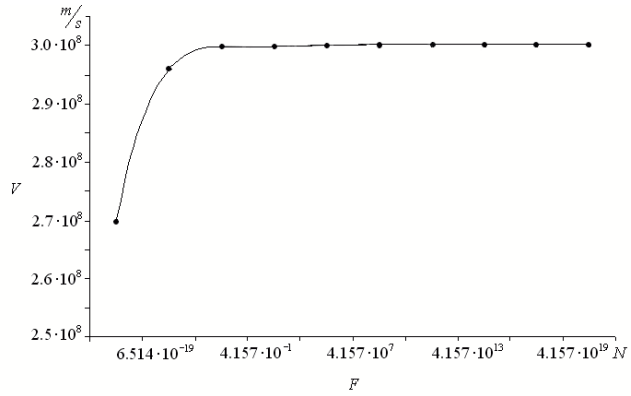


Figure 2: The dependence of the tidal force $F$ on the speed of the proton $V$.

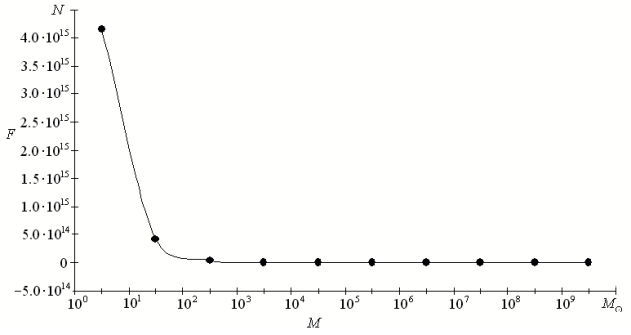


Figure 3: The dependence of the tidal force $F$ on the black hole mass $M$.

black hole. Also if there is an increase of specific angular momentum of the black hole then there is an increase of the tidal forces near the horizon.

*Acknowledgements.* The author expresses her sincere gratitude to her research supervisor Professor Andrei Grib for the problem statement and numerous discussions. The work was supported by Russian Foundation for Basic Research, grant 15-02-06818-a.

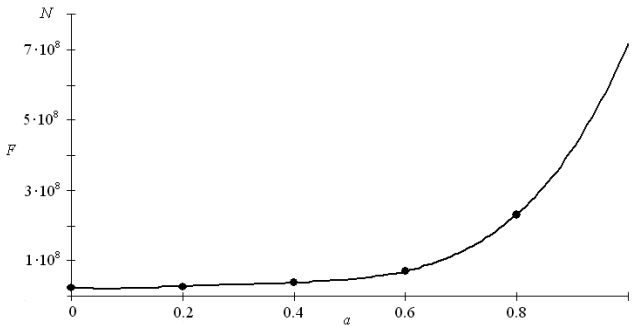


Figure 4: The dependence of the tidal force $F$ on the specific angular momentum of the black hole $a$.

**References**

1. Levi-Civita T.: 1926, *The absolute differential calculus*, London: Blackie and Son.
2. Synge J.L.: 1934, *Element Ann. Math.*, **35**, 705.
3. Synge J.L.: 1960, *Relativity: The General Theory*, North-Holland, Amsterdam; Interscience, New-York.
4. Shapiro S.L., Teukolsky S.A.: 1983, *Black Holes, White Dwarfs and Neutron Stars*, Cornell Univ., Ithaca, New York.
5. Chandrasekhar S.: 1983, *The Mathematical Theory of Black Holes*, Oxford Univ. Press, Oxford.
6. Misner C.W., Thorne K.S., Wheeler J.A.: 1973, Gravitation, Freeman and Company Limited.

# X-RAY SPECTRAL PROPERTIES OF THE ISOLATED AGNs: NGC 1050, NGC 2989, ESO 317-038, ESO 438-009

I.B. Vavilova, A.A. Vasylenko, Iu.V. Babyk, N.G. Pulatova

Main Astronomical Observatory of the NAS of Ukraine,
27 Akademika Zabolotnogo St., Kyiv, MSP 03680, Ukraine, *irivav@mao.kiev.ua*

ABSTRACT. We have analyzed the spectral data obtained by XMM-Newton, Swift, Chandra, and INTEGRAL space observatories for several isolated AGNs from 2MIG catalogue, for which the available X-ray data were accessed. Among these objects were CGCG 179-005, NGC 6300, NGC 1050, NGC 2989, WKK 3050, ESO 438-009, and ESO 317-038. We determined corresponding spectral models and values of their parameters (spectral index, intrinsic absorption etc.). X-ray spectra for bright galaxies, NGC 6300 and Circinus, were analyzed up to 250 keV and their characteristics of emission features were determined in 6-7 keV range.

We present the results for NGC 1050, NGC 2989, ESO 317-038, and ESO 438-009, for which their spectral parameters were obtained for the first time.

**Keywords:** Active galaxy nuclei – X-ray; Objects: NGC 1050, NGC 2989, ESO 317-038, ESO 438-009

## 1. Introduction

The most galaxies with active nuclei (AGNs) in the Local Universe are in a low-luminosity state (Ptak et al., 2000; Ho et al., 2009; Maia et al., 2003; Pulatova et al., 2015). In this sense, the principal question is why this state is related also to X-ray activity of the isolated galaxies with active nuclei (AGNs). The answer will be helpful to explain the AGN's paradigm in detail as well as to get a response to the internal evolution of galaxy activity as well as to investigate the influence of halo matter (baryonic/dark) on the formation and productivity of AGN's engine.

With this goal we have analyzed the data obtained by XMM-Newton, Swift, Chandra, and INTEG-RAL X-ray observatories to find the X-ray spectra of a good quality for several isolated AGNs from 2MIG catalogue (Karachentseva et al., 2010). We have selected such objects as CGCG 179-005, NGC 6300, NGC 1050, NGC 2989, WKK 3050, ESO 438-009, and ESO 317-038 and determined their main spectral properties. In this paper we describe briefly our results for NGC 1050, NGC 2989, ESO 438-009, and ESO 317-038, for which their spectral parameters were not previously studied.

## 2. Data processing

The Swift/BAT spectra were derived from the 70-month hard X-ray Survey (Baumgartner et al. 2013). The reduced Swift /XRT products were taken by using the XRT products generator (http://www.swift.ac.uk/user_objects/) (Evans et al. 2007, 2009, 2010) with HEASOFT 6.15.1 software package in UKSSDC (UK Swift Science Data Centre) archive. We only used the data taken in the photon counting (PC) mode in such a manner that we were able to identify the precise locations of our targets without any contamination. Only events with energy in the range of 0.3–10 keV with grades 0–12 were included.

The XMM-Newton MOS and PN data were pro-cessed using the standard software packages XMM SAS ver. 11.0 (Science Analysis Software) according to the guidelines of XMM-Newton User's Manual. Because of its higher sensitivity, we use the EPIC/PN spectrum for the analysis of NGC 1050, although duration of exposure for EPIC/MOS has been slightly longer (but it has less data as compared to PN). Only patterns corresponding to single and double events (pattern ≤4) were taken into account for the PN camera. Filter FLAG=0 was applied to exclude bad pixels and events that are at the edge of a CCD. The ARFGEN and RMFGEN tasks were used to create ancillary and response files. Spectra were binned according to the luminosity of each source.

The XMM-Newton/XRT and BAT spectra were treated together and analyzed using XSpec ver.12.6 software. Since observations for each instrument are not simultaneous, a cross-calibration constants $C$ have been introduced in our models. In order to derive the luminosities we used the standard ΛCDM cosmological model with parameters $H_0$ =70 (km·s)/Mpc, Λ=0.73, $\Omega_m$=0.27 (Bennett, 2003) as well as the Galactic absorption (see Table 1) has already been taken into account in the fitting.

The Chandra data was analyzed with CIAO software package (Chandra Interactive Analysis of Observations, version 4.7 (Fruscione et al. 2006) and the latest realize of calibration files. The standard reprocessing and screening routines to create new level=2 event files were made using *chandra repro* script. To extract the source and background spectra with ARF and RMF files we have used *specextract* script. The XSpec environment version 12.6.0 was used to model all spectra with absorbed power law model. The errors of best-fit parameters correspond of 1σ confidence level.

## 3. Results

The main spectral parameters of NGC 1050, NGC 2989, ESO 317-038 and ESO 438-009 are given in Table 1, namely, Column (1): Object name; Column (2): Right Ascension from NASA/IPAC Extragalactic Data base (NED); Column (3): Declination (NED); Column (4): Redshift (NED); Column (5): X-ray Observatory/ Instrument; Column (6): Observation exposures in ks; Column (7): Galactic absorption in units of $10^{20}$ cm$^{-2}$ (by Kalberla

Table 1. The main spectral parameters of NGC 1050, NGC 2989, ESO 317-038 and ESO 438-009 for the absorbed power law fits to the data

| (1) Object (Type) | (2) RA (deg) (J2000) | (3) Dec. (deg) (J2000) | (4) z | (5) Instrument | (6) Exposure (ks) | (7) $N_H$ $10^{20}$ cm$^{-2}$ | (8) L, $10^{40}$ erg/s | (9) $N_H$ | (10) Phot. index |
|---|---|---|---|---|---|---|---|---|---|
| NGC 1050 (Sy2) | 40.648 | 34.764 | 0.013 | XMM-Newton/ EPIC PN | 9.507* | 5.67 | 2.15±0.23 (0,5-2 keV) | 47.43±0.81 ($10^{22}$ cm$^{-2}$) | 2.0 (fixed) |
| NGC 2989 (AGN) | 146.355 | -18.374 | 0.014 | Swift/ XRT | 27.8* | 4.34 | 2.19 (0,5-2 keV) | $5.07^{+0.10}_{-0.05}$ ($10^{20}$ cm$^{-2}$) | 1.69±0.68 |
| ESO 317-038 (AGN) | 157.440 | -38.349 | 0.015 | Swift/ XRT+BAT | 14.4*+8482 | 6.0 | 27.1 | $17.05^{+32.59}_{-14.12}$ ($10^{22}$ cm$^{-2}$) | 1.7 (fixed) |
| ESO 438-009 (Sy1.5) | 167.700 | -28.501 | 0.024 | Swift/ XRT+BAT | 17.4*+7242 | 5.26 | 357 | $4.61^{+4.76}_{-3.40}$ ($10^{21}$ cm$^{-2}$) | 1.89±0.08 |
| * Exposure time in ks (EPIC PN/Swift XRT) after the data screening | | | | | | | | | |

et al. 2005 (LAB map)); Column (8): Luminosity, L, in units of $10^{40}$ erg/s in 2-10 кеV range; Column (9): Intrinsic absorption in units of $10^{22}$ cm$^{-2}$; Column (10): Photon Index.

***NGC 1050*** has been observed by XMM-Newton (2013-02-27, ID 0693540201). X-ray spectrum has a bad quality and the data beyond ~5 keV are absent. It was fitted by the model *phabs*(zbbody+zpo)*, where *tbabs* corresponds to the Galactic absorption. Because of a lack of data in the middle range, we have fixed a value of the photon index as $\Gamma$ = 2.0. We determined the values of flux in 0.5-2.0 keV as $(5.64\pm0.59)\cdot10^{14}$ ergs/cm$^2$/s and black-

body model as $kT$ = 189±23 eV ($\chi^2$/dof = 15.41/11 = 1.4). Other parameters are summarized in Table 1 and the best fitting spectrum is presented in Figure 1 (left panel).

X-ray observational data for NGC 1050 are presented for the first time.

***NGC 2989*** has been observed twice by Swift/ XRT (2008-10-06/08), duration of exposure in XRT/PC mode was 14125 s та 13672 s. A lower limit of spectrum was 2.5 keV. We fitted it by the model *phabs* zphbs*zpo*, where *phabs* corresponds to the Galactic absorption. A value of the photon index was determined as $\Gamma$=1.69±0.68, $\chi^2$/dof = 9.06/9. The main parameters are summarized in Table 1 and its spectrum is presented in Figure 1 (left panel). The errors are caused by the poor quality of the XRT data.

***ESO 317-038*** has been observed six times by Swift/XRT from 2011-02-24 to 2011-03-20, duration of exposure in XRT/PC mode was 623 ÷ 4909 s. A spectral analysis was conducted altogether with the Swift/BAT observational data and allowed us to enlarge a spectral range till 195 keV. A lower limit of spectrum was also 2.5 keV. We fitted its spectrum by the model *phabs*zphbs* cutoffpl*, where *phabs* corresponds to the Galactic absorption. We fixed a value of the photon index as $\Gamma$=1.7 and energy as $E_{cut\text{-}off}$= 500 keV. Luminosity is $2.71\cdot10^{41}$ ergs/s in 2.0-10 keV, $6.31\cdot10^{42}$ ergs/s in 14-195 keV (Swift BAT 70-Month Hard X-ray Survey). The main parameters are summarized in Table 1 and its spectrum is presented in Figure 1 (right panel). The errors are caused by the poor quality of the XRT data.

***ESO 438-009*** has been observed three times by Swift/XRT from 2010-11-02 to 2010-11-08, duration of exposure in the XRT/PC mode is 1172÷6429 s. A spectral analysis was conducted altogether with the Swift/BAT observational data and allowed us to enlarge a spectral range till 195 keV. A lower limit of spectrum is 0.5 keV. We fitted its spectrum by the model phabs**zxicpf*cut offpl*, where *zxipcf* corresponds to the absorption by the ionized matter with the overlap factor $C$ (we fixed $C$=1). We determined the photon index as $\Gamma$=1.86±0.06, cut-off energy was fixed as $E_{cut\text{-}off}$ = 500 keV. Intrinsic ionized absorption is $N_H = 4.61^{+4.76}_{-3.40}\ 10^{21}$ cm$^{-2}$ and ionization rate log $\xi = 2.35^{-0.44}_{+0.68}$; $\chi^2$/dof=134.51/116. Luminosity is $L_x$=2.73 $10^{42}$ ergs/s in 0.5-2.0 keV, $4.94\cdot10^{41}$ ergs/s in 2.0-10 keV, $1.24\cdot10^{43}$ ergs/s in 14-195 keV (Swift BAT 70-Month Hard X-ray Survey). The main parameters are summarized in Table 1 and its spectrum is presented in Figure 1 (right panel).

## 4. Brief discussion

One can see, the studied galaxies are of low activity (X-ray luminosity is less than $10^{42}$ ergs/s) that is consistent with our previous research (Pulatova et al., 2015), where we found that isolated AGNs in the Local Universe are mostly faint in X-ray. Altogether with these new data, a mean luminosity for 17 the 2MIG isolated AGNs without companions is $L_x$ ~$1.9\cdot10^{42}$ ergs/s in the soft 2-10 keV range (see, for comparison, results by Halderson (2001). The same estimations were derived by Anderson et al. (2013) for subsets of 2MIG galaxies: the average luminosity $L_X$ within 50 kpc is $1.0\cdot10^{40}$ ergs/s. They found also that that 1/2 of the total emission is extended and about 1/3 of the extended emission comes from hot gas.

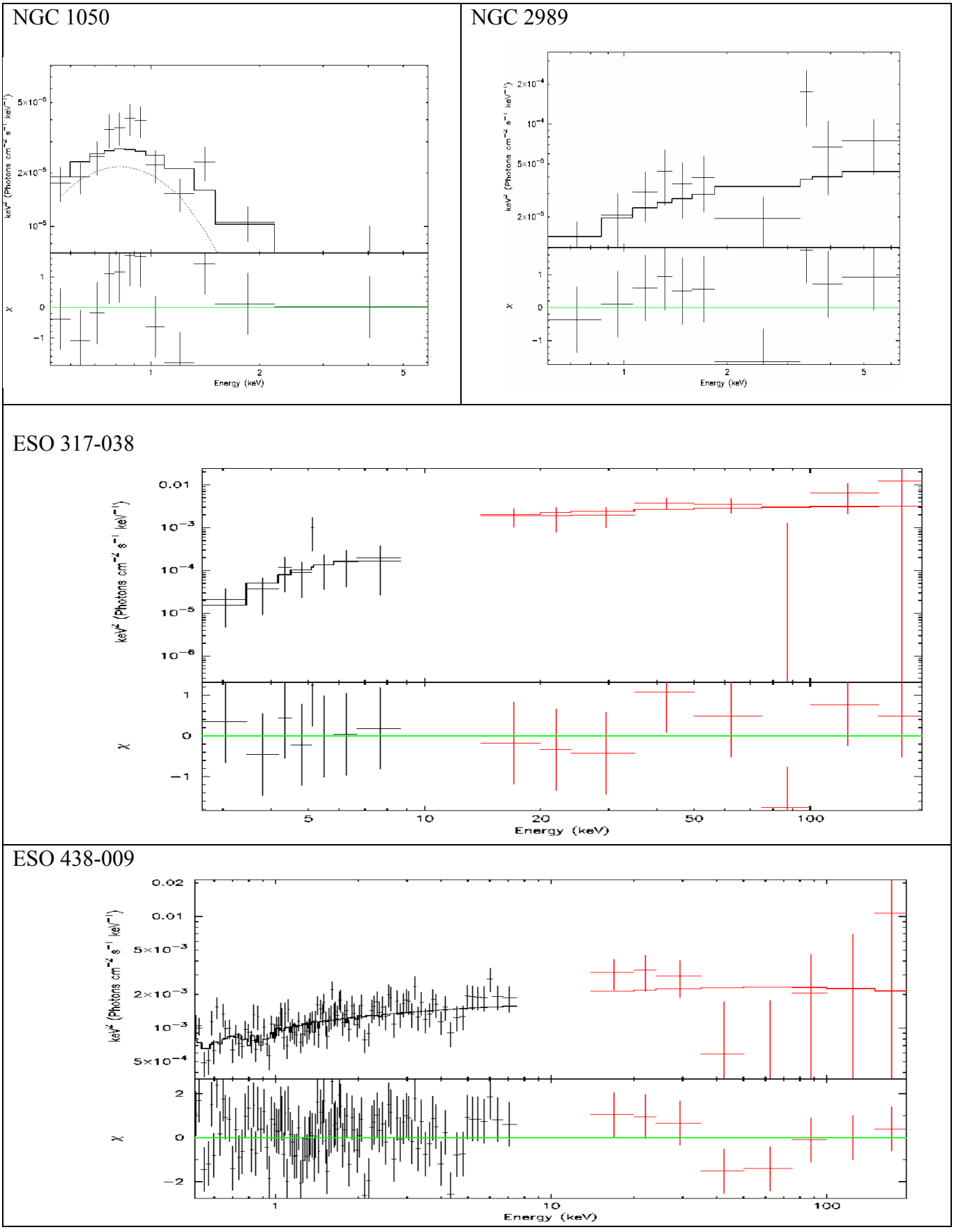


Figure 1: Unfolded spectrum of the isolated galaxies with active nuclei (their parameters are in Table 1).
*Top*: NGC 1050 and NGC 2989; the spectra were obtained in 0,5-10 keV range with XMM-Newton/XRT/BAT (best fitting spectra) and Swift respectively. *Down*: ESO 317-038 and ESO 438-009; the broad-band spectra were obtained in 0,5-150 keV range with Swift and INTEGRAL (red)

The authors (Melnyk et al., 2013) in their research with two selected samples XMM-LSS field (X-ray galaxies and AGNs) have studied an environment effect and found that AGNs, including soft X-ray AGNs, when comparing to X-ray galaxies, prefer to be located in lower galaxy overdensities. It is in a good agreement with our estimations on the influence of choice of isolation criteria for spatial analysis and physical/morphological properties of host galaxies (Vavilova, 2009; Elyiv, 2009). At the same time, we do not confirm the conclusion that the softest AGNs are of Sy1 type.

We noted in our research (Pulatova et al., 2015) that Sy 1 type galaxies appear to be more luminous that of Sy 2 type. Some AGNs of our sample have the spectral energy distribution almost flat from the infrared to X-ray part of spectrum, as result the spectral index is ~ 1, although it is usually steeper.

The stronger X-ray flux, than X-ray continuum is produced by lower energy photons. These photons are scattered to higher energies by relativistic electrons using Compton scattering. The fraction of the power emitted in the X-ray flux is almost four times bigger in AGNs than in normal galaxies. Using such property, we conclude that X-ray soft emission from the studied objects is in favor of the presence of AGN's engine. Additional evidences are the normalized excess variances (variability amplitudes) that anti-correlate with black hole masses. Our preliminary estimations point out (Chesnok et al., 2010) that the isolated AGNs in the Local Universe posses a low-mass black holes (intermediate values, $10^5$-$10^6$ $M_{Sun}$) being closer to their primordial mass (Ludlam et al., 2015).

To investigate the correlation between photon index of power law model and X-ray flux for each AGNs we have used additional data of XMM-Newton and Chandra observatories. Figure 2 shows the distribution of slopes of spectra of the isolated AGNs over X-ray flux. It was found a clear correlation between these values: the slope is 1.3. At the same time, we did not find correlation between the photon index and luminosity of the studied X-ray isolated AGNs.

*Acknowledgements.* This study is partially supported in frame of the Target Program of Scientific Space Research of the National Academy of Sciences of Ukraine (2012-2016).

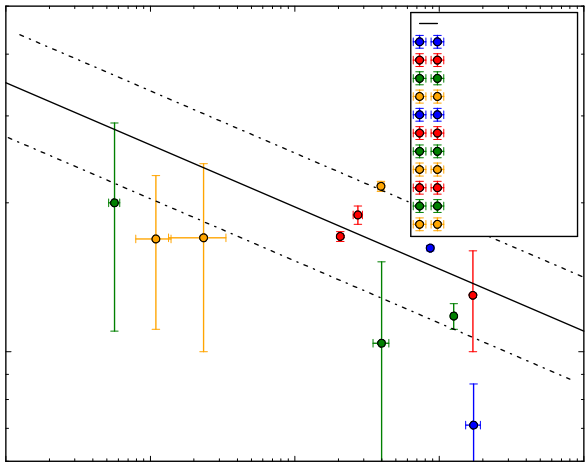

Figure 2: The Flux - Photon Index relation for X-ray sample of the isolated AGNs. The solid line corresponds to the simple power law model with slope 1.3, while two dotted lines correspond to the standard deviation.

**References**

Anderson M.E. et al.: 2013, *ApJ*, **762**, Is. 2, article id. 106.
Baumgartner W. H. et al.: 2013, *ApJSS*, **207**, 19.
Bennett C.L. et al.: 2003, *ApJSS*, **148**, 1.
Chesnok et al.: 2009, *Kinemat. Phys. Celest. Bodies*, **25**, issue 2, 107.
Chesnok N. et al.: 2010, *AIP Conf. Series*., **1206**, 328.
Elyiv A.A. et al.: 2009, *MNRAS*, **394**, Is. 3, 1409.
Evans P. A. et al.: 2007, *A&A*, **469**, 379.
Evans P. A. et al.: 2009, *MNRAS*, **397**, 1177.
Evans P. A. et al.: 2010, *A&A*, **519**, A102.
Fruscione et al.: 2006, SPIE Proc. 6270, 62701V, D.R. Silvia & R.E. Doxsey, eds.
Halderson E.L. et al.: 2001, *AJ*, **122**, 637.
Ho L.C.: 2009, *ApJ*, **699**, 626.
Hwang H.S. et al.: 2012, *A&A*, **538**, A15.
Kalberla P. M. et al.: 2005, *A&A*, **440**, 775.
Karachentseva V.E. et al.: 2010, *Astrophys. Bull*., **65**, 1.
Ludlam R.M. et al.: 2015, *MNRAS*, **447**, 2112.
Maia M.A.G. et al.: 2003, *ApJ*, **126**, 1750.
Melnyk O.V. et al.: 2013, *A&A*, **557**, id. A81.
Ptak A. et al.: 1999, *ApJSS*, **120**, 179.
Pulatova N.G.et al.: 2015, *MNRAS*, **447**, 2209.
Vasylenko A.A. et al.: 2015, *Ap&SS*, DOI: 10.1007/s10509-015-2585-z
Vavilova I. B. et al: 2009, *Astron. Nachr*., **330**, 1004.
Vol'vach A.E. et al.: 2011, *Astron. Reports*, **55**, 608.